



National Library
of Canada

Bibliothèque nationale
du Canada

Canadian Theses Service

Service des thèses canadiennes

Ottawa Canada
K1A 0N4

NOTICE

The quality of this microform is heavily dependent upon the quality of the original thesis submitted for microfilming. Every effort has been made to ensure the highest quality of reproduction possible.

If pages are missing, contact the university which granted the degree.

Some pages may have indistinct print especially if the original pages were typed with a poor typewriter ribbon or if the university sent us an inferior photocopy.

Reproduction in full or in part of this microform is governed by the Canadian Copyright Act, R.S.C. 1970, c. C-30, and subsequent amendments.

AVIS

La qualité de cette microforme dépend grandement de la qualité de la thèse soumise au microfilmage. Nous avons tout fait pour assurer une qualité supérieure de reproduction.

S'il manque des pages, veuillez communiquer avec l'université qui a conféré le grade.

La qualité d'impression de certaines pages peut laisser à désirer, surtout si les pages originales ont été dactylographiées à l'aide d'un ruban usé ou si l'université nous a fait parvenir une photocopie de qualité inférieure.

La reproduction, même partielle, de cette microforme est soumise à la Loi canadienne sur le droit d'auteur, SRC 1970, c. C-30, et ses amendements subséquents.



National Library
of Canada

Bibliothèque nationale
du Canada

Canadian Theses Service Service des thèses canadiennes

Ottawa, Canada
K1A 0N4

The author has granted an irrevocable non-exclusive licence allowing the National Library of Canada to reproduce, loan, distribute or sell copies of his/her thesis by any means and in any form or format, making this thesis available to interested persons.

The author retains ownership of the copyright in his/her thesis. Neither the thesis nor substantial extracts from it may be printed or otherwise reproduced without his/her permission.

L'auteur a accordé une licence irrévocable et non exclusive permettant à la Bibliothèque nationale du Canada de reproduire, prêter, distribuer ou vendre des copies de sa thèse de quelque manière et sous quelque forme que ce soit pour mettre des exemplaires de cette thèse à la disposition des personnes intéressées.

L'auteur conserve la propriété du droit d'auteur qui protège sa thèse. Ni la thèse ni des extraits substantiels de celle-ci ne doivent être imprimés ou autrement reproduits sans son autorisation.

ISBN 0-315-56059-2

Canada

**A Computer Method for Dynamic Analysis of HVAC system - Building
Interaction and Control Applications**

Menelaos Stylianou

A Thesis

in

The Centre for Building Studies

**Presented in Partial Fulfilment of the Requirements
for the Degree of Master of Engineering at
Concordia University
Montréal, Québec, Canada**

September 1989

© Menelaos Stylianou, 1989

ABSTRACT

A Computer Method for Dynamic Analysis of HVAC System - Building Interaction and Control Applications

Menelaos Stylianou

Use of computers within energy management and control systems now permits the implementation of dynamic control strategies that attempt to exploit the interaction between the building mass and the HVAC system for improvement of the building's overall performance; capabilities not intrinsic in conventional feedback control systems.

To accomplish a high level of integration, however, it is necessary first to study the interaction between the room air and the envelope mass thermal dynamics. In this thesis, the effect of short and long term fluctuations in the loads for rooms with different thermal mass was considered in order to explore this interaction. Using frequency response methods, it was determined that, especially with respect to massive buildings, for convective loads there is a relatively clear separation between short and long term dynamics at an approximate frequency of 36 cycles/day (periods of about 40 min.). However, for radiative loads no such separation exists, which implies that feedback control cannot properly limit the room temperature swings imposed by such loads.

To counteract this shortcoming associated with feedback control, theoretical, comparative, studies were carried out to investigate the feedforward control system which incorporates in its design, consideration for the interaction of the building envelope mass with the HVAC system and

which, by virtue of its algorithmic nature, has anticipatory capabilities and the capacity for supervisory action.

These studies, performed using DYCON, a computer program developed as part of this work, showed that the hybrid feedforward-feedback control system greatly improved the performance of an HVAC system over the conventional feedback control system by substantially limiting the temperature fluctuations. This stems directly from the fact that this system treats the HVAC system and the building enclosure as one integrated system and possesses the capability to react to disturbances that are in the region where neither short nor long term dynamic strategies can be applied.

ACKNOWLEDGEMENTS

This thesis would not have been possible without the help of many people.

I would like to express my gratitude to my supervisor Dr. A. K. Athienitis for his expert guidance, encouragement and support during my graduate studies.

Special thanks and appreciation also go to my wife, Susan, for her patience, understanding, encouragement and moral support. I would also like to thank my parents for their support and guidance throughout my studies.

Finally, I wish to acknowledge the support and encouragement of my friends and colleagues for their valuable contributions.

TABLE OF CONTENTS

LIST OF FIGURES	x
LIST OF TABLES	xiii
NOMENCLATURE	xiv
CHAPTER 1 INTRODUCTION	1
1.1 Introduction	1
1.2 Motivation	4
1.3 Objectives	5
CHAPTER 2 LITERATURE REVIEW	7
2.1 Introduction	7
2.2 HVAC system component modelling	7
2.2.1 Fans	11
2.2.2 Air ducts	13
2.2.3 Heating coils	17
2.2.4 Cooling and dehumidifying coils	20
2.2.5 Control valves	22
2.2.6 Sensors	24
2.2.7 Controllers	24
2.3 HVAC system modelling	25
2.4 Room models	28

2.5 Relationship between HVAC control system and building envelope with respect to energy consumption and thermal comfort	30
2.6 Discussion	36

CHAPTER 3 COMPARISON OF ROOM MODELS FOR BUILDING OPERATION DYNAMIC

STUDIES AND THE EFFECT OF ENVELOPE AND AIR MASS	40
3.1 Introduction	40
3.2 Room models	41
3.2.1 Description of room models	43
3.2.2 Comparison of model 3 to a detailed model	53
3.3 Nyquist and Bode plots	54
3.4 Frequency response differences among models	56
3.5 Discussion	59
3.6 Effect of envelope and air mass on building operation dynamics	59
3.6.1 Frequency response study for short and long term dynamics	60
3.6.3 Discussion	64

CHAPTER 4 DYNAMIC CONTROL STRATEGIES USING THE MASS OF THE

BUILDING	80
4.1 Introduction	80
4.2 Using the mass for frequencies of 1 cycle per day	80
4.2.1 Problems associated with square set-back profile and possible solutions	82

4.2.2 Setpoint temperature variation for frequencies of 1 cycle per day	84
4.2.2.1 The discrete frequency domain approach and discrete Fourier transforms	84
4.2.2.2 The algorithm	86
4.2.3 Discussion	91
4.3 Utilizing the mass for frequencies higher than 1 cycle/day	92
4.3.1 Methodology	93
4.3.2 Discussion of results	95
4.4 Conclusions	96

CHAPTER 5 A THEORETICAL STUDY OF INTEGRATED BUILDING - HVAC SYSTEM

DYNAMIC CONTROL	97
5.1 Introduction	97
5.2 Control system design approaches	99
5.2.1 Comparison of feedforward and feedback control systems	103
5.2.2 Feedforward-feedback control	104
5.3 A comparative study of the different control system design approaches	106
5.3.1 Numerical inversion of Laplace transforms	107
5.3.2 DYCON: A program for time and frequency domain studies of HVAC system dynamics	111
5.3.2.1 Air ducts	113
5.3.2.2 Heat exchangers	115

5.3.2.3 Control valves	115
5.3.2.4 Sensors	117
5.3.2.5 Controller	117
5.3.3 Feedback control of the system	118
5.3.4 Feedforward control system	125
5.3.5 Feedforward-feedback control system	129
5.4 Conclusion	133
CHAPTER 6 CONCLUSIONS AND EXTENSIONS OF WORK	135
6.1 Extensions of the current work	136
REFERENCES	138
APPENDIX A	
Input data for chapter 5	148
APPENDIX B	
Listing of DYCONFOR, the FORTRAN program of DYCON	155
APPENDIX C	
Heat exchanger model used in DYCON	190

LIST OF FIGURES

3.1 Schematic of room used in study	45
3.2 Network analogue of room	45
3.3 Model 1 representation of the floor	46
3.4 Model 2 representation of the floor	46
3.5 Network representation of model 2	46
3.6 Norton equivalent for the floor sub-network	46
3.7 Calculating the Norton equivalent for model 2	49
3.8 Schematic of the slab	49
3.9 Example of magnitude and phase difference	58
3.10 Polar plot of $Z(1,1)$ variation: model 2	65
3.11 Plot of magnitude ratio for $Z(1,1)$: model 2	65
3.12 Plot of phase angle of $Z(1,1)$: model 2	66
3.13 Polar plot of $Z(1,1)$ Variation: model 3	66
3.14 Plot of magnitude ratio for $Z(1,1)$: model 3	67
3.15 Plot of phase angle of $Z(1,1)$: model 3	67
3.16 Magnitude error for $Z(1,1)$ of model 2 compared to model 3 . . .	68
3.17 Polar plot of $Z(1,1)$ Variation: model 1	68
3.18 Plot of magnitude ratio for $Z(1,1)$: model 1	69
3.19 Plot of phase angle of $Z(1,1)$: model 1	69
3.20 Magnitude error for $Z(1,1)$ of model 1 compared to model 3 . . .	70
3.21 Magnitude error for $Z(1,2)$ of model 2 compared to model 3 . . .	70
3.22 Magnitude error for $Z(1,2)$ of model 1 compared to model 3 . . .	71
3.23 Plot of magnitude ratio for $Z(1,2)$: model 1	71

3.24 Plot of phase angle of $Z(1,2)$: model 1	72
3.25 Plot of magnitude ratio for $Z(1,2)$: model 2	72
3.26 Plot of phase angle of $Z(1,2)$: model 2	73
3.27 Plot of magnitude ratio for $Z(1,2)$: model 2	73
3.28 Plot of phase angle of $Z(1,2)$: model 3	74
3.29 Magnitude error for $Z(1,1)$ of model 2 compared to model 3 . . .	74
3.30 Magnitude error for $Z(1,1)$ of model 1 compared to model 3 . . .	75
3.31 Magnitude error for $Z(1,2)$ of model 2 compared to model 3 . . .	75
3.32 Polar Plot of $Z(1,1)$ variation: model 3 (gypsum board)	76
3.33 Plot of magnitude ratio for $Z(1,1)$: model 3	76
3.34 Plot of phase angle of $Z(1,1)$: model 3 (gypsum board)	77
3.35 Plot of magnitude ratio for $Z(1,2)$: model 3	77
3.36 Plot of phase angle of $Z(1,2)$: model 3 (gypsum board)	78
3.37 Plot time lag for $Z(1,1)$ of model 3 for concrete and gypsum board	78
3.38 Plot of time lag for $Z(1,2)$ of model 3 for concrete and gypsum board	79
4.1 Simple setback	81
4.2 Auxiliary energy requirements for the square profile	81
4.3 The system block diagram	87
4.4 Algorithm for generating setpoint profiles	88
4.5 Profile 1	90
4.6 Profile 2	90
4.7 Comparison of the different profiles and energy requirements . .	91
4.8 Convective, radiative and total load variation	94
4.9 Temperature setpoint variation	94

4.10 Cooling energy required for constant and varying setpoint . . .	95
5.1 Structure of (a) feedforward and (b) feedback control loops . .	99
5.2 Block diagrams for (a) process (b) feedforward loop (c) feedforward loop with measuring device and final control element	102
5.3 Diagram for feedforward-feedback control loop	105
5.4 The structure of DYCON	112
5.5 (a) Schematic of room and HVAC system (b) block diagram of the system	119
5.6 Time response at the stability limit for calculation of K_p and τ_i : base case	122
5.7 Time response at the stability limit for calculation of K_p and τ_i : system with 300 seconds delay	122
5.8 Time response of feedback loop : base case	123
5.9 Time response of feedback loop : System with 300 seconds delay	123
5.10 Frequency response of the system: base case	124
5.11 Frequency response of the system: system with 300 seconds delay	124
5.12 Feedforward loop	127
5.13 Feedforward loop response	127
5.14 Block diagram for feedforward-feedback control	131
5.15 Feedforward-feedback time response of system: base Case . . .	132
5.16 Feedforward-feedback time response of system: system with 300 seconds delay	132

LIST OF TABLES

3.1 Room model data 44

3.2 Comparison of Z(1,1) computed using model 3 and the detailed
mode 55

3.3 Comparison of Z(1,2) computed using model 3 and the detailed
mode 55

NOMENCLATURE

a	constant used for duct
c_p	specific heat (J/kgK)
dd	weight of duct per unit length (kg/m)
e	base of natural logarithms
h	heat transfer coefficient ($W/^\circ C m^2$)
i	current (A)
j	$\sqrt{-1}$
k	conductivity ($W/m^\circ C$)
m	mass flow rate (kg/sec)
q	heat flow (W)
s	Laplace operator
t	time (sec)
x	horizontal distance (m)
y	vertical distance (m)
z_1, z_2, z_3	impedance ($^\circ C/W$)
z	variable in numerical inversion of Laplace transform
A	area (m^2)
F	Fourier transform
G_o	Transfer function relating outside temperature variations to inside air temperature
G_q	Transfer function relating the auxiliary energy variations to inside air temperature
G_f	Transfer function representing the final control element
G_m	Transfer function representing the measuring device

G_{duct}	Transfer function representing the change of fluid temperature along the duct
G_{valve}	Transfer function representing the change of water mass flow rate to a change in the valve position
G_{coil}	Transfer function representing the change in outlet air temperature for a step change in the water flow rate in a heat exchanger
G'_{duct}	$G_{duct}Cp_a m_a$
G_x	$G_{valve}G_{coil}G'_{duct}Z_{11}$
K	gain
K_i	variable in numerical inversion of Laplace transform
L	length (m)
Q	heat flow (W)
V	volume flow rate (m ³ /sec)
T_f	fluid temperature (°C)
T	temperature (°C)
U	conductance (W/m ² °C)
UF	conductance between floor and basement (W/m ² °C)
UFA	conductance between floor and air (W/m ² °C)
UFK	conductance between the middle of floor slab and basement (W/m ² °C)
UFT	conductance between the middle of floor slab and floor surface (W/m ² °C)
UO	conductance between inside and outside air (W/m ² °C)
$Y_{1,1}$	wall self admittance (W/°C)
$Y_{1,2}$	wall transfer admittance (W/°C)

Z(1,1) wall self impedance ($^{\circ}\text{C}/\text{W}$)
Z11 wall self impedance ($^{\circ}\text{C}/\text{W}$)
Z(1,2) wall transfer impedance ($^{\circ}\text{C}/\text{W}$)
Z12 wall transfer impedance ($^{\circ}\text{C}/\text{W}$)

SUBSCRIPTS

a air
ai room air
ap approximate
aux auxiliary
b basement
conv convective
d duct
f floor
i inside
ia inlet air
m measured
o outside
oa outlet air
out outlet
p proportional
rad radiative
s sensor
sc short circuit
sf floor surface
SP set point

ss	steady state
v	valve
w	water
wi	water inlet
wo	water outlet
c	concrete
g	gypsum board

SUPERSCRIPTS

°	outlet
x	horizontal distance

GREEK

α	thermal diffusivity
γ	$\sqrt{(s/\alpha)}$
Δ	difference
ϵ	error
ρ	density
τ	time constant
τ_1	integral (or reset) time
ϕ	phase angle
ω	frequency

CHAPTER 1

INTRODUCTION

1.1 Introduction

The primary concern of many in the area of HVAC system dynamics has been the study of closed loop control. However, the dynamic interaction between the building envelope and HVAC systems and their controls has received limited attention. Due to the lack of an extensive knowledge base on which to examine this interaction, it is preferable to approach the study of this interaction at a fundamental level using modelling for analysis and simulation studies.

There are mainly two approaches for studying HVAC system - building envelope interaction; analysis through simulation using time or frequency domain methods and direct analysis using frequency domain methods. The majority of studies whose objectives are related to this interaction use the former method (Zhang and Warren 1988) while the latter is used for feedback control loop studies (Hamilton et al 1974).

Time domain methods are based on discretization in space and time of the processes occurring in the system. They include a large number of procedures whose use is dependent on the application being considered. The main advantage of these methods over frequency domain methods is their ability to model system non-linearities. In order to accommodate modelling of non-linearities, a new system of simultaneous equations would have to be solved at every time step, making the inclusion of non-linearities time consuming.

Although very useful for simulating non-linearities in the system, time domain methods have limited application to the analysis and design of systems. This stems from the need for repeated simulations to examine different design alternatives, which leads to computational inefficiency. Frequency domain methods by-pass this inefficiency since, as in the case of discrete frequency response methods, no simulation is needed. The response of a system whose transfer function is known is simply calculated for the frequency of interest. If the response to periodic inputs is desired, the inverse discrete Fourier transform can be used to establish it. It may therefore be desirable to linearize the system for computational efficiency reasons, in which case it could be conveniently modelled for both frequency and time domain studies.

Computer aided studies require the establishment of model complexity requirements. By using a model that is detailed enough to produce results that are representative of the dynamic characteristics of buildings, it would be possible to establish a better understanding of the building properties and how they affect HVAC system performance.

Frequency response characteristics determined from room thermal network models provide insights into the influence the presence of a massive element has on the air temperature variation in response to disturbances at the air and floor surface nodes. To gain more information regarding this interaction, the thermal impedances relating the effect of loads at the air and floor nodes will be calculated for rooms with highly different amounts of thermal mass.

After examining the frequency response characteristics of enclosures with significant thermal mass and those without, the use of the mass to

limit equipment sizes and improve thermal comfort will be examined. Dynamic control strategies are based on the principle that the mass of the building should be a factor in the design and operation of HVAC systems. This principle, however, has been used without a structured methodology to obtain optimal results. It is therefore necessary to demonstrate a structured approach to the use of mass to limit peak loads upon start-up, as well as show that the thermal mass can also be used for relatively high frequencies of the order of 8 cycles per day with significant lowering of the peak load.

Finally, having discussed the dynamic effect of the building's thermal mass on the room air temperature and the mass's use as a thermal reservoir by the use of controlled temperature swings, the control system design approach to accomplish this will be addressed. Dynamic control strategies are based on the knowledge of the building's thermal behaviour. Such knowledge, however, whether acquired through modelling or measurements, can only be useful if it can be used to facilitate the achievement of thermal comfort and reduced energy consumption.

By its nature, the building mass introduces high thermal lag which conventional control systems, such as feedback control, are intrinsically unable to compensate for effectively. This is because they are local loop control systems which tend to ignore the dynamic interaction between the HVAC system and the building mass, resulting sometimes in discomfort and energy waste. A control system that would be able to accommodate this interaction is clearly one that would possess "knowledge" of the building and the system. It would allow the integration of HVAC system and building dynamics and be able to anticipate the effects of load changes on comfort.

energy consumption and stability considerations. It is apparent, therefore, that such a system would rely heavily on feedforward control algorithms and controllers, which although having been applied for a number of years in the process control industry, are a new concept in EMCS (Energy Management and Control Systems).

1.2 Motivation

Predictive control in conjunction with integrated control are the two basic differences between dynamic control and the other types of control (Hartman 1988). Predictive control requires a weather predictor to continuously project the upcoming outdoor conditions to establish the set-point temperature. The integrated or supervisory control tries to attain this temperature by orchestrating the operation of individual components, (for example by varying fan speed, coil air discharge set-point temperature, water temperature and flow rates through the coil, among others), together with exploiting the thermal storage mass of the building.

The use, however, of the weather predictor may be dispensed with for short term dynamics (of the order of less than 3 hours) if the disturbances, due to changing outdoor conditions, can be reliably measured. This may be possible through the use of sensors for outdoor temperature and solar radiation which would feed information to a processor with either a knowledge base or a detailed model of the building and which would instruct the integrated control system as to the strategy best suited for the operation of the system.

This approach is comparable to the feedforward control approach and

its use may improve comfort and energy conservation. In addition, this strategy may be of use not only during the operating stage, but also at the design stage through the use of detailed simulation and/or analysis to help establish optimum equipment sizes. In a study of a predictive control algorithm for energy conservation and reduction of room temperature swing, Athienitis (1988) used simulation of a detailed one room model under different set-point profiles. It was found that while a simple night set-back (square wave) saved energy over a constant set-point, a 40% increase in peak heating load resulted on sunny, cold days. Use of smoother profiles, involving ramping through the use of continuously changing set-points, produced a peak heating load increase of only 11%, as compared to the constant set-point, while the temperature swing was lowered by 1 °C.

Findings such as these offer proof to the earlier statements regarding the effective use of dynamic control strategies at the design stage to limit the size of equipment while at the same time maintaining thermal comfort. In addition, integrated control may be used to allow for more efficient operation of equipment through feedforward control strategies.

1.3 Objectives

The objectives of this thesis therefore are the following:

1. To establish quantitatively the effects of high and low frequency variations of radiative and convective loads on room air temperature.

2. To study feedforward control algorithms for improved control of both short and long term building thermal performance.
3. To develop a computer method to perform such building operation dynamics studies.

CHAPTER 2

LITERATURE REVIEW

2.1 Introduction

Extensive research has been conducted by many on the dynamics of HVAC systems. Their primary concern, however, has been the study of local loop control, such as stable control of the supply air temperature of a heating coil. Within this area, modelling of the HVAC systems and their controls has been extensively exploited as the venue to a better understanding of the dynamics of heating and cooling processes in buildings. Examination of the dynamics of the interaction between the building envelope and the HVAC systems and their controls, has, however, received limited attention. This chapter will deal with both (1) the methodology followed by these researchers in modelling the individual system components as well as the HVAC system and building integration and (2) the study of work done towards understanding and exploiting the HVAC system-building enclosure interaction as a means for improving overall building performance.

2.2 HVAC system component modelling

There are two approaches to the study of HVAC system - building envelope interaction; analysis through simulation using time or frequency domain methods and direct analysis using frequency domain transform methods. The majority of studies whose objectives are related to this interaction use the former method (Miller, 1982) while the latter is used

for closed loop stability studies.

Although very useful for simulating non-linearities in the system, time domain methods have limited application to the analysis and design of systems. This stems from the need for repeated simulations to examine different design alternatives and leads to computational inefficiency. In addition, it may indeed be desirable to assume that the HVAC system behaves in a linear fashion, an assumption that is not incorrect provided the system is operating within certain bounds. The main reasons for linearizing the system are:

1. Exact solutions of linear systems can be easily found.
2. Modelling of non-linear behaviour in systems is peculiar to the situation being evaluated and with respect to this careful consideration is required to avoid overgeneralization.

It may therefore be desirable to linearize the system for computational efficiency reasons, in which case it could be conveniently modelled for both frequency and time domain studies as the Laplace transform of the energy balance equations for a thermal network.

In developing methods for the simulation and analysis of HVAC system dynamics, three basic steps are usually taken:

1. Development of mathematical models to describe the components of the system. The detail with which the models describe the actual components, however, has a significant effect on the results of studies performed. Although detail is required to ensure a realistic

representation of a model's behaviour, extreme complexity of the model would lead to results that are influenced by parameters that are not adequately accounted for.

2. Integrating these models into representations of the actual system through the use of systems of algebraic and differential equations or block diagrams representing a set of interconnected transfer functions.
3. Solution of the resulting sets of differential and algebraic equations for the variables of interest. As previously mentioned, time domain methods have the ability to model system non-linearities; the two kinds of which are processes with hard and soft non-linearities. The former are characterized by being described by different equations under different circumstances, as is the case with limiting control or proportional controllers with a dead band. The latter are characterized by the fact that the equations that describe them are non-linear differential or algebraic equations, as is the case with equal percentage valves. To accommodate modelling of non-linearities, a new system of simultaneous equations would have to be solved at every time step, making the inclusion of non-linearities time consuming.

It has to be kept in mind that there should be an optimum complexity in the description of the models so that extremely large models or extremely simple ones do not obstruct the objectives of the studies they are meant to perform.

Regardless of the approach, the system components, each described

by either differential equations or transfer functions, are related to each other through the airflow, control signals and thermal media flow (such as chilled or hot water) to compose sets of differential equations or transfer functions describing the HVAC system. Two of the most common methods for representation and solution of these sets are:

1. Transfer function-block diagram representation of systems (e.g. Zhang and Warren 1988)

Block diagram representation of a system is a vital tool for visualizing the design of complex systems. A set of symbols can be used to develop a powerful block diagram algebra for manipulating system transfer functions, developing system equivalencies, simplifying system transfer functions and generally visualizing the system design and the interactions among the system's many elements. Within a block diagram, the flow of signals is easily visualized and the component transfer functions, usually derived from thermal network models solved in the Laplace domain, can be easily integrated to form the system transfer function. The resultant transfer function can then be used for frequency domain analysis, simulation using response factor methods, inverse discrete Fourier transform and other methods as well.

2. System representation in state variable form (e.g. Park et al 1985) and solution using numerical methods

This method is also termed vector-matrix formulation and is somewhat removed from the physical system representation, its main advantage

being that the analyst gains mathematical insights into the system's characteristics that add to his understanding of a system's physical properties. The state of a system is described by a set of first-order differential equations written in terms of the state variables (e.g. temperature). These equations may be solved using a number of numerical methods (e.g. forward difference techniques)

Still others proceed directly with the solution of the coupled differential equations (Shavit and Brandt 1982) using one of a number of numerical methods. This approach, however, does not lend itself to the detailed analysis of the system, an advantage that is gained from utilizing the above representation methods.

2.2.1 Fans

Three variables are required from a fan model: the temperature and pressure rise in the air stream produced and the energy consumption for full and part load conditions. In general, the fan's effect on the air stream is ignored (Miller 1982, Zhang and Warren 1988) or is incorporated in a fan-duct model (Thompson 1981). Larger programs, however, provide for fan models that at least relate one of the three variables to the air flow rate and to the size of the fan. DOE2 (Curtis et al 1984) accounts for temperature rise and energy consumption for full and part load operation based on the size of the fan and the static pressure of the system.

Simulation studies performed (Patterson and Alwin 1978) have shown that air movement in commercial buildings may account for up to 23.9% of the total energy consumption. It is therefore imperative that a fan model

have the capability to calculate the energy consumption for both part and full load performance, in addition to any temperature rise and pressure increase in the air stream flowing through the fan.

The model used by DOE2 (Curtis et al 1984) requires air pressures and fan efficiencies to be specified and assumes that all fan energy consumption causes an air-stream temperature rise.

At design load, the temperature rise due to the supply fan ΔT^{sf} is then found using:

$$DT^{sf} = \frac{P_s^{sf}}{\eta^{sf}} \quad (2.1)$$

$$\Delta T^{sf} = DT^{sf} * k_1^{sf} \quad (2.2)$$

where

P_s^{sf} = supply static pressure

η^{sf} = supply fan efficiency

k_1^{sf} = variable that depends on the state of air

while the power consumption is:

$$psf = \frac{V_{da}^{sf} * DT^{sf}}{c} \quad (2.3)$$

where c = conversion factor

V_{da}^{sf} = design supply air flow rate

At part load the model computes the power consumption and temperature rise in the fans as follows; first the fraction of the design

volume flow rate is calculated:

$$PL_v = V_{da}/V_a \quad (2.4)$$

where

V_{da} = design flow rate

V_a = actual flow rate

Following this, the part-load ratio (PLR^f) of energy input to the fan rated energy input is found depending on the method of fan control i.e. speed, inlet vanes, discharge, or cycling according to constants suggested by the program. This ratio is subsequently used to calculate the temperature rise and energy consumption under part-load conditions.

Finally, HVACSIM⁺ calculates the temperature rise and energy consumption also based on the efficiency and air pressures, but does not recommend any values for part load performance (Clark, 1985) relying on the user to supply the different constants describing it. In addition, instead of considering that all energy supplied to the fan contributes to the temperature rise, it assumes that only the inefficiencies heat the air.

2.2.2 Air ducts

The ductwork's effect on the dynamics of an HVAC system is similar to that of the fan in that it affects both the pressure and the temperature of the air stream. The effect of the fan is much more pronounced but if the ductwork is extensive, studying it separately from

the fans provides an insight into a number of problems encountered, particularly with VAV systems.

Models for the temperature response of the air stream within the duct should account for thermal losses to the surroundings and the transport delay. Clark et al (1985) present an approximate model which accounts for both conditions. The model, implemented in HVACSIM*, uses a fifth order time dependent polynomial to model the temperature distribution in a duct or pipe which accounts for the transport delay:

$$T(x,t) = \sum_{i=0}^5 a_i(t)x^i \quad (2.5)$$

where a_i = time dependent coefficients of the polynomial

x = normalized position in pipe or duct

At t' , after a time Δt (i.e $t' = t + \Delta t$), the temperature distribution is shifted by a distance Δx which is the distance travelled along the duct at a velocity V after a time Δt ($\Delta x = V \Delta t / L$, where L is the length of the duct).

Therefore:

$$T(x,t') = T(x-\Delta x,t) \quad \Delta x < x \leq 1 \quad (2.6)$$

Between $x = 0$ and $x = \Delta x$ linear interpolation is used to evaluate temperatures:

$$T(x,t') = T(0,t') + [T(0,t) - T(0,t')] * x / \Delta x \quad 0 < x < \Delta x \quad (2.7)$$

The temperatures are evaluated at five points at each time step, while a new set of coefficients for the polynomial is found by Gaussian elimination. Clark et al (1985) observed that for a stable solution, the evaluation points should be equally spaced along the duct provided that one of the points be located at $x = \Delta x$ and one or more points be in the region between zero and Δx if Δx is greater than $1/5$. Since the program allows for variable time step within user defined minimum and maximum values, this method of representing time delays is necessary for the methods of solution of the differential equations employed in HVACSIM* which use backward differential formulas. The temperature change of the fluid in the duct, the other important variable that should be accounted for in a proper duct model, is found by considering the steady state energy balance as a function of the distance travelled along the duct, as well as the dynamic relationship between the duct's temperature and the flow of the fluid within it. Finally, the model assumes that the thermal losses to ambient conditions occur at a steady rate, and that an equilibrium exists between the last average duct temperature and the outlet temperature of the fluid, which allows for the elimination of the duct's temperature from the resulting equation:

$$\frac{dT}{dt} = \frac{(T_{ss} - T_{out})}{\tau} \quad (2.8)$$

$$\tau = \frac{h_i}{h_i + h_o} * \frac{M_d * C_d}{m_a * c_p} \quad (2.9)$$

where:

- T_{ss} - steady state air outlet temperature
- T_{out} - outlet air temperature
- h_i - inside heat transfer coefficient per unit length
- h_o - outside heat transfer coefficient per unit length
- M_d - mass of duct
- C_d - specific heat of duct
- m_a - air mass flow rate
- c_p - specific heat of air

The last step in the process of estimating the air's outlet temperature is to send the value calculated from the above equation to the subroutine used to estimate the transport delay.

Results obtained from the implementation of the above method were consistent with results from the more exact transfer function developed by Tobias (1973) except where the outside heat transfer coefficient is high and when the temperature oscillations are much faster than the transport delay.

The transfer function developed by Tobias (1973) is obtained by means of the Laplace transform of the two partial differential equations describing the temperature of a fluid flowing through a conduit when the ambient temperature is constant and uniform:

$$\rho A c_p \frac{\delta T_f}{\delta t} + m_a c_p \frac{\delta T_f}{\delta y} + h_i (T_f - T_d) = 0 \quad (2.10)$$

and

$$ddc_{pd} \frac{\delta T_d}{\delta t} + (h_i + h_o) T_d - h_i T_f = 0 \quad (2.11)$$

where

- T_f - air temperature
- T_d - duct temperature
- ρ - air density
- A - cross sectional area of duct
- c_p - specific heat capacity of air
- m_a - air mass flow rate
- dd - weight of duct per unit length
- c_{pd} - specific heat capacity of duct material

The transfer function obtained contains similarities with the Clark model but is more exact in its formulation of the process. It also presents the capabilities inherent in the use of transfer functions in that it is possible to be used in both frequency analysis and simulation by using the inverse discrete Fourier transformation. More extensive discussion of this transfer function will be presented in chapter 5 during the discussion on the models used for the purpose of this research.

2.2.3 Heating coils

Extensive research has been conducted, resulting in the development of transfer functions representing the dynamic behaviour of heat exchangers. The transfer functions thus developed were primarily used to enable control engineers to design control systems that would be stable,

accurate and responsive, resulting in a more optimum design and thus reducing energy consumption. Gartner and Harrison (1963) were the first to develop a model for a straight tube in cross-flow by considering variations in various temperatures along the axis of the tube, treating them in the radial direction. Dynamic equations of the coil, based on energy balance considerations were partial differential equations in space and time which produced complicated transcendental transfer functions which were difficult to use. A number of simplifications of this model were subsequently presented by several researchers (Gartner and Harrison 1965, Gartner and Daane 1969, Gartner 1972, Bhargava et al 1975, Stoecker et al 1978). The resulting first and second order transfer functions agreed favourably with the original transcendental functions (Bhargava et al 1975).

Bhargava et al (1975), presented the six transfer functions that describe the dynamics of a single row heat exchanger (a_i , b_i are constants for the coil in question):

$T_{oa}(s)/\Delta V_w(s)$ Representing the response of the average air outlet temperature to a change in the water velocity:

$$T_{oa}(s)/\Delta V_w(s) = a_1/(1+b_1s) \quad (2.12)$$

$T_{wo}(s)/\Delta V_w(s)$ Representing the response of the water outlet temperature to a change in the water velocity:

$$T_{wo}(s)/\Delta V_w(s) = a_2/(1+b_2s) \quad (2.13)$$

$T_{wo}(s)/T_{wi}(s)$ Representing the response of the water outlet temperature to a change in the water inlet temperature:

$$T_{wo}(s)/T_{wi}(s) = e^{-s} \{ (a_3 + a_4 s) / (b_3 + s) \} \quad (2.14)$$

$T_{oa}(s)/T_{wi}(s)$ Representing the response of the air outlet temperature to a change in the water inlet temperature:

$$T_{oa}(s)/T_{wi}(s) = a_5 / (1 + b_4 s + b_5 s^2) \quad (2.15)$$

$T_{wo}(s)/T_{ia}(s)$ Representing the response of the water outlet temperature to a change in the air inlet temperature:

$$T_{wo}(s)/T_{ia}(s) = a_6 / (1 + b_6 s + b_7 s^2) \quad (2.16)$$

$T_{oa}(s)/T_{ia}(s)$ Representing the response of the outlet air temperature to a change in the inlet air temperature:

$$T_{oa}(s)/T_{ia}(s) = a_7 / (1 + b_8 s) \quad (2.17)$$

Pearson et al (1974), through analysis, experiment and computer simulation, arrived at a first order model describing the outlet air temperature response to changes in water mass flow rate for serpentine cross flow heat exchangers. The model accounts for the fin efficiency, air and water side heat transfer coefficients, parameters that were not included in other models. This model was subsequently improved (Boot et

al 1977) and the time constant and gain of the heat exchanger were presented in an algebraic form. In addition, constraints were imposed on its applicability. This depends on the heat capacity of the fins relative to the heat capacity of the exchanger, since a high value for the fin time constant would dominate the dynamic response characteristic of the coil.

HVAC system simulation programs discussed in the literature make use of a variety of models representing the dynamic characteristics of heating coils. Clark et al (1985), in describing the models used in HVACSIM⁺, use simplified models developed by Gartner and Harrison (1965), while others use either similar simplifications (Hamilton et al 1974, Stoecker et al 1978, Gondal 1987), or empirical relationships (Thompson 1981, Shavit and Brand 1982).

2.2.4 Cooling and dehumidifying coils

The dynamic characteristics of cooling and dehumidifying coils have received much less attention than the dynamic characteristics of heating coils. This stems from the unpredictability of the combined effects of heat and mass transfer. While the sensible heat aspect of a cooling coil can be represented with existing models of heat exchangers, its behaviour during dehumidification is largely uncertain. In studies performed for multi-row cooling and dehumidifying coils (Shekar et al 1970), a number of observations were made:

1. Dry coils showed faster response than wet coils because the dry coil resistance to heat flow is less than that of the wet

coil.

2. The transient response characteristic of humidity ratio in a wet coil was similar to that of the air temperature response. One difference between the two was a time delay in the response of the humidity ratio, of the order of 2 seconds. This was the result of the transition from sensible heat transfer to latent heat transfer. As the coil temperature dropped below the dew point of the air stream, both mass and sensible heat transfer commenced.
3. The transient response of the dry coil model differed slightly from that of the wet coil. It may, therefore, be presumed that the approximation of a wet coil to a dry is satisfactory for practical problems.

Due to the complexity of heat and mass transfer in cooling and dehumidifying, other workers have opted to use empirical relationships based on the steady state characteristics of cooling coils (Miller, 1982). Zhang and Warren (1988) used such steady state relationships to model the sensible gain of a cooling coil based on the air- and water-side effectiveness of the coil, as described in the ASHRAE 1986 Fundamentals (1986), for a counterflow heat exchanger. The time constant in the function was computed on the assumption that the coil was a block of metal and was therefore equal to the product of the heat resistance and capacitance of the coil material.

2.2.5 Control valves

Two types of control valves are widely modelled in the literature reviewed:

1. Linear (or proportional) valves, whose flow characteristic is linear (or proportional).
2. Equal percentage valves whose flow characteristic gives an exponential relationship between the valve stroke and the flow rate.

As a result of the flow characteristics of the two kinds of valves, linear algebraic equations are used to describe the gain (K_v) of the linear valve (Gondal 1987, Shavit and Brandt 1982) and non linear are used to describe the gain of the equal percentage valve (Shavit and Brandt 1982, Miller 1982).

The inherent flow characteristic, which is based on a constant pressure drop across the valve body for a linear valve, is described by the following expression:

$$Q = ky \quad (2.18)$$

where

Q - flow at constant pressure drop

k - constant

y - valve opening

The expression for the inherent flow characteristic of an equal percentage valve is;

$$Q = be^{ay} \quad (2.19)$$

where

Q = flow at constant pressure drop

a and b = constants

y = valve opening

From the above equations the non-linearity of the equal percentage valve is evident. This, however, is misleading in that the installed flow characteristics of the two valves which is influenced considerably by the rest of the pipe circuit, may actually cause the equal percentage valve to exhibit a more linear response than the proportional one. Hamilton et al (1974) observed that while a better response of a discharge air temperature loop was obtained using the linear valve at full load, the use of the same valve for part load performance resulted in instability. An equal percentage valve, however, compensated for the non-linearities present at part load performance resulting in a stable performance of the loop.

Although different equations can be used to relate the flow rate increase per unit valve stem rise, the transfer function representation of the response is:

$$\frac{\Delta m_w(s)}{\Delta y} = \frac{K_v}{1 + \tau_v s} \quad (2.20)$$

where $\Delta m_w(s)$ = mass flow rate variation in s-domain

Δy = change in valve stroke

K_v = valve gain

τ_v = valve time constant

In addition to the time constant, under certain conditions such as lack of a positioner, the actuator of the valve may experience hysteresis, both in linear and equal percentage valves.

2.2.6 Sensors

Sensors are generally modelled as first order transfer functions or differential equations. The differential equation representing a sensor is expressed as follows (Hill 1985, Shavit and Brandt 1982):

$$\frac{dT_s}{dt} = \frac{T_m - T_s}{\tau_s} \quad (2.21)$$

where T_s = sensor output temperature

T_m = measured temperature

τ_s = sensor time constant

The transfer function representation is:

$$G_s(s) = \frac{1}{1 + \tau_s s} \quad (2.22)$$

In cases where the distance of the sensing element is significant, a transport delay can be included in the transfer function.

2.2.7 Controllers

Apart from simple on/off thermostats (which often contain an anticipator), two types of controllers are used extensively in HVAC systems: proportional and proportional plus integral. Proportional controllers are modelled by a simple gain (K_p), while proportional plus

integral are described by the following transfer function (Zhang and Warren 1988):

$$G_{\text{control}}(s) = K_p \left(1 + \frac{1}{\tau_i s} \right) \quad (2.23)$$

The integro-differential equation representation of this controller is

$$C = K_p \cdot \epsilon + K_i \int \epsilon \cdot dt \quad (2.24)$$

where C = controller output

The third mode of control, namely the derivative, is rarely employed because of potential instabilities resulting from apparent rapid changes in temperature induced by, for example, local turbulence.

2.3 HVAC system modelling

Before describing the room models used for HVAC system studies, it is necessary to present the different programs used for studying HVAC systems. Evidently, a significant effort has been made in the modelling of HVAC systems and their components and the computer programs that have been developed may be separated into four categories:

1. Programs such as BESA (CandaPlan Group Inc. 1987) that are used primarily for energy analysis of buildings. These programs contain predefined HVAC systems and utilize the Cooling Load Temperature Difference (CLTD) and Cooling Load Factor (CLF) methods, outlined in the ASHRAE 1986 Fundamentals Handbook, in their cooling load calculations and steady state

calculations for heating loads.

2. Programs that are similar in purpose as the ones mentioned above but which utilize more detailed modelling of the thermal processes. This category includes DOE2 (Curtis et al 1984) and BLAST (Hittle 1979), programs that perform hourly simulation for the calculation of loads and provide predefined systems.
3. Completely modularized programs such as HVACSIM⁺ (Clark, 1985) that allow for variable time steps and can be used to construct an HVAC system and its control from individual components providing the flexibility lacking in the previous two categories.
4. Programs developed by researchers (Zhang and Warren, 1988) in the area of HVAC system dynamics and control which can simulate the system and its controls with time steps of the order of 10's of seconds, that is, the short term dynamics.

Programs such as BESA are intended primarily for energy analysis of buildings and do not have the capability to analyze the dynamic behaviour of the system they are simulating.

Although DOE2 and BLAST are also geared primarily for energy analysis purposes, their capability for simulating the system on an hour by hour basis provides some opportunity to study the effect of a limited range of control strategies such as pre-cooling and pre-heating to shift

the loads and thus reduce peak demands. They cannot, however, account for processes which take place within one hour and are restricted to analysis through simulation, an approach which can be computationally inefficient. Furthermore, these programs are also restricted by the fact that the user has to be content with employing predefined systems, which adversely affects design flexibility, since it is impossible to represent all possible design combinations and control strategies.

Investigation of the dynamic interaction between the building envelope and the HVAC system can be served by a computer program with the flexibility inherent to the modularization and the varying time step found in HVACSIM⁺. The approach HVACSIM⁺ takes in dealing with the problem encountered when trying to simulate components with widely different time constants, such as the building envelope (from several 100's to 1000's of seconds) and a valve (≈ 2 seconds), is to have a user-defined time step for the building envelope while a variable time step is used for the HVAC and control system simulation. In this program, the user can compose a system by selecting individual components and controls. This affords one the flexibility to compare variations of systems and allows for the examination of a large variety of control strategies.

The approach taken by this program, namely, analysis through simulation, results in prohibitively high computational times. As well, HVACSIM⁺ needs a large amount of input data, which, apart from taking up significant time to gather and input to the program, also tends to introduce errors due to improper choices for various parameter values. In addition to these limitations, the detail with which HVACSIM⁺ models the mechanical components, as well as the building, does not mean that it will

produce an accurate simulation. The validation of this program actually produced simulations that introduced errors of up to 2.5°C in zone temperature calculations (Park et al 1989).

Finally, programs developed by other researchers in the area of HVAC system control utilize small time steps (5 sec - 1 min) for the investigation of control system dynamics. However, due to the limits imposed by the size of the time step, these programs can not be used for the study of medium ($1/2$ -3 hours) to long term (3+ hours) effects from the implementation of control strategies. In these cases as well, the simulation approach towards the study of control strategies necessitates considerable computational time and generally requires approximations that can be avoided if frequency domain methods are used.

2.4 Room models

An important component of any HVAC system study is the model describing the thermal behaviour of the building. Such models vary widely in complexity, from simple, first order ones that consider only the air mass and account approximately for the thermal properties of the enclosure (Zhang and Warren 1989) to very detailed ones that describe all modes of heat transfer and that are generally used in programs such as BLAST and DOE2. These so-called detailed building energy analysis programs differ in the way they model the effect of radiation and other thermal effects. A program that handles the coupled radiation-conduction heat transfer in detail is BEEP (Athienitis et al 1986). This frequency domain detailed thermal network program has been compared with TARP (a response factor program which is a research version of BLAST) by Haghghat and Athienitis

(1988).

For the purposes of studying the fundamentals in the dynamic interaction between the HVAC system and the building, there must be an optimization of the model's complexity, such that the building's dynamic and steady state characteristics are reasonably retained while the model's complexity does not interfere with the fundamental studies it is meant to be the basis for. Park et al (1989), in their discussion regarding the validation of HVACSIM⁺, state that "...the most difficult task was the preparation of input data.". Such an extreme approach to detail, i.e. one that poses problems with respect to the definition of the system, causes distraction from the focal point of the research, results in more attention being given to the tool instead of the task and does not guarantee accuracy as is shown by the results of the validation of HVACSIM⁺ (Park et al 1989).

In order to examine the fundamentals behind building dynamics, the model complexity requirements for studies related to the optimization of the HVAC system - building interaction need to be established. By using a model that is detailed enough to produce results that are representative of the dynamic characteristics of buildings, it would be possible to establish a reliable methodology that would lead to a better understanding of these building properties and to improved building systems design and operation.

Room models provide the basis on which the behaviour of HVAC systems is studied. This has to be stressed, since room models are generally regarded as being part of an HVAC system study. This point of view can easily be seen from the different types of room models that exist in the

literature, each adapted to serve a particular HVAC system study.

Building models are used, among other purposes, for:

1. Calculating the energy consumed by HVAC systems such as by DOE2 (Eto and Powel 1985)
2. Studying the air temperature variation for different types of controllers (Mehta,1987) and
3. A combination of the above such as in HVACSIM[†] (Clark 1985).

The emphasis of the uses of building models is on the behaviour of the HVAC system model. It is, however, apparent that whether it is with respect to energy consumption or thermal comfort, HVAC system behaviour depends strongly on the building model's characteristics and therefore, by extension, the HVAC system behaviour depends on the building's characteristics. Consequently, it is imperative that the building dynamics be well understood before trying to study the behaviour of the building with the HVAC system. The result of such an approach would be an HVAC system that works with the building instead of against it in order to optimize the overall performance as dictated by the building's function.

2.5 Relation between HVAC control system and building envelope with respect to energy consumption and thermal comfort

The dynamic control of HVAC systems and its effect on energy consumption and thermal comfort has received limited attention as has the dynamic interaction between the control strategy implemented in HVAC

systems and the building envelope.

Studies related to control have been concentrated on stability studies of the HVAC control systems (Zhang and Warren 1988, Borresen 1981). While extensive research has been conducted in the performance of control systems, the effect this performance has on energy consumption and thermal comfort has not been widely studied. Hamilton et al (1974), explored the performance characteristics of a typical discharge air temperature control system (DATCS) under various loads for heating and attempted to determine the components responsible for the system's poor performance. It was observed that linear valves, while performing satisfactorily at full load conditions, exhibited limit cycle performance at part load, i.e. they were oscillating between the minimum and maximum stroke positions and, as a result, producing oscillating air temperatures. Although the oscillations, according to the authors, were relatively small and therefore would not cause comfort problems, their effect on the equipment might have been detrimental. The problem was eliminated by using a smaller controller gain which, however, caused the system to become sluggish. Equal percentage valves performed well under part load conditions but produced a decaying sinusoidal response at full load. Based on these observations, it was recommended that the above undesirable behaviour could be eliminated if a design criterion were developed, which would be based on the dynamics of the components of the DATCS, to aid the designer in selecting components for the system. This criterion, according to the authors, should predict the nature of the dynamic response of the DATCS. By selecting the components based on this criterion, energy consumption would be minimized. Current practice involves resetting the

water temperature according to the outside temperature. This causes increased flow rate, thus eliminating the undesirable oscillations in the discharge temperature. A better practice would be to reset the water temperature based upon the load. This approach, however, would necessitate extensive knowledge of the system's dynamics and relationship to the thermal response of the building. It would also require a control system approach not unlike the feedforward control used by the process control industry. This control action, i.e. feedforward control, uses information concerning one or more conditions that can disturb the controlled variable and converts it into corrective action to minimize deviations of the controlled variable (Considine, 1985). This implies that all deviations of this variable may be prevented, whereas in feedback control a deviation should exist before the feedback controller takes action.

More research that links control performance with energy consumption and also thermal comfort is presented by Stoecker et al (1978) and by Mehta (1987). Stoecker et al related the throttling range of air temperature controllers to energy consumption and stability. Their study was concentrated on dual duct systems, but the observations and recommendations can be applied to any system that requires simultaneous heating and cooling, such, as reheat systems.

Their research concluded that with a very low gain setting, i.e. large throttling range the extra heating and cooling energy required by the experimental system was appreciable. Reduction of the throttling range, resulted in lower energy consumption. Care, however, had to be taken as the system became unstable at a very low throttling range. The resulting system, with a smaller throttling range, had reduced energy

consumption, while the discharge air temperature was oscillating only between ± 1 degrees Celsius. Mehta (1987) took the findings of Stoecker et al (1978) one step further. In an experimental validation of the dynamic performance of PI controllers, he studied the effect of the magnitude of the throttling range and of the reset time in a PI controller on thermal comfort in addition to energy consumption. The criteria he used for estimating thermal comfort were those proposed by Sprague and McNall (1970) and by Griffiths and McIntyre (1974). Based on their models for thermal comfort, analytical and experimental results, the following conclusions were drawn:

1. The reset time (τ_1) should not exceed 131 minutes if the thermal comfort criteria are to be satisfied. This was based on the findings of Sprague and McNall (1970) and Griffiths and McIntyre (1974). According to studies performed by Sprague and McNall (1970), no serious occupancy complaints would occur if

$$\Delta T^2 * CPH \leq 4.63 \quad (2.25)$$

where ΔT = peak-to-peak amplitude of the
temperature fluctuation

CPH = cycling frequency (cycles per hour)

Griffiths and McIntyre (1974) recommended a maximum deviation of ± 2.25 °C from the mean comfort temperature for minimum discomfort conditions. Mehta (1987) using these two recommendations arrived to the maximum reset time value of 131 min as follows:

$$CPH = \frac{4.63}{(4.50)^2} = 0.2286$$

$$r_{\max} = \frac{60}{2 * 0.2286} = 131 \text{ minutes/repeat}$$

2. PI controllers would result in reduced energy consumption if they were operated with higher reset times under full heating load and when heating demand increases (negative offsets) and with lower reset times under part load and when heating demand decreases (positive offsets). The reverse was true for cooling, an application possibility for adaptive control techniques to HVAC system operation.

The way to achieve the above conditions is through the use of a programmable controller. The problem encountered by this proposition is that the rate of change of the throttling range and other parameters required to achieve changes in the reset time (which would result in lower energy consumption) has to be established. This points to the requirement of knowledge about the system and building dynamics so that modelling of their interaction could be used to manipulate system parameters, such as reset times, to achieve an optimum system performance.

Reduction of energy consumption, however, does not only result from single, closed loop control performance considerations but also from open loop or steering control. This approach can be seen as supervisory control strategies that dictate the operation of the whole HVAC system with consideration given to the performance of its individual components. Before attempting to discuss supervisory control strategies, the response of the building to changes in loads and/or setpoints needs to be

understood. More effort is needed in this area to extend the work already done in projects commissioned by ASHRAE related to the dynamic operation of HVAC systems in buildings (321-RP,409-RP,539-RP), to cover the interactions of these systems with the thermal response of buildings.

There has been limited research into the response of buildings to changes in conditions which would provide the knowledge to put the building's thermal mass into effective use. The basic feature of the building's response to changing outside conditions is the delay introduced by the building storage mass. Zmeareanu et al (1987) used the variation of the room air temperature (no solar radiation, no infiltration and no internal mass present) in response to a step-function change of the outdoor temperature to compare an analytical solution developed by Pratt (1981) to a computer simulation. His results indicated that a delay of about 3 hours occurs before the step-function change starts to affect the room air temperature. The delay is comparable to the results obtained by Athienitis (1988) in his study of a predictive control strategy. A detailed room model was used, the parameters of which differed from that of Zmeareanu et al, to study the effect of different set-point profiles on energy consumption and temperature swings for three different days. The base case of the study considered an outdoor mean temperature of -15°C with a range of $\pm 8^{\circ}\text{C}$ and a constant set-point. In this case, which is currently of interest, the effect of the peak solar gains, at solar noon, affected the room air temperature 3 to $3\frac{1}{2}$ hours later. Both of these studies provide the evidence that buildings with some thermal mass introduce a substantial delay in the effect a change in outdoor conditions has on the room air temperature.

Athienitis (1988) also used a predictive control strategy to make use of the thermal mass of a room. His findings point to the advantages of using the building mass as a thermal reservoir and the effect this has on limiting equipment sizes.

Finally, Ngan (1985) used a weather predictor together with a first order room model to control a simple HVAC system in a test hut. Based on the thermal properties of the hut and the expected weather conditions, the hut was precooled or preheated in advance making use of cooler outside air and internal gains respectively, thus lowering the energy consumption of the system.

As was previously mentioned, knowledge of the thermal response of a building can lead to improved design and operating procedures. This improvement, however, has to be done in conjunction with a control system that uses this knowledge to integrate both the building and the HVAC system dynamics into a single operating system. Ngan (1985) attempted to accomplish this but only with respect to where free energy was available, thus excluding a wider application of the predictive or feedforward control system. Instead, the conventional feedback control system was used to maintain the desired room temperature, with the predictive control system in use only where precooling or preheating was required.

2.6 Discussion

Traditionally, HVAC control has been based on steady-state strategies, which means that the HVAC system reacts with the heat flow

necessary to counteract the sum of gains or losses in the building. Although effective in maintaining a constant temperature set-point, this approach is not able to respond properly to rapid changes in indoor or outdoor conditions which often prevent the system from attaining the required stable conditions. Furthermore, it does not take full advantage of the microprocessor based control system approach which is used extensively by the process control industry.

This started changing with the advent of Direct Digital Controllers (DDC). Their flexibility over the traditional pneumatic controllers is unquestionable but their effective application has been hampered by the fact that they are implemented, not in innovative ways but in accordance with guidelines passed on from the traditional pneumatic controls. As such, many Energy Management and Control Systems (EMCS) combine steady-state control with "add-on" energy reduction strategies which frequently work counter to each other, resulting in routines too complicated to understand and monitor effectively, and which contribute neither to efficiency nor to comfort (Hartman 1988).

Traditional control seeks to maintain the steady state balance of heat flows through stable control of HVAC equipment, most likely at part-load conditions. Consequently, the equipment operates at less than its rated performance and may be less efficient than it could be. Dynamic control, on the other hand, seeks to intelligently manage the disequilibrium and optimize the operation of the system so that it acts in accordance with the prevailing loads and requirements. A deciding

factor in the success of dynamic control strategies is the use of the building's thermal mass to achieve the desired system performance.

In designing the HVAC system and its controls, the engineer bases the estimation of loads and sizes of equipment on design days, days that occur for less than 10% of the year. This means that both the HVAC system and its (steady-state) control strategies operate for most of the time under conditions for which they are not designed. The successful design of HVAC systems and their controls depends heavily on the understanding that the HVAC system is not an "add-on" to the building, but rather an integral part of it. This understanding is vital in that dynamic control strategies should seek to manipulate the building's thermal storage capacity to extract heating and cooling energy, thus lowering the peak demands which would consequently result in smaller equipment sizes. It would therefore be more effective if the design of the HVAC system were based not only on design days but also on the average conditions. By giving consideration to dynamic control strategies at the design stage, use is made of the thermal storage mass to provide the required energy in the cases where extraordinary conditions exist, thus providing indoor conditions that are within the constraints imposed by thermal comfort considerations, without the energy consumption that would otherwise be required.

To arrive at dynamic control strategies that would successfully employ the thermal mass of the building knowledge regarding the dynamic interaction of this mass with the air temperature is required. By

exploiting this knowledge, apart from establishing effective dynamic control strategies, improved control system approaches can be introduced which would allow for more efficient system operation and improved thermal comfort. Feedforward control is such an approach which can be used extensively, provided that the behaviour of both the building and its HVAC system are well known.

CHAPTER 3

COMPARISON OF ROOM MODELS FOR BUILDING OPERATION DYNAMIC STUDIES AND THE EFFECT OF ENVELOPE AND AIR MASS

3.1 Introduction

The complexity of a room model has been shown to have a significant influence on the type of study such a model can be used for (Borresen 1981). In order to examine the fundamentals behind building dynamics, it is necessary to establish the model complexity requirements that are needed to study the dynamic interaction between the building and the HVAC system. By using a model that is detailed enough to produce results that are representative of the dynamic characteristics of buildings, it will be possible to establish a reliable methodology that will lead to a better understanding of these building properties and to improved building systems design and operation.

In addition, it is necessary to establish a methodology that can be used in recognizing and exploiting the short and long term characteristics of buildings for improved thermal comfort and energy savings.

This separation into short (periods of about 15 min.) and long (periods in excess of 3 hours) term dynamics, is the result of the interaction of the air mass and the envelope mass in their response to disturbances. The air mass reacts faster to disturbances with higher frequencies and is therefore associated with short term dynamics, and the envelope mass, by virtue of its high thermal capacitance, reacts to

disturbances with lower frequencies at which frequencies the air mass is almost at steady state. Therefore, the time scales at which the separation affects the system, whether at the local loop level or at the control strategy level, have to be established so that the full potential of the building envelope mass can be achieved.

3.2 Room models

To reach this point, the study has to begin at a fundamental level. However, the model that satisfies the fundamental nature of the analysis must do so without compromising realism.

Borresen (1981) attempted to categorize models according to how well they simulated short term dynamics i.e. with periods of the order of up to 10-15 minutes, and long term dynamics i.e. with periods greater than 3 hours up to steady state. The simplification level reflected this classification by having four models of increasing detail:

Model I: This simplest of the four models focused on short term dynamics and was first order. It completely ignored the thermal properties of the envelope (both steady state and transient) and considered only the response resulting from the thermal dynamics of the room air mass which was treated as a lumped element.

Model II: In addition to the properties of Model I, Model II included the steady state characteristics of the envelope resulting in accurate steady state conditions while the first order nature of model I was retained.

Model III: This model was a modified version of model II with similar characteristics.

Model IV: This was the most detailed of the four models. It was a second order model that, in addition to the properties already described, accounted for the transient nature of heat conduction through the walls by modelling them as lumped elements.

By submitting each of the models to a step change in the supply air temperature, Borresen studied the response of each model according to its performance with respect to short term dynamics and steady state. He concluded that,

- (a) model I is adequate for short term response analysis in the area of 0.5 to 10 minutes,
- (b) model II produces reasonable results only for short term and steady state,
- (c) model III results are reasonable for short term and to some extent long term responses,
- (d) model IV results are the most accurate, but because this model will reach steady state very slowly, it would be preferable to use model II for analyzing dynamic control loops without great loss of accuracy and
- (e) using model I or model II for adjusting controllers will give conservative values for control parameters.

The conclusions drawn from the study were related to room air temperature control analysis and simulation. As such, they provide little information about the models' characteristics as they relate to dynamic control strategies, but centre instead on the air temperature responses to step changes in supply air temperature, restricting the applicability of the results to these types of studies only.

3.2.1 Description of room models

To establish the model complexity required for realistic building dynamic studies, two models that are studied by Borresen (1981) and used widely by others (Thompson 1981) are compared to a model which, although simple in all other respects, describes in detail the distributed nature of a massive element (the floor) present in the room. The massive element is represented by the Norton equivalent (Athienitis et al 1986) of the sub-network for each of the three models. Figure 3.1 shows the schematic of the room considered, figure 3.2 shows the network equivalent to it and table 3.1 indicates the room dimensions and material characteristics.

Model 1: This type of model is used extensively in studies of short term dynamics. Figure 3.3 shows that only the steady state characteristics of the floor are considered. It is similar to Borresen's model II and is described by equation (3.1).

$$C_a \frac{dT_{ai}}{dt} = UT(T_b - T_{ai}) + UO(T_0 - T_{ai}) \quad (3.1)$$

where

$$UT = \left(\frac{1}{U_{FT}} + \frac{1}{U_{FK}} + \frac{1}{U_{FA}} \right)^{-1}$$

Model 2: Used extensively in studies involving both short and long term dynamics (Thompson 1981), its representation of the floor subnetwork is shown in figure 3.4; transient thermal properties are modelled, with the massive element (the floor) modelled as a separate lumped capacitance. It is similar to Borresen's model IV with similar steady state thermal properties to model 1 and is described by equations (3.2) and (3.3).

$$C_a \frac{dT_{ai}}{dt} = UO(T_0 - T_{ai}) + UKA(T_f - T_{ai}) \quad (3.2)$$

$$C_f \frac{dT_f}{dt} = UFT(T_b - T_f) + UKA(T_{ai} - T_f) \quad (3.3)$$

where

$$UKA = \left(\frac{1}{UFK} + \frac{1}{UFA} \right)^{-1}$$

The Norton equivalent of the sub-network representing the floor for model 2 needs to be found first and the self and transfer admittances (Y_{11} and Y_{12} respectively), to be defined. The formulation used for model 2 can be used for model 1, since it is the same as model 2 with the capacitance representing the floor mass equal to zero. Figure 3.5 shows the part of the circuit representing the floor mass. The conductances UFT and UFK as well as the floor capacitance C_f are represented by phasors as their equivalent impedances. The Norton equivalent is found by first setting the temperature source (T_b) to zero and calculating the equivalent

Table 3.1 Room model data

<u>DIMENSIONS</u>				
Room Depth	: 6.71 m	Window	Height	: 1.93 m
	Height		Width	: 5.74 m
	Width			
	: 7.32 m			
<u>MATERIAL PROPERTIES</u>				
R-values				
	Window	:	0.4	m ² °C/W
	Walls and ceiling	:	3.5	m ² °C/W
	Floor	:	1	m ² °C/W
	Thickness	Density	Conduct.	Specific Heat
	(m)	(kg/m ³)	(W/m°C)	(J/kg°C)
Gypsum Board	0.013	750	0.16	800
Concrete	0.042	2100	1.7	800

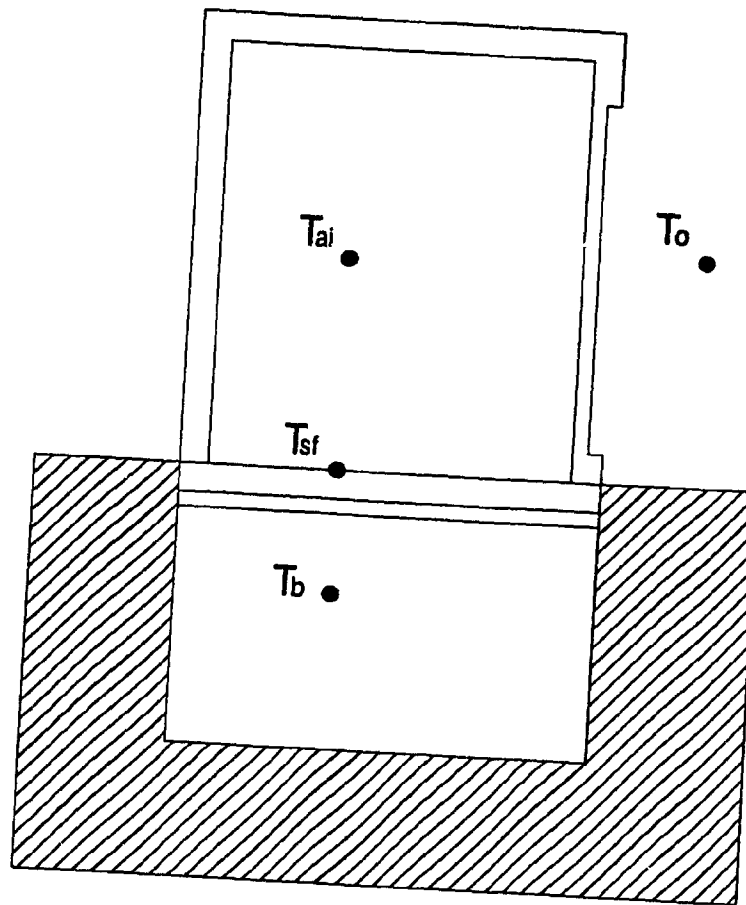


Figure 3.1 Schematic of room used in study

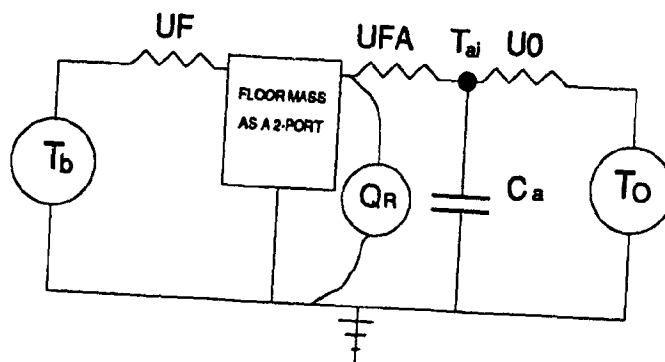


Figure 3.2 Network analog of room

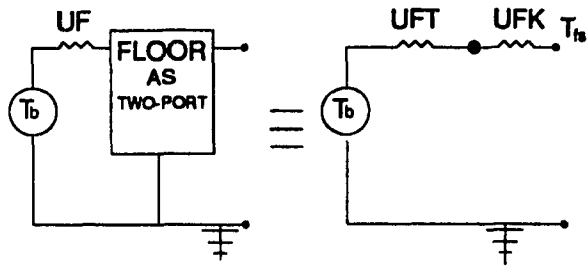


Figure 3.3 Model 1 representation of the floor

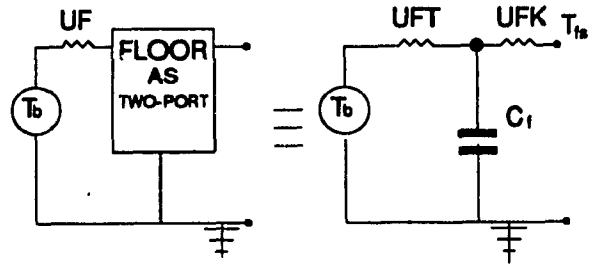


Figure 3.4 Model 2 representation of the floor

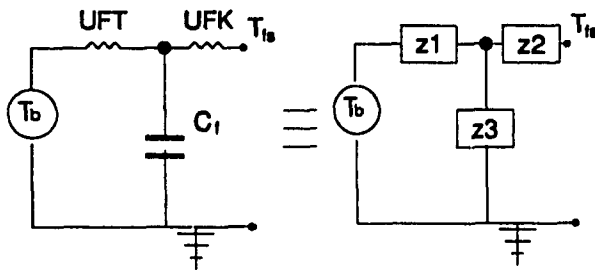


Figure 3.5 Network representation of model 2

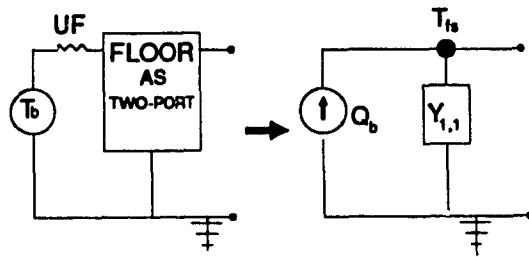


Figure 3.6 Norton equivalent for the floor sub-network

impedance of the circuit which is defined by :

$$z_1 = 1/UFT \quad (3.4)$$

$$z_2 = 1/UFK \quad (3.5)$$

$$z_3 = 1/C_f s \quad (3.6)$$

therefore

$$z = z_3 + ((1/z_1) + (1/z_2))^{-1} \quad (3.7)$$

$$\text{therefore} \quad Y_{11} = 1/z \quad (3.8)$$

The second step is to short circuit the circuit in figure 3.5, which results in the one shown in figure 3.7, and to calculate the equivalent temperature source Q_b .

$$z_1 i_1 + z_2 (i_1 - i_{sc}) = T \quad (3.9)$$

$$z_3 i_{sc} - z_2 (i_1 - i_{sc}) = 0 \quad (3.10)$$

$$\text{therefore} \quad i_1 = (z_3 i_{sc} + z_2 i_{sc}) / z_2 \quad (3.11)$$

solving for i_{sc} we get

$$i_{sc} = T_b / (((z_1/z_2) * (z_3 + z_2)) + (z_2 * (((z_3 + z_2)/z_2) - 1))) \quad (3.12)$$

$$\text{therefore} \quad Y_{12} = (((z_1/z_2) * (z_3 + z_2)) + (z_2 * (((z_3 + z_2)/z_2) - 1)))^{-1} \quad (3.13)$$

Therefore figure 3.4 reduces to figure 3.6 with

$$Q_b = T_b Y_{12} \quad (3.14)$$

Model 3: The only difference between model 2 and this one is the description of the massive element. While model 2 describes this mass as a lumped element, model 3 describes it as a distributed element. To describe how the distributed nature of the model is derived it is necessary to start with the basics. Consider figure 3.8; the equation (Carslaw and Jaeger, 1959) describing the heat transfer through the slab is:

$$\alpha * (\delta^2 T / \delta x^2) = \delta T / \delta t \quad (3.15)$$

or in the Laplace domain:

$$\alpha \left(\frac{\partial^2 T}{\partial x^2} \right) = sT \quad (3.16)$$

Solving for $T(x)$ and treating s as a constant

$$T(x,s) = c_1 e^{\gamma x} + c_2 e^{-\gamma x} \quad (3.17)$$

where $\gamma = \sqrt{(s/\alpha)}$

Rewriting:

$$T(x,s) = M \cosh \gamma x + N \sinh \gamma x \quad (3.18)$$

$$\text{since } q' = -k \frac{dT}{dx} \quad (3.19)$$

then

$$q'(x,s) = -M \gamma \sinh \gamma x - N \gamma \cosh \gamma x \quad (3.20)$$

therefore at each surface

$$T_1(x=0, s) = M \quad (3.21)$$

$$q'_1(x=0, s) = -N \gamma \quad (3.22)$$

$$T_2(x=L, s) = M \cosh \gamma L + N \sinh \gamma L \quad (3.23)$$

$$q'_2(x=L, s) = -M \gamma \sinh \gamma L - N \gamma \cosh \gamma L \quad (3.24)$$

or in matrix form (Athienitis, 1986):

$$\begin{bmatrix} T_1 \\ q_1 \end{bmatrix} = \begin{bmatrix} \cosh(\gamma L) & (\sinh(\gamma L))/k\gamma \\ k\gamma \sinh(\gamma L) & \cosh(\gamma L) \end{bmatrix} \begin{bmatrix} T_2 \\ -q_2 \end{bmatrix} \quad (3.25)$$

This is the two port cascade matrix representing the behaviour of the slab. Since, however, there exists an insulation layer beneath the floor and above the basement, this matrix has to be multiplied by the insulation cascade matrix giving:

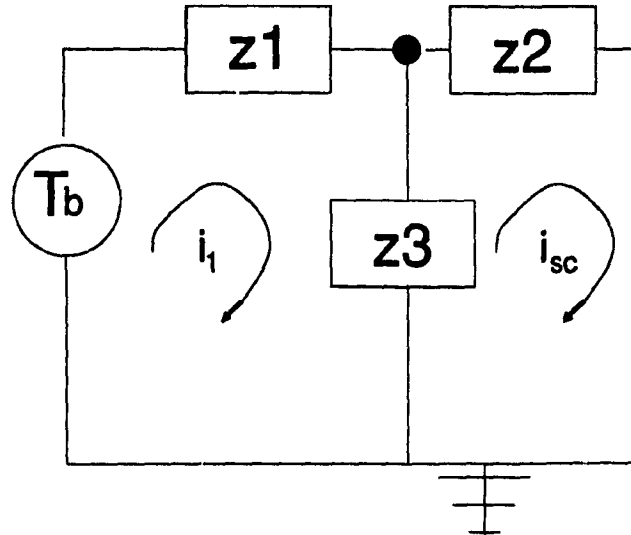


Figure 3.7 Calculating the Norton equivalent for model 2

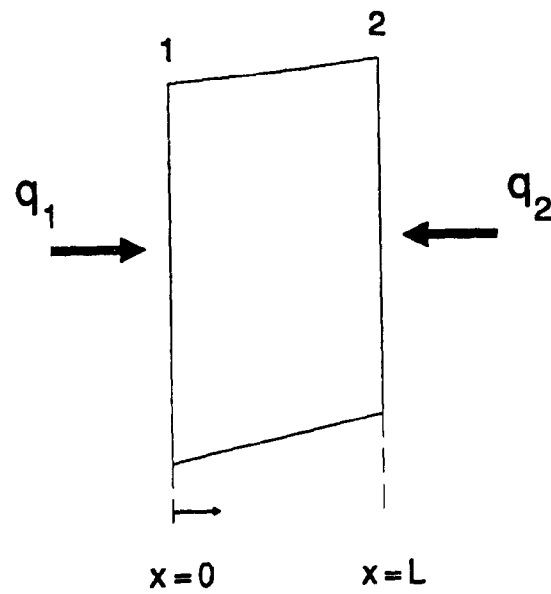


Figure 3.8 Schematic of the slab

$$\begin{bmatrix} T_1 \\ q_1' \end{bmatrix} = \begin{bmatrix} A & B \\ C & D \end{bmatrix} \begin{bmatrix} 1 & 1/u \\ 0 & 1 \end{bmatrix} \begin{bmatrix} T_2 \\ -q_2' \end{bmatrix} \quad (3.26)$$

In a similar manner as with model 1, Y_{11} and Y_{12} are calculated using the Norton equivalent of the floor subnetwork (Athienitis et al, 1987).

Therefore setting T_2 to zero Y_{11} is defined by

$$Y_{11} = q_1/T_1 = A_f q_1'/T_1 \quad (3.27)$$

$$Y_{11} = (U_f + A_f k \gamma \tanh(\gamma L)) / ((U_f / (k \gamma A_f)) \tanh(\gamma L) + 1) \quad (3.28)$$

and Y_{12} is defined by setting $T_1 = 0$

$$Y_{12} = q_1/T_2 = A_f q_1'/T_2 \quad (3.29)$$

$$Y_{12} = A_f / ((A_f / U_f) \cosh(\gamma L) + (1/\gamma k) \sinh(\gamma L)) \quad (3.30)$$

To facilitate the mathematical description of the models, the nodal formulation is used, i.e. the heat flows are balanced at each of the two nodes considered: the air node (node 1) and the floor surface node (node 2). The formulation for a model with N nodes (Athienitis et al, 1987) is as follows :

$$[Y]_{N \times N} [T]_N = [Q]_N \quad (3.31)$$

where [Y] = Admittance Matrix
 [T] = Temperature Matrix
 [Q] = Source or Input Matrix

The input matrix [Q] is made up of actual sources acting at nodes 1 to N (e.g. solar radiation, internal gains) plus the equivalent sources obtained from the application of the Norton theorem. The nodal admittance matrix [Y] is automatically formulated by inspection of the network and is of size NxN. A diagonal entry Y(i,i) is equal to the sum of the component admittances connected to node i, while an off diagonal entry Y(i,j) is given by the sum of component admittances connected between nodes i and j, multiplied by -1 (Athienitis et al, 1987).

In the case of the network in figure 3.2 the admittance matrix is therefore:

$$[Y] = \begin{bmatrix} C_a s + U_0 + U_{FA} & -U_{FA} \\ -U_{FA} & Y_{11} + U_{FA} \end{bmatrix} \quad (3.32)$$

Rearranging, the relation between the input and the resulting temperature is therefore:

$$[T]_N = [Y]_{N \times N}^{-1} [Q] \quad (3.33)$$

The inverse of the admittance matrix being the impedance matrix [Z], the temperature at node i can be found as follows:

$$T(i) = \sum Z(i, j) * Q(j) \quad (3.34)$$

which implies that

$$Z(i, j) = \left[\frac{T(i)}{Q(j)} \right]_{\text{All other sources}=0} \quad (3.35)$$

where $Z(i, j)$ can be found as:

$$\frac{1}{(Y_{11} + UFA)(C_a s + UO + UFA) - (UFA)^2} \begin{bmatrix} Y_{11} + UFA & UFA \\ UFA & C_a s + UO + UFA \end{bmatrix} \quad (3.36)$$

From the above mathematical representation, the impedance $Z(i, j)$, is defined as the function that relates the effect of a source, Q , acting at node j , on the temperature of node i . Since there are only two nodes in each of the three models considered, there are two impedance transfer functions affecting the behaviour of the air temperature. These are, **Z(1,1)** which relates the effect of a source, acting at the air node, on the air node temperature. This can be viewed as the function that relates the effect that changes in air supply temperature have on the room air temperature. The equation expressing this function is therefore:

$$Z(1,1) = \frac{Y_{11} + UFA}{(Y_{11} + UFA)(C_a s + UO + UFA) - (UFA)^2} \quad (3.37)$$

Z(1,2) which relates the effect of a source acting at the floor surface (node 2), on the air node temperature. This can be viewed as the function that relates changes in radiation incident on the floor surface, to the room air temperature fluctuations. $Z(1,2)$ is therefore:

$$Z(1,2) = \frac{UFA}{(Y_{11}+UFA)(C_a s+U0+UFA)-(UFA)^2} \quad (3.38)$$

These two functions are strongly influenced by the degree of modelling used and their study will not only indicate excessive modelling approximation, but also provide insights into the behaviour of actual buildings.

3.2.2 Comparison of model 3 to a detailed model

In spite of the detail with which model 3 represents the massive element, the approximate way of describing long wave interchange between the surfaces raises questions as to its ability to give a realistic picture of the building's behaviour and thus be used as the standard against which the other two models are to be judged. Having this in mind, it was decided to check its validity by comparing $Z(1,1)$ and $Z(1,2)$ calculated using model 3 and using a validated model. The model used for comparison has been validated using actual data (Athienitis et al, 1987), and describes in detail the thermal dynamics of buildings, with all walls being modelled as distributed elements and the radiant exchange factors calculated in detail. For comparison purposes, the mass of the room was also considered to be on the floor while a lumped element represented the room air mass. Table 3.2 compares $Z(1,1)$ of each model which incidentally has the same meaning in both, that is, the impedance of the room as seen from the air point, while table 3.3 compares the impedance of the floor surface with respect to the air, denoted here as $Z(1,2)$ but $Z(1,7)$ in the

detailed model.

Both tables show very close values for both impedances, a factor that allows the use of model 3 as a standard against which to compare the other two models. It is important to note that while in all other respects model 3 is simple, it is detailed with respect to the modelling of the mass. The complexity of such a model is thus kept within reasonable limits, in that it allows fundamental types of studies to be performed without compromising realism.

3.3 Nyquist and Bode plots

To compare and study $Z(1,1)$ and $Z(1,2)$ for each of the three models, their frequency response was calculated and plotted on two types of plots widely used for dynamic and control systems analysis: the Nyquist and Bode plots.

Both sets of diagrams provide information over a frequency range for each transfer function, called the frequency response of the function. This response is represented by a complex number of the form $a+jb$ which provides information regarding the magnitude ($|Z(i,j)| = (a^2+b^2)^{1/2}$) and phase angle ($\phi = \tan^{-1}(b/a)$) associated with the transfer function at that particular frequency. The magnitude of the transfer function is the amplitude ratio of the output over the input, while the phase angle may be interpreted as the angle by which the output lags the input. As will be explained later, the phase lag imparted by the transfer function to the input can also be expressed as the time delay of that input at particular frequencies. The approach is only valid if the transfer functions ($Z(1,1)$ and $Z(1,2)$ in this study) can be approximated to be linear functions for

Table 3.2 Comparison of Z(1,1) computed using model 3 and using the detailed model

FREQUENCY (Cyc./day)	PERIOD (sec)	DETAILED MODEL			MODEL 3			DIFFERENCE (z)
		REAL (W/K)	IMAGINARY (W/K)	MAGNITUDE (W/K)	REAL (W/K)	IMAGINARY (W/K)	MAGNITUDE (W/K)	
1	86400	0.003636	-0.00277	0.004576	0.003217	-0.00288	0.004320	5.589068
2	43200	0.002916	-0.00163	0.003343	0.002517	-0.00164	0.003007	10.04195
3	28800	0.002758	-0.00123	0.003022	0.002368	-0.00120	0.002658	12.00778
4	21600	0.002690	-0.00106	0.002892	0.002307	-0.00101	0.002519	12.80366
6	14400	0.002608	-0.00095	0.002778	0.002242	-0.00086	0.002402	13.54390
8	10800	0.002537	-0.00096	0.002715	0.002190	-0.00083	0.002345	13.63828
9	9600	0.002499	-0.00098	0.002688	0.002163	-0.00084	0.002322	13.59867
STEADY STATE Z(1,1):				0.011066			0.011590	-4.74319

Table 3.3 Comparison of Z(1,2) computed using model 3 and the detailed model

FREQUENCY (Cyc./day)	PERIOD (sec)	DETAILED MODEL			MODEL3			DIFFERENCE (z)
		REAL (W/K)	IMAGINARY (W/K)	MAGNITUDE (W/K)	REAL (W/K)	IMAGINARY (W/K)	MAGNITUDE (W/K)	
1	86400	0.001140	-0.00301	0.003224	0.001107	-0.00311	0.003305	-2.51918
2	43200	0.000344	-0.00165	0.001691	0.000341	-0.00169	0.001724	-1.93892
3	28800	0.000179	-0.00112	0.001142	0.000185	-0.00114	0.001163	-1.86063
4	21600	0.000120	-0.00085	0.000864	0.000128	-0.00087	0.000880	-1.88010
6	14400	0.000076	-0.00058	0.000585	0.000087	-0.00059	0.000597	-2.02770
8	10800	0.000058	-0.00044	0.000447	0.000070	-0.00045	0.000457	-2.26069
9	9600	0.000053	-0.00039	0.000402	0.000065	-0.00040	0.000411	-2.40193
STEADY STATE Z(1,2):				0.009428			0.010330	-9.56737

the frequencies considered.

The Bode plots used for this study consist of a pair of diagrams showing:

1. How the logarithm of the magnitude ratio (MR) of the function varies with the logarithm of the frequency (ω cycles per day), where magnitude ratio is the ratio of the function magnitude at a particular frequency to the steady state value, and
2. How the phase angle (ϕ°) of the function varies with the logarithm of the frequency.

A Nyquist plot is an alternate representation of the frequency response characteristics of system transfer functions. It uses the real and imaginary parts of the response as abscissa and ordinate and plots the value of the response a distance $|Z(i,j)|$ from the origin at an angle ϕ° from the real axis. In effect, a Nyquist plot provides the information present in both Bode plots but from a different point of view.

The combination of both sets of diagrams will be used to first compare the models and subsequently provide information on the dynamics of buildings that can be used for developing efficient HVAC system operation algorithms that effectively utilize the building's thermal mass to improve overall performance.

3.4 Frequency response differences among models

The frequency responses of the functions $Z(1,1)$ and $Z(1,2)$ for models whose massive element (the floor) was considered to be concrete

were calculated for frequencies of up to 8640 cycles per day and were plotted in accordance with the previously described Bode and Nyquist plots.

The plots for $Z(1,1)$ for each model, figures 3.10-3.18, show that the diagrams for the frequency response of $Z(1,1)$ for model 2 (figures 3.10,3.11,3.12) and model 3 (figures 3.13,3.14,3.15), the models that account for the transient nature of heat conduction, are almost identical. The plot of the percentage magnitude difference between the two (figure 3.16), shows a maximum difference of 2.7 % at about 16 cycles per day (Period = 5550 sec). The similarities, however, do not extend to model 1. The shapes of the Nyquist (figure 3.17) and Bode (figures 3.18,3.19) plots of model 1 are radically different from those of both models 2 and 3, the differences resulting from the first order nature of model 1. The magnitude difference of the frequency response between models 1 and 3 is less than 10% for frequencies that exceed 90 cycles per day (or periods of 960 sec), the phase lag difference at this frequency being 18° . This implies that for disturbances with frequencies lower than 90 cycles per day, model 1 will predict an effect on the air temperature, the magnitude of which would be as if the disturbance were at least 1.1 times greater and 18° (or 48 sec) ahead than if the more accurate model 3 were used. Consider, for example, a study of oscillations of the air supply temperature whose frequency is, say, 90 cycles per day. If model 1 were used and the supply air temperature oscillations had an amplitude of $\theta^\circ\text{C}$, the predicted effect on the room air temperature would be the same as the effect predicted by the more accurate model 3 with a disturbance whose amplitude was $1.1*\theta^\circ\text{C}$ and which started 48 sec earlier. An example of the

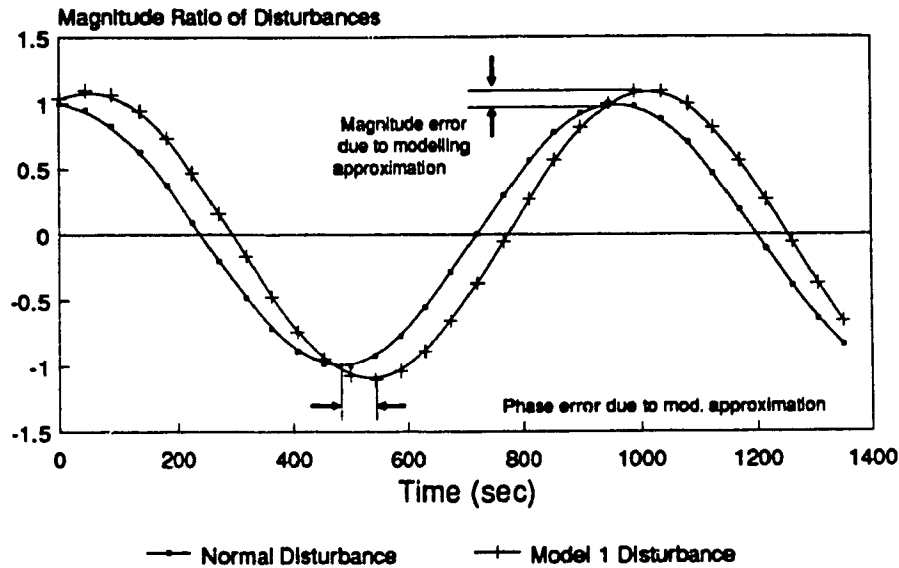


Figure 3.9 Example of Magnitude and Phase difference

nature of the difference is shown in figure 3.9. Although this error might seem minor at first, its significance becomes apparent when the throttling range and reset times are to be sized, based on this model.

The differences between the models regarding impedance $Z(1,2)$ are quite different from those of $Z(1,1)$. This is manifested primarily in the fact that the maximum deviations of model 2 from model 3 occur for frequencies in excess of 14.76 cycles per day, or for periods less than 6000 sec (figure 3.21), while the response from model 1 agrees reasonably only when steady state is encountered (figure 3.22). The deviation is best observed when the Bode plots of the three models for the frequency response of $Z(1,2)$ are compared (figures 3.23-3.28). The significance of this lies in the frequencies at which the maximum errors occur: the

frequencies that are generally associated with local loop control and short term dynamics. If disturbances of high frequency from radiative sources were considered, their effect on the air temperature would be greatly miscalculated unless model 3 were used. It should be noted, however, that the magnitude of $Z(1,2)$ is lesser than the magnitude of $Z(1,1)$ and therefore disturbances at node 2 have to be relatively large in amplitude to significantly contribute to the effect at the air node, especially if node 1 is also experiencing disturbances.

3.5 Discussion

It is apparent from the studies performed here that using simple models in studies without verifying their applicability may lead to significant errors. This was demonstrated conclusively here through the frequency response study which revealed the deficiencies of models 1 and 2 with respect to floor mass-air temperature relationship.

Finally, the comparison of model 3 with a detailed, verified, model produced results that allow its use in dynamic control studies which, by their nature, require reliable modelling of the relationship between mass and air.

3.6 Effect of envelope and air mass on building operation dynamics

The preceding discussion on the differences in frequency response between the three models provide, in an indirect way, some insights into the influence the presence of a massive element has on the air temperature variation in response to disturbances at the air and floor surface nodes. To gain more information regarding this interaction, $Z(1,1)$ and $Z(1,2)$ for

models 1,2 and 3 were calculated again, but instead of concrete, the material considered was gypsum board, a material of lower conductivity and thermal capacitance.

The variations of $Z(1,1)$ and $Z(1,2)$ for these three models are not unlike the results from the models with the concrete element, i.e.:

1. Very good correlation between $Z(1,1)$ of model 2_G (G for gypsum board) and model 3_G , with a maximum magnitude difference of 4.7 % for disturbances with frequencies of about 34 cycles per day (figure 3.29).
2. The magnitude of model 1_G produces an error with respect to model 3_G excess of 10% if the disturbances at node 1 have frequencies lower than 96 cycles per day (figure 3.30).

In addition, the magnitude error for $Z(1,2)$ of model 2_G with respect to model 3_G was in excess of 10 % for disturbances at node 2 of frequencies greater than 60 cycles per day (figure 3.31) in a manner similar to models with the concrete element.

3.6.1 Frequency response study for short and long term dynamics

The purpose of this section is the establishment of a methodology in recognizing the short and long term thermal characteristics of buildings for improved thermal comfort and energy savings.

It is generally acknowledged that in this respect, short term dynamics involve changes associated with local loop control, which implies

frequencies of greater than 96 cycles per day (periods of about 15 min.). Long term dynamics, on the other hand, involve changes related with control strategies which are associated with frequencies lower than 8 cycles per day (periods longer than 3 hours).

This separation is the result of the interaction of the air mass and the envelope mass in their response to disturbances, with the air mass reacting faster to higher frequencies and therefore associated with short term dynamics and the envelope mass dominating the dynamics at lower frequencies (long term dynamics).

Such a separation is immediately evident upon studying the Nyquist plot of $Z(1,1)$ for model 3_c (C for concrete) in figure 3.13, with the small cusp representing the short term dynamics and the larger one that of the long term dynamics. The minimum of the small cusp occurs for frequencies of about 36 cycles/day (period=2390 sec), while the depression separating the small and large cusps occurs at frequencies of about 8 cycles/day (period=10800 sec). This separation can also be seen clearly on the variation of the magnitude ratio with respect to frequency in the Bode plot of the model in figure 3.12. The shape of the magnitude ratio is associated with the existence of this separation. The two stages in the increase of the magnitude of the impedance present represent the two types of dynamics associated with the building, the first steep rise in the magnitude ratio occurs at frequencies closely associated with the first cusp of the Nyquist plot, that is, frequencies greater than 36 cycles per day. For these frequencies, the air mass dominates the frequency response of the impedance and is associated with short term dynamics. Long term dynamics are associated with the second step increase in impedance

magnitude ratio and consequently, with the second cusp in the Nyquist plot. This behaviour is related to disturbances with frequencies lower than 6 cycles per day and is dominated by the dynamics of the concrete mass. Disturbances with frequencies between 6 and 36 cycles per day are influenced by both the thermal behaviour of the air mass and of the concrete in degrees proportional approximately to how close they are to each end of the spectrum.

On the other hand, the Nyquist (figure 3.32) and Bode (figures 3.33, 3.34) plots for $Z(1,1)$ of model 3_G show only a slight indication of the existence of such a separation. This is indicative of the extent of the coupling of the gypsum board with the air mass. Plots of $Z(1,1)$ for model 3_G and model 1_G compared to plots for model 3_C and model 1_C show the effect of the higher thermal capacitance of the concrete, while for disturbances with frequencies of less than 36.15 cycles per day both gypsum and concrete produce responses of similar magnitude ratio, gypsum board reaches the steady state value at much higher frequencies than the concrete, in a manner not unlike the air mass would if no mass were present.

The dynamics of $Z(1,2)$ for both models do not display any obvious separation between the short and long term. From the Nyquist plots (figures 3.35, 3.36) it can be seen that the models behave as second order systems, even though, since they contain distributed elements, they are of infinite order. This lack of clear separation in high and low frequency behaviour is the result of two quite opposite effects. On the one hand, the coupling of the gypsum board with the air mass causes any separation to be vague, while, on the other hand, the domination of the concrete over

the air mass at this node produces responses that are associated to disturbances with low frequencies; completely overshadowing to a large extent any contribution from the air mass.

In addition to observations as to the magnitude changes that the transfer functions $Z(1,1)$ and $Z(1,2)$ will impart on the disturbances, the phase lag they will cause needs to be examined, since it is an indication of the speed with which a disturbance will be felt at the air node. This becomes quite clear when the phase lag (or lead) ϕ° is converted to an equivalent time lag (or lead) τ sec. This is done by simply dividing the phase angle (in radians) by the corresponding frequency (in radians/sec).

Studying plots for time delays associated with $Z(1,1)$ and $Z(1,2)$ for models 3_c and 3_g gives further insights into the role of the mass in the building and its effect on the air temperature response to disturbances at both nodes 1 and 2.

Figure 3.37 shows that the presence of elements with low thermal capacitance and conductivity, such as found in gypsum board, will delay the sensing of a disturbance at the air node by the air temperature longer than the presence of an element with higher thermal capacitance and conductivity. This occurs for disturbances with frequencies higher than 3 cycles per day and points to a coupling of the air and gypsum thermal masses, an observation already made with respect to the frequencies at which gypsum reaches steady state. Disturbances with lower frequencies, however, lead to a steady state of this coupled response, but affect the dynamics of the elements with higher thermal capacitance and conductivity, resulting in higher time lags.

Figure 3.38 displays the time lags for $Z(1,2)$ of models 3_c and 3_g

plotted against frequency. The separation of the two plots is not very distinct but important observations can be made from them. For disturbances with frequencies lower than 16 cycles per day (period=5360 sec), the time lag caused by $Z(1,2)$ of model 3_c is 10% greater than the time lag caused by $Z(1,2)$ of model 3_g due to the same reasons cited previously, i.e. the less massive gypsum board tends to reach steady state at higher frequencies. For disturbances with frequencies greater than 16 cycles per day, the maximum time lag oscillates between model 3_g (for disturbances with frequencies greater than 16 and lower than 83 cycles per day) and model 3_c (for disturbances with frequencies greater than 83 cycles per day), but the difference never exceeds 10%. The implications of the behaviour of the time lag can only be an indication of the lack of the type of separation between short term dynamics and long term dynamics that exists for $Z(1,1)$.

3.6.3 Discussion

The above discussion indicates that although highly varying radiative loads in buildings can have a significant effect on the room air temperature, the process can be so slow as to inhibit the performance of feedback control. For convective loads however, there is a relatively clear separation between short and long term dynamics at an approximate frequency of 36 cycles/day (periods of about 40 min.). Its absence for radiative loads implies that feedback control cannot properly limit the room temperature swings imposed by such loads.

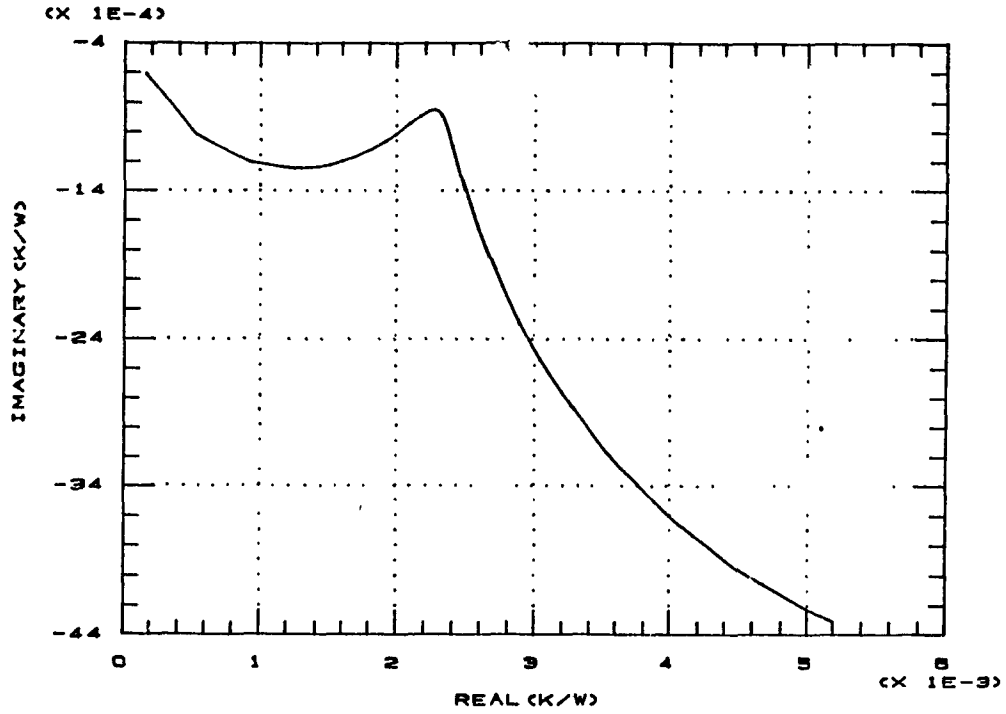


Figure 3.10 Polar plot of Z(1,1) variation: model 2

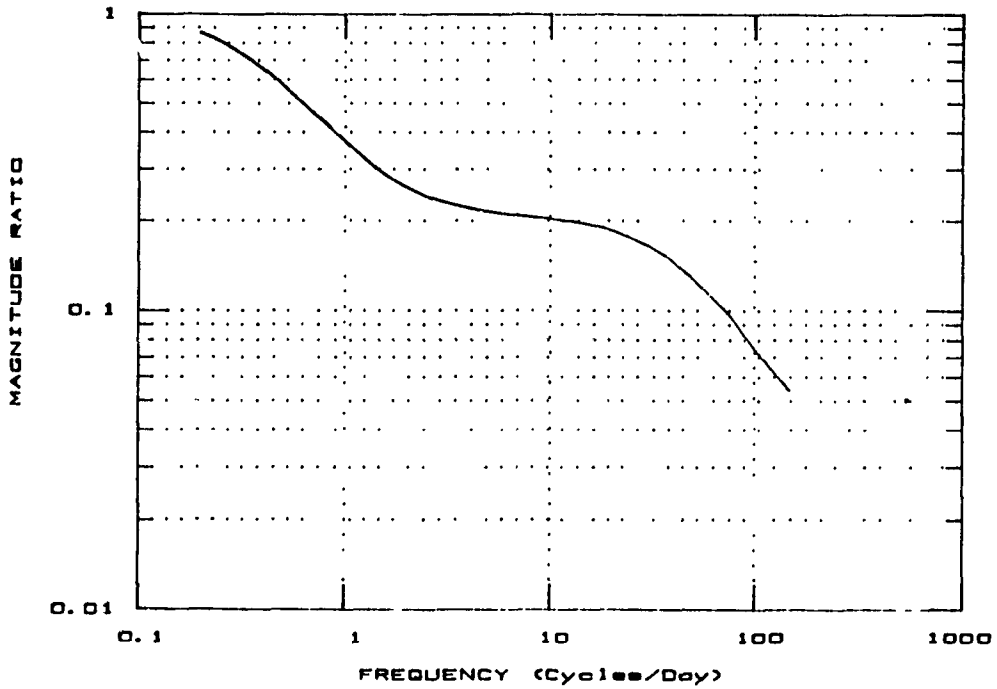


Figure 3.11 Plot of magnitude ratio for Z(1,1) : model 2

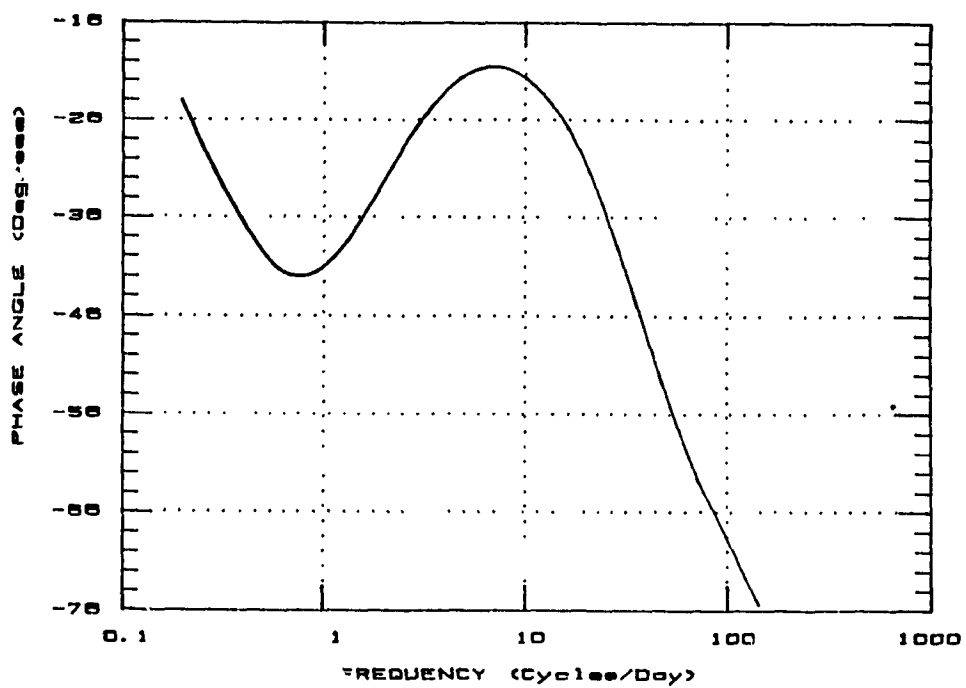


Figure 3.12 Plot of phase angle of $Z(1,1)$: model 2

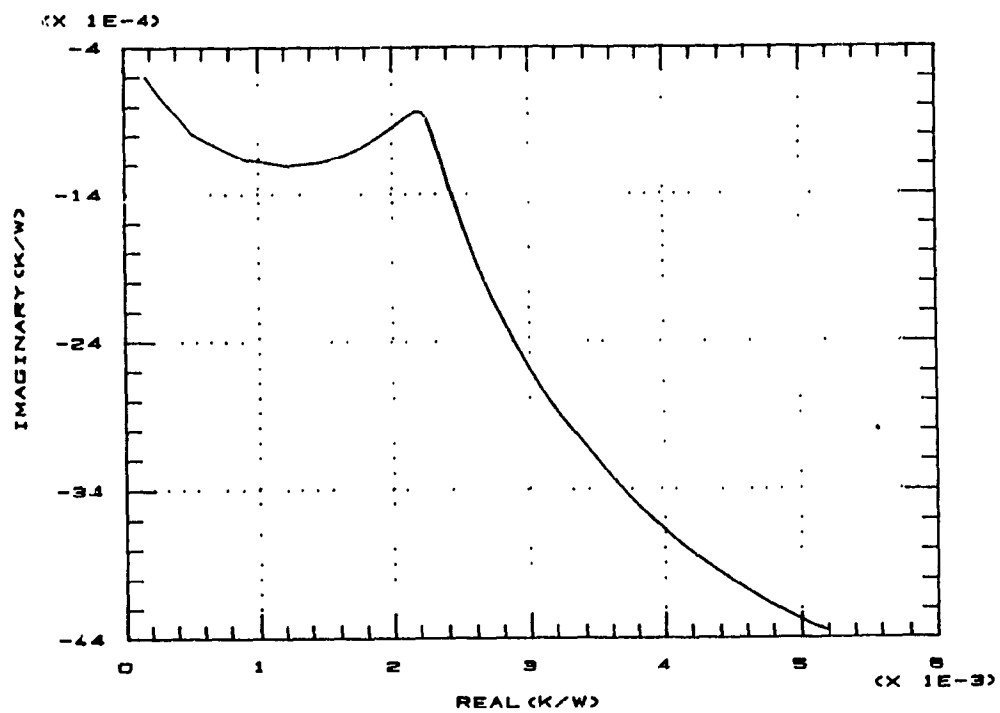


Figure 3.13 Polar plot of $Z(1,1)$ variation: model 3

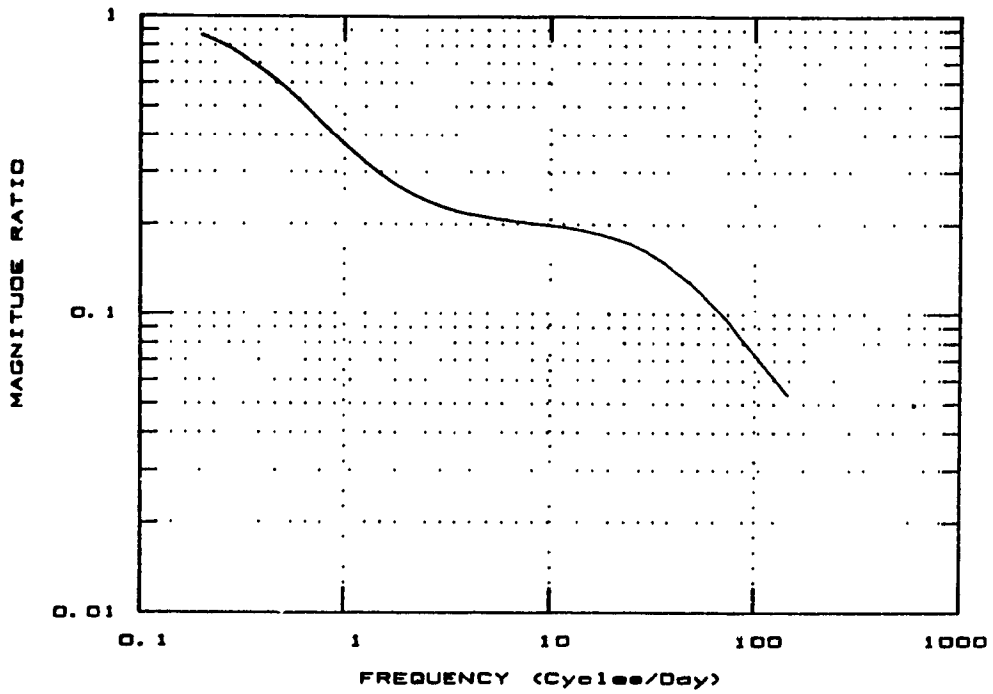


Figure 3.14 Plot of magnitude ratio for Z(1,1) : model 3

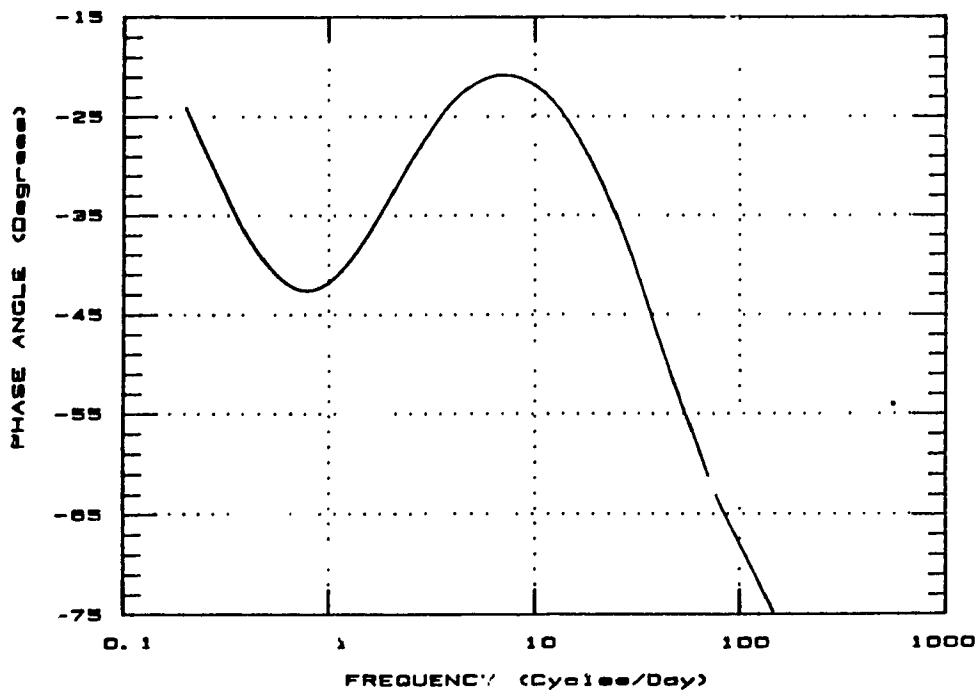


Figure 3.15 Plot of phase angle of Z(1,1) : model 3

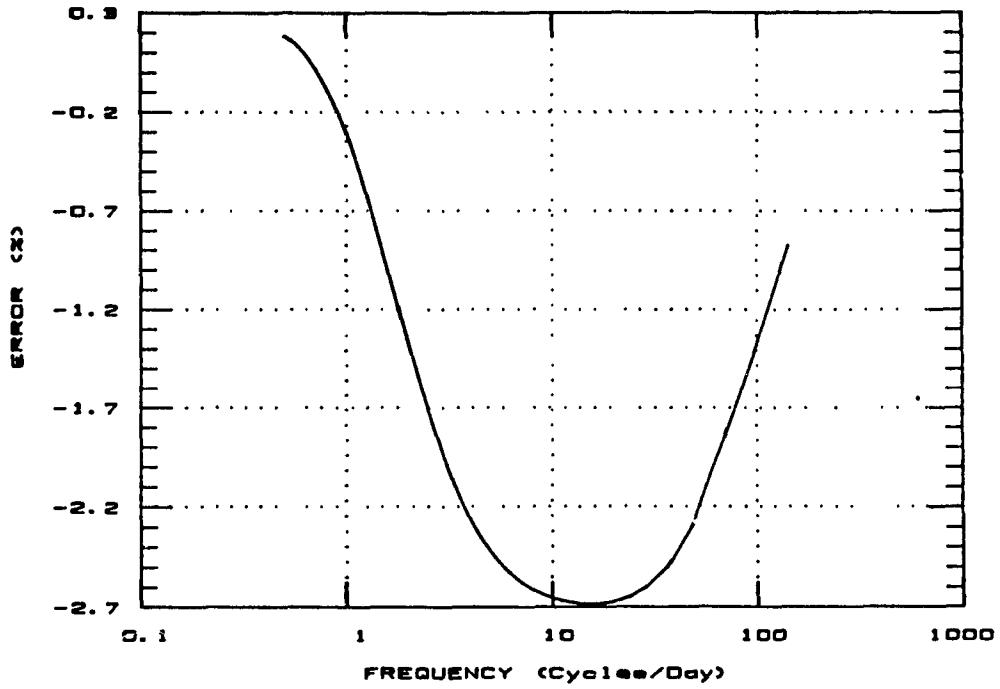


Figure 3.16 Magnitude error for Z(1,1) of model 2 compared to model 3

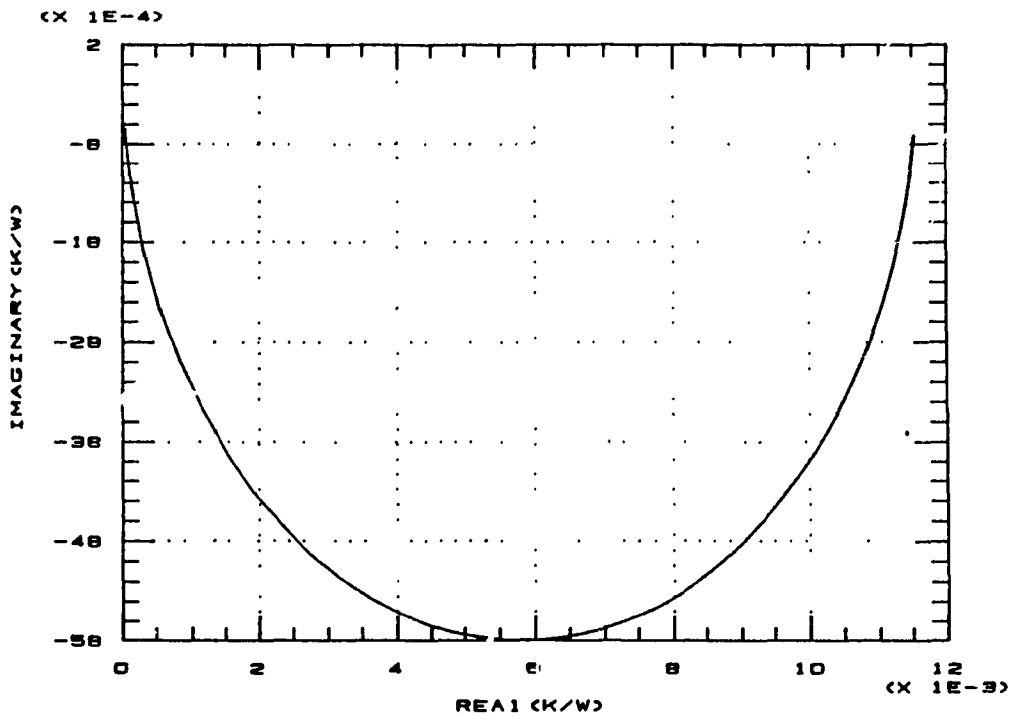


Figure 3.17 Polar plot of Z(1,1) variation: model 1

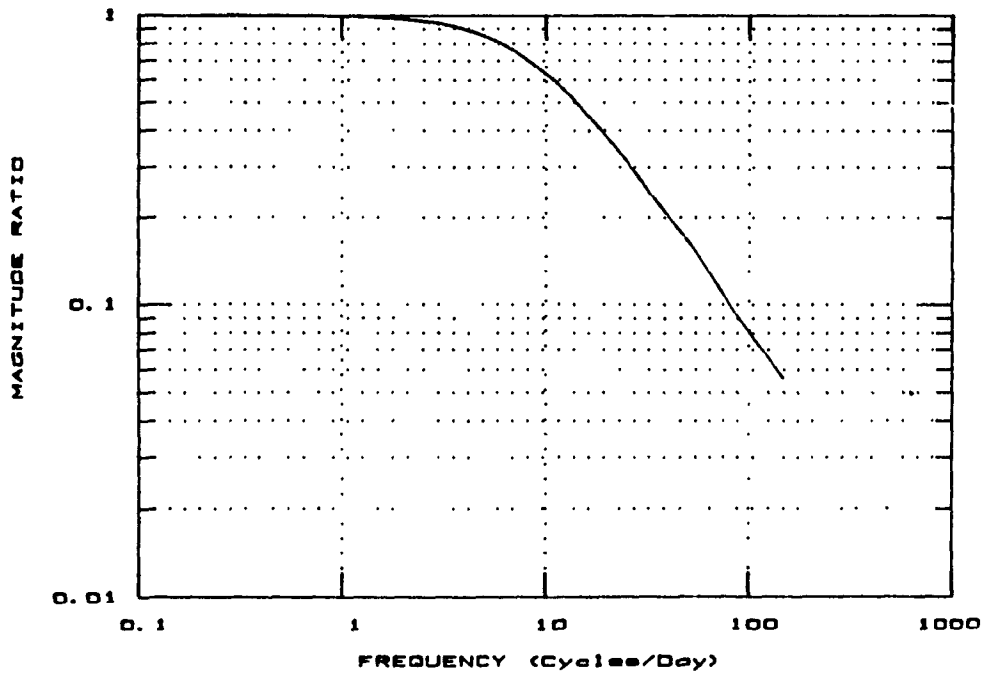


Figure 3.18 Plot of magnitude ratio for Z(1,1) : model 1

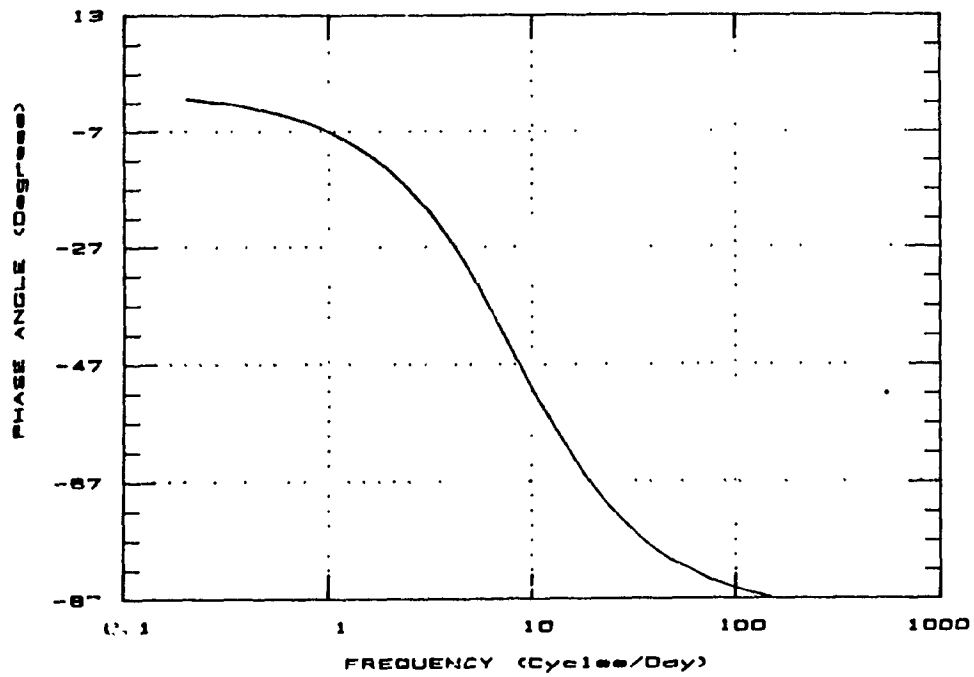


Figure 3.19 Plot of phase angle of Z(1,1) : model 1

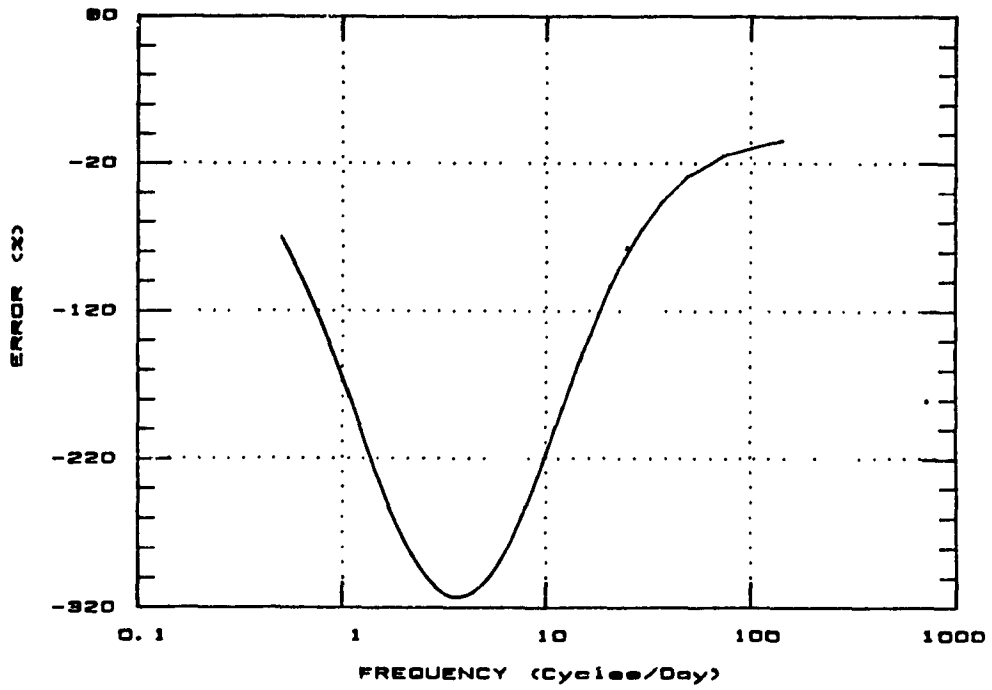


Figure 3.20 Magnitude error for $Z(1,1)$ of model 1 compared to model 3

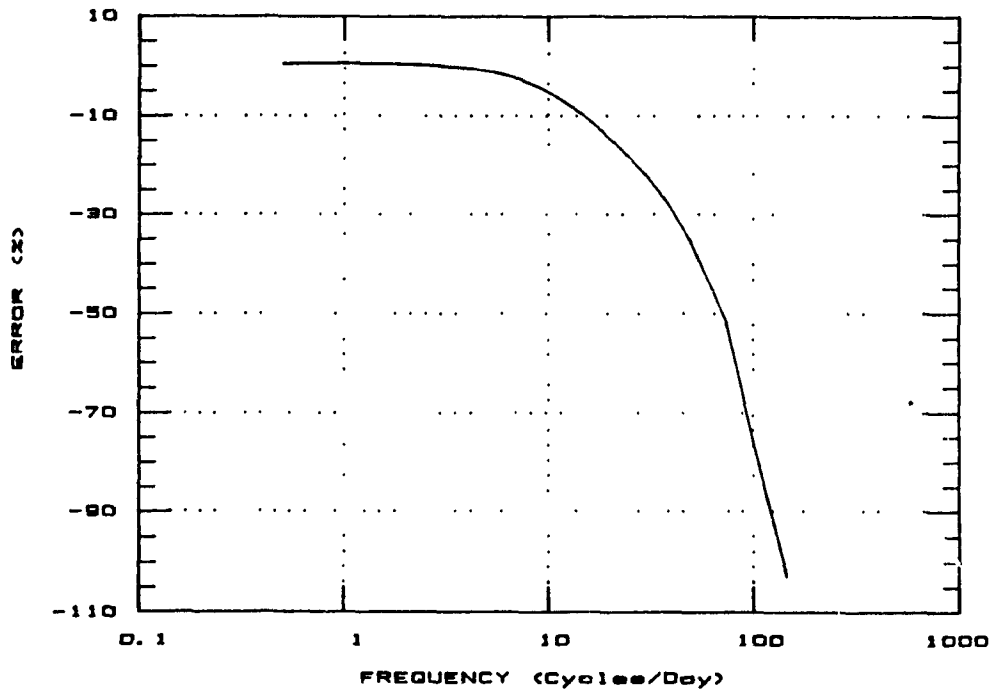


Figure 3.21 Magnitude error for $Z(1,2)$ of model 2 compared to model 3

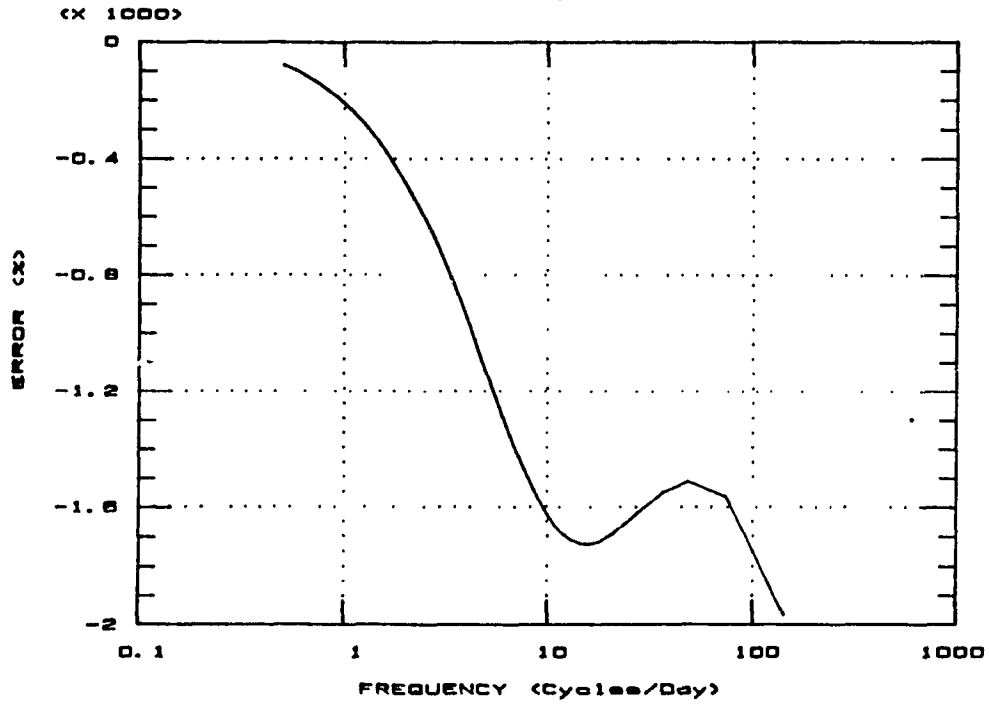


Figure 3.22 Magnitude error for Z(1,2) of model 1 compared to model 3

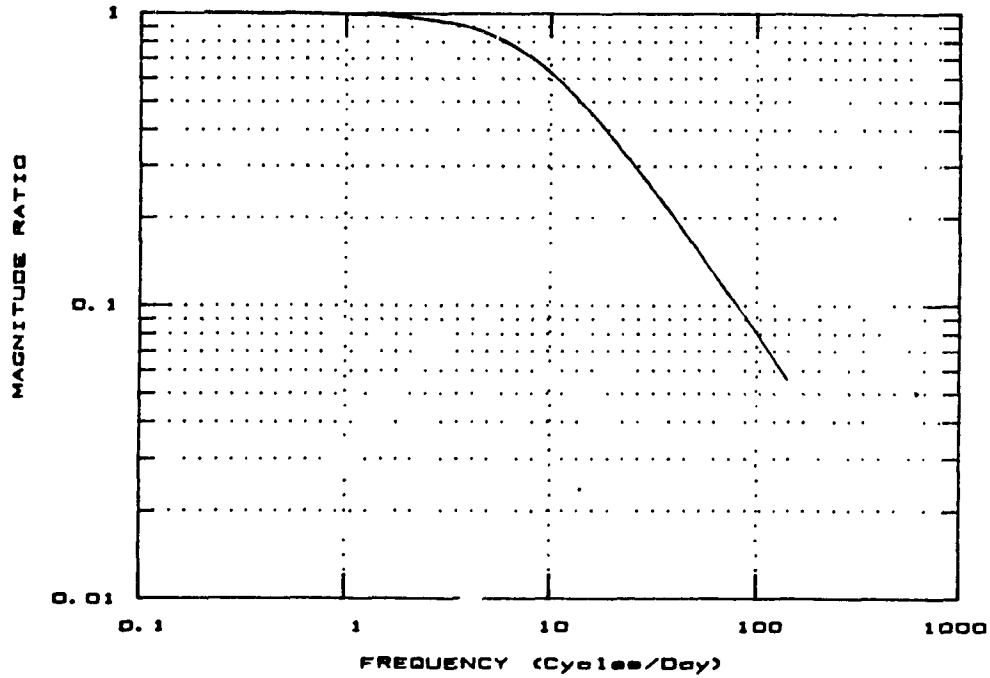


Figure 3.23 Plot of Magnitude ratio for Z(1,2) : Model 1

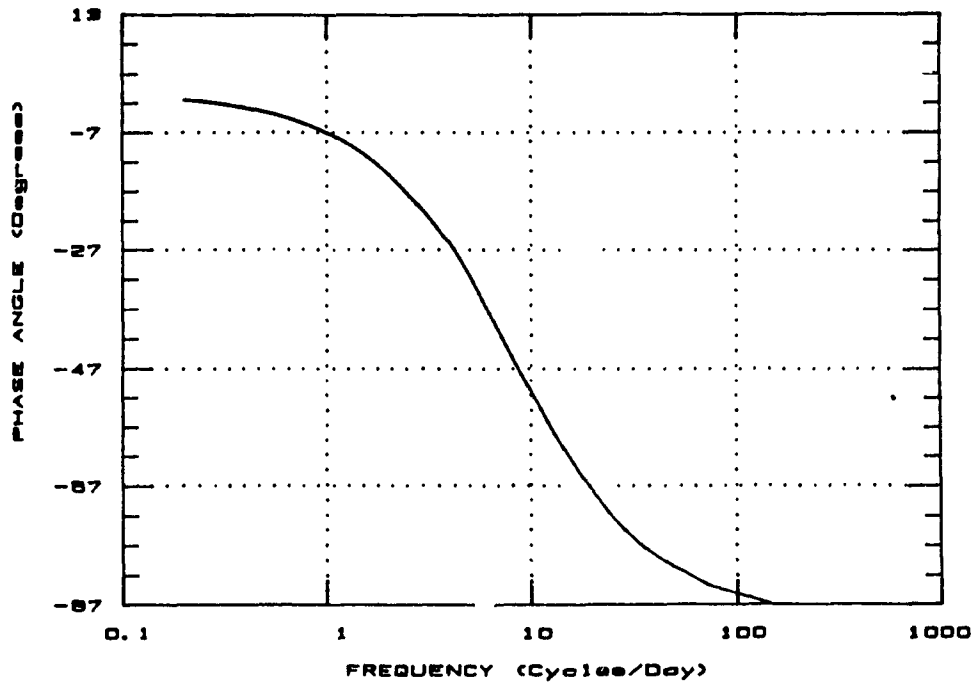


Figure 3.24 Plot of Phase angle of $Z(1,2)$: Model 1

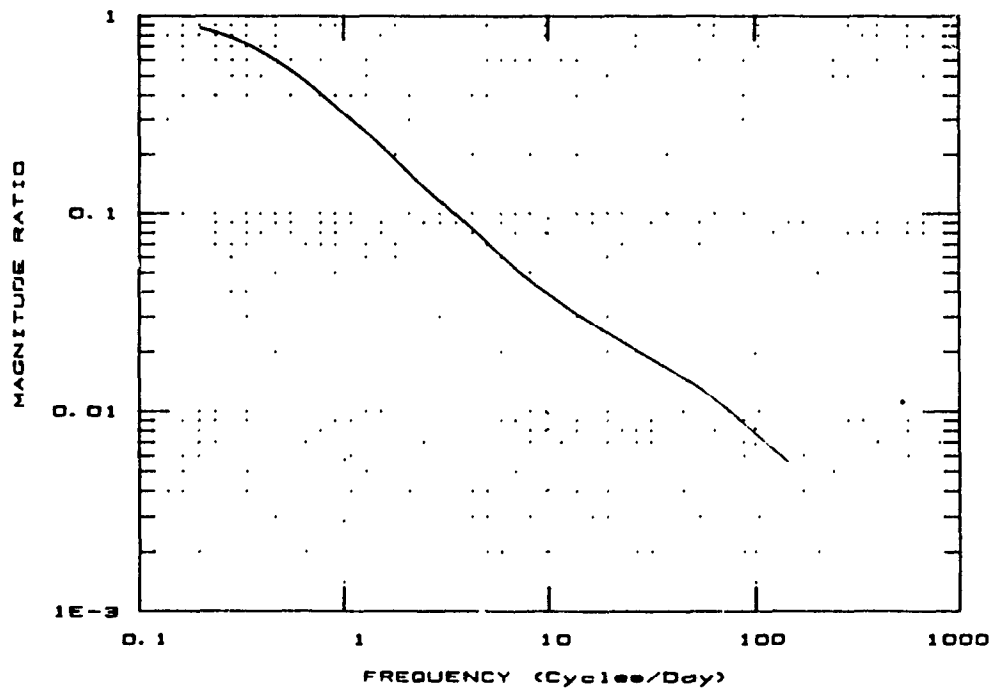


Figure 3.25 Plot of Magnitude ratio for $Z(1,2)$: Model 2

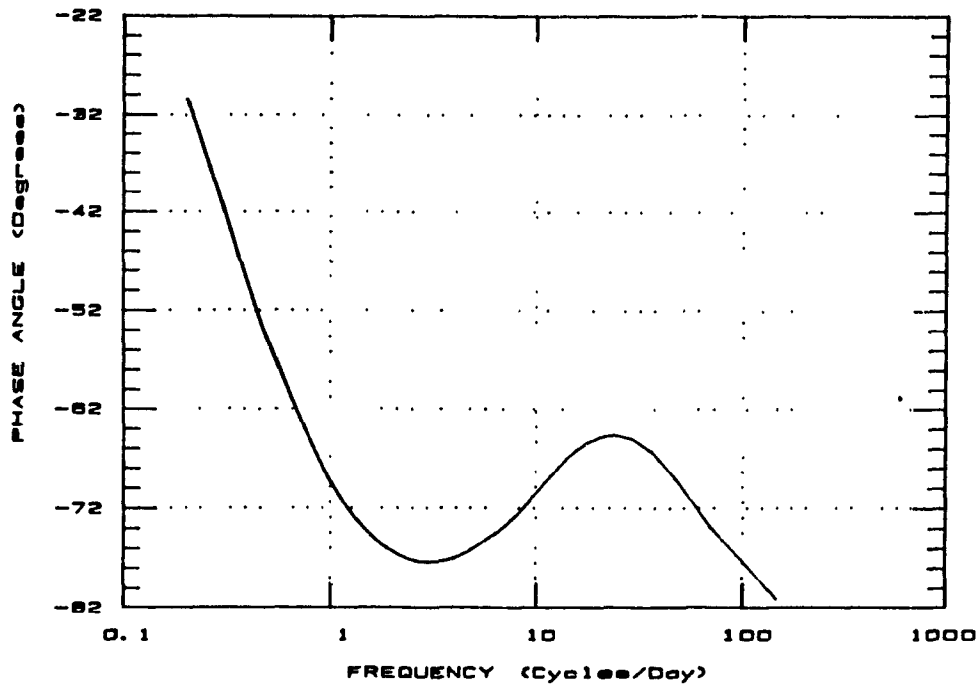


Figure 3.26 Plot of Phase angle of $Z(1,2)$: Model 2

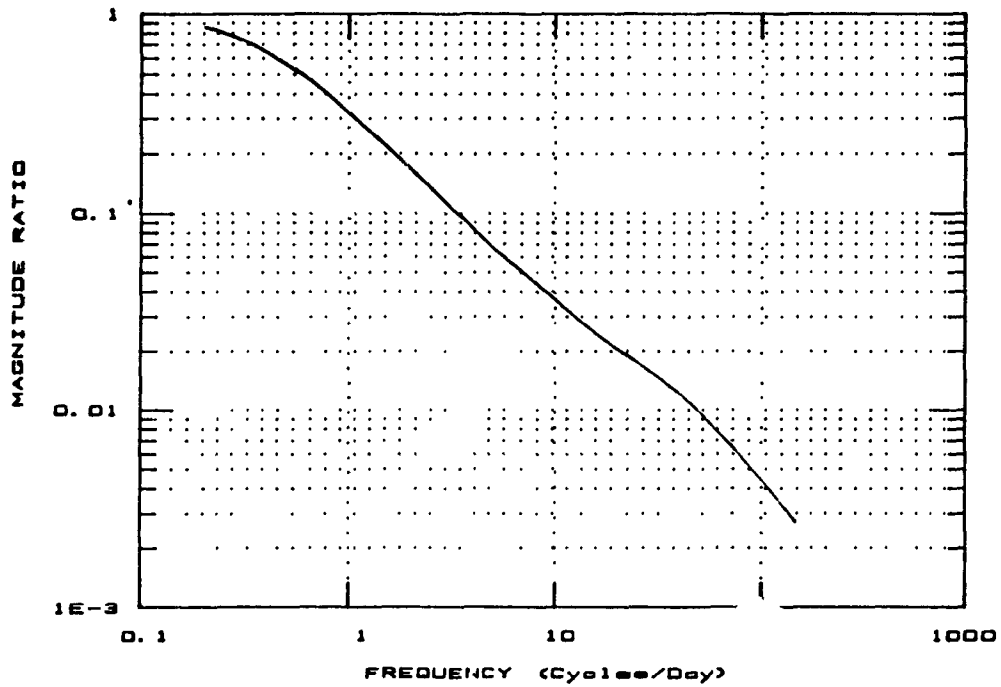


Figure 3.27 Plot of Magnitude ratio for $Z(1,2)$: Model 3

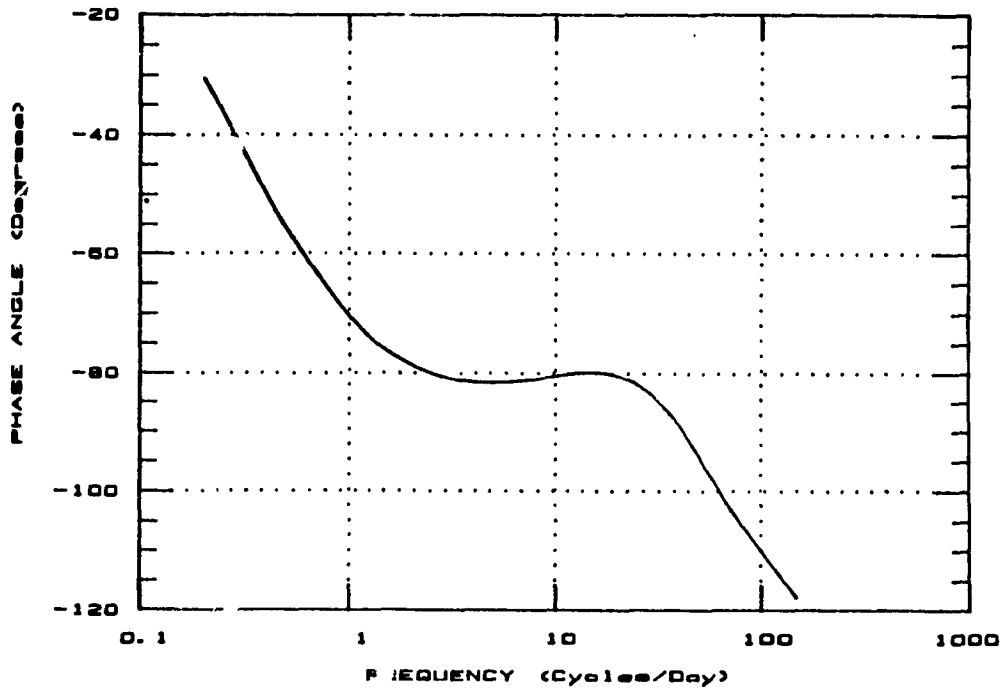


Figure 3.28 Plot of Phase angle of $Z(1,2)$: Model 3

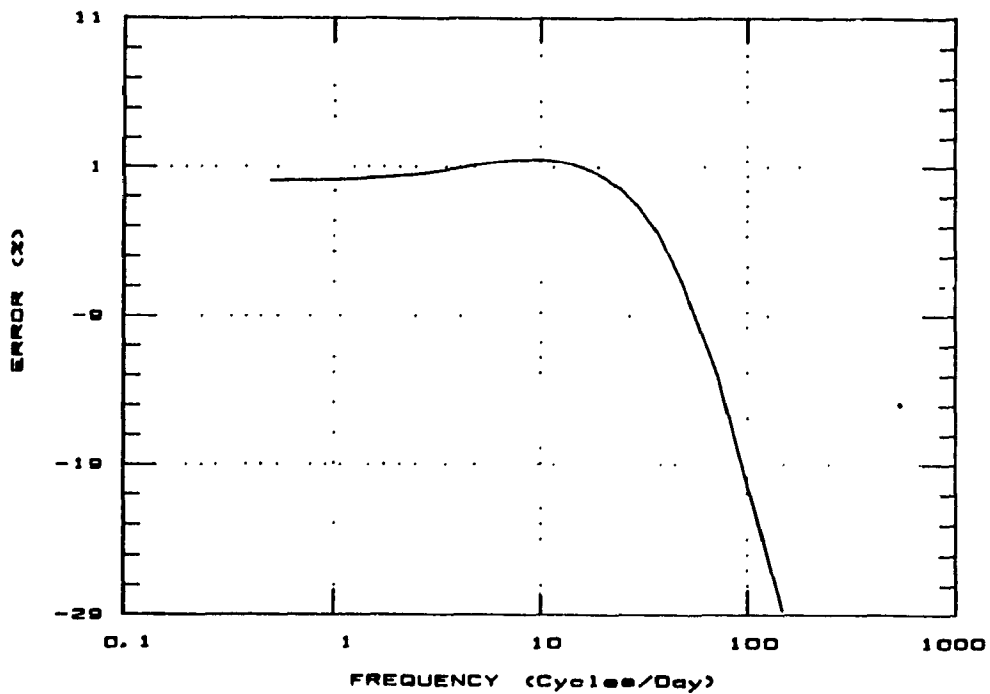


Figure 3.29 Magnitude error for $Z(1,1)$ of Model 2 compared to Model 3 (Gypsum board)

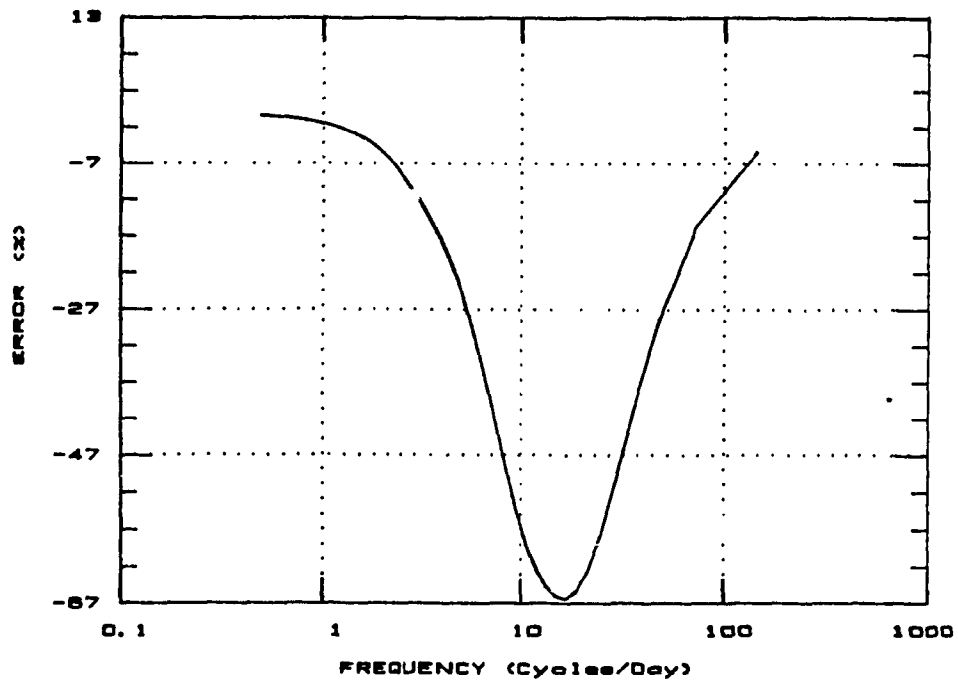


Figure 3.30 Magnitude error for $Z(1,1)$ of model 1 compared to model 3 (gypsum board)

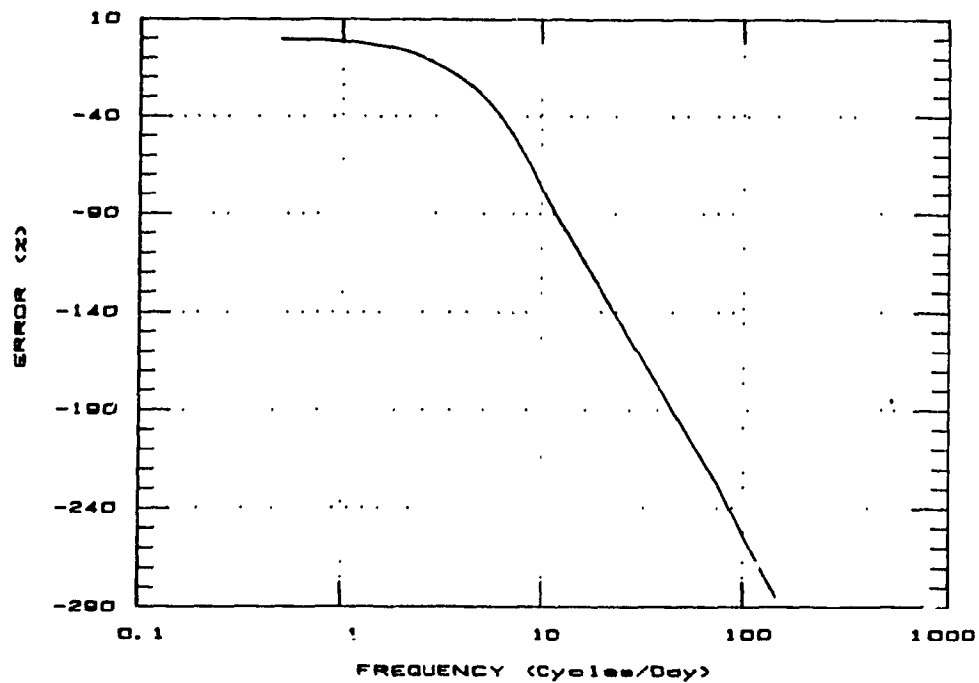


Figure 3.31 Magnitude error for $Z(1,2)$ of model 2 compared to model 3 (gypsum board)

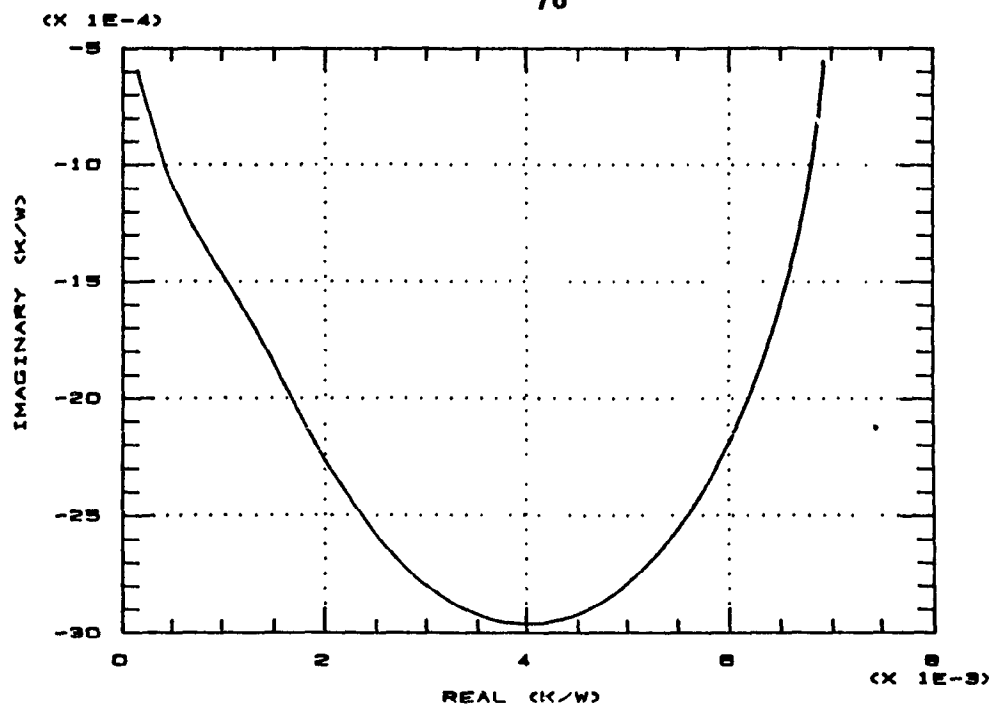


Figure 3.32 Polar plot of $Z(1,1)$ variation: model 3 (gypsum board)

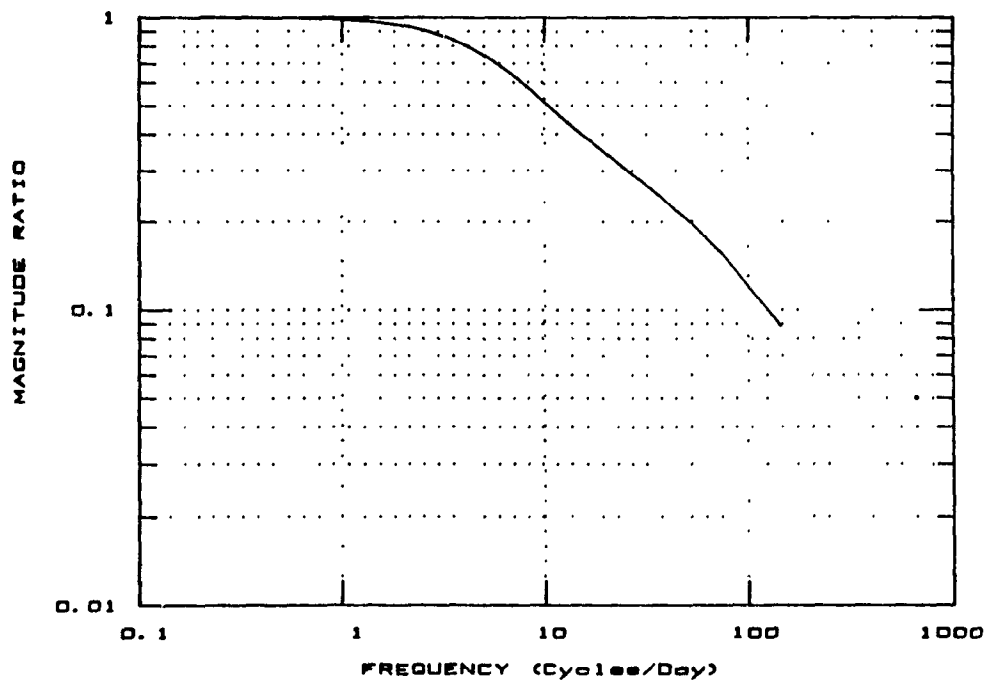


Figure 3.33 Plot of magnitude ratio for $Z(1,1)$: model 3 (gypsum board)

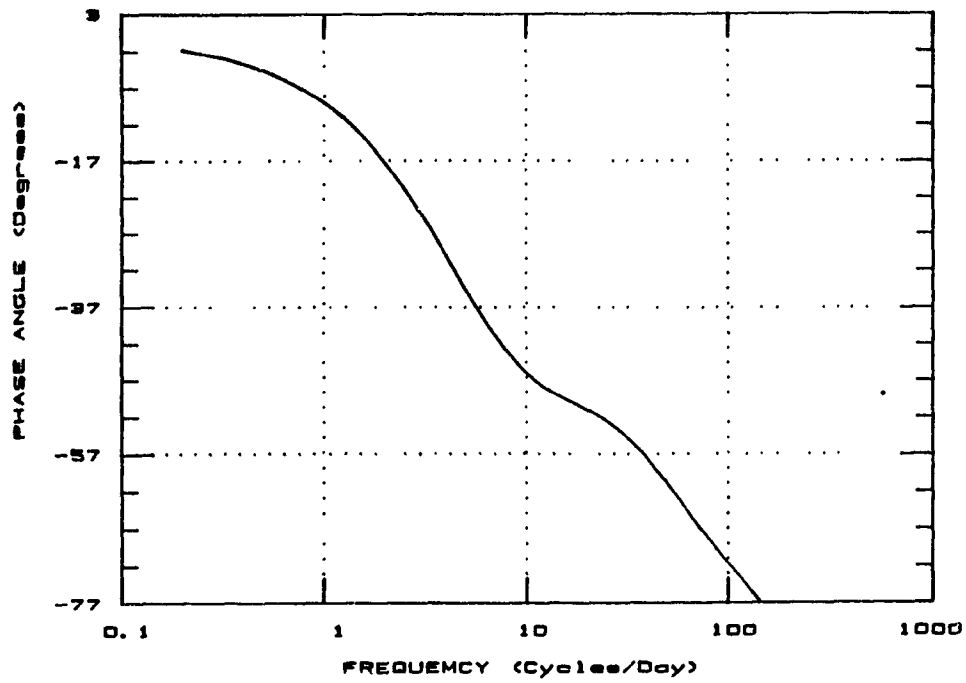


Figure 3.34 Plot of phase angle of $Z(1,1)$: model 3 (gypsum board)

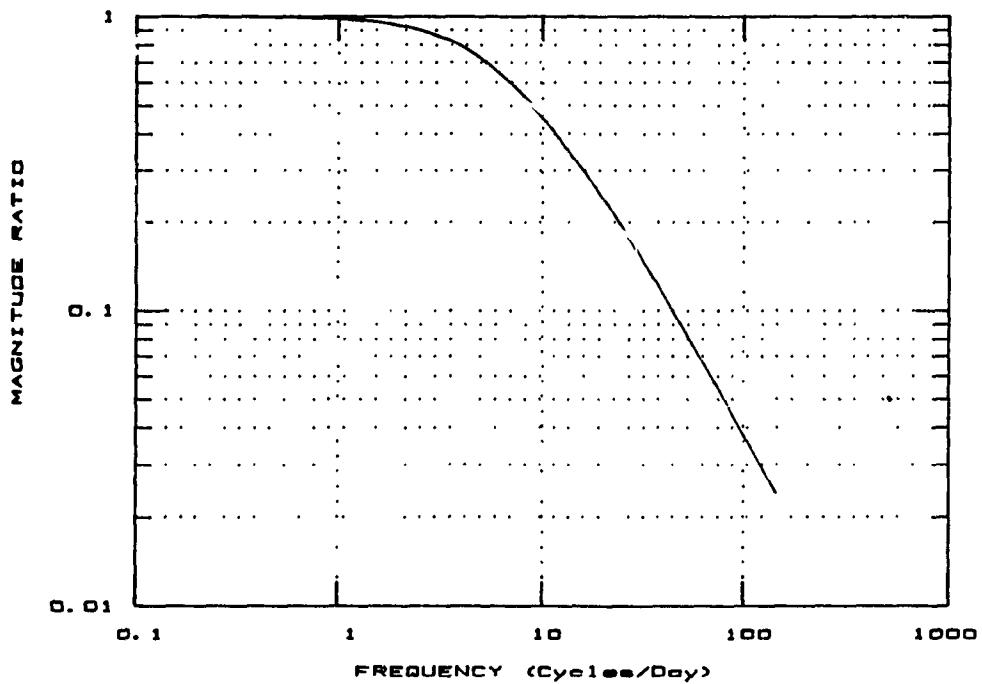


Figure 3.35 Plot of magnitude ratio for $Z(1,2)$: model 3 (gypsum board)

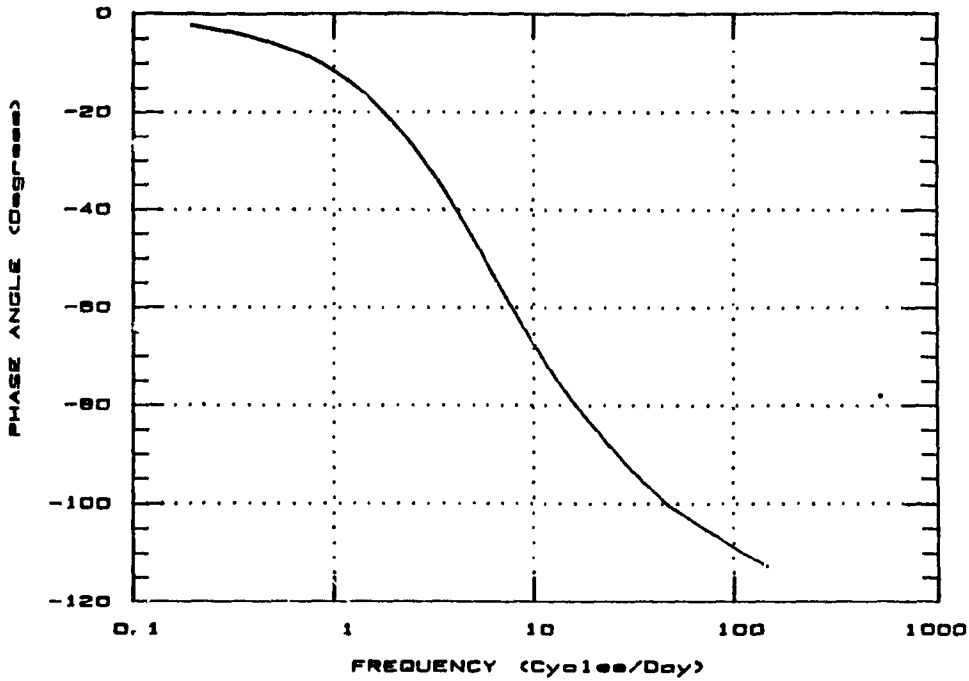


Figure 3.36 Plot of phase angle of Z(1,2) : model 3 (gypsum board)

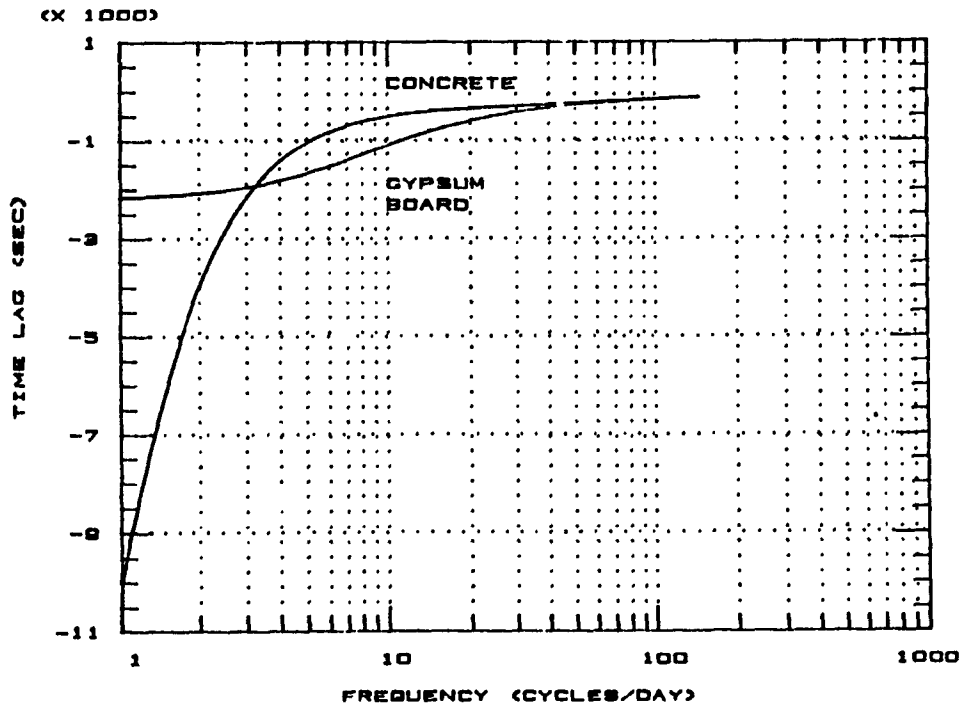


Figure 3.37 Plot time lag for Z(1,1) of model 3 for concrete and gypsum board

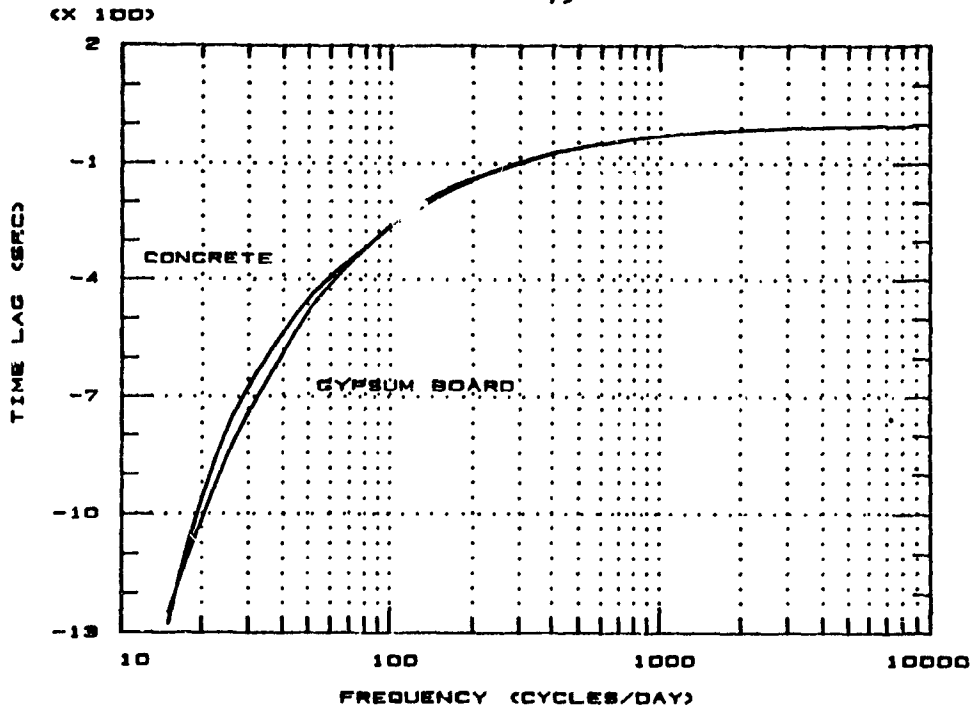


Figure 3.38 Plot of time lag for Z(1,2) of model 3 for concrete and gypsum board

CHAPTER 4

DYNAMIC CONTROL STRATEGIES USING THE MASS OF THE BUILDING

4.1 Introduction

Dynamic control strategies are based on the principle that the mass of the building should be a factor in the design and operation of HVAC systems. This principle, however, has been used without a rigorous methodology to obtain optimal results. This section seeks to demonstrate a simple and rigorous algorithm for use of the envelope mass to limit peak loads upon start-up, as well as show that the thermal mass can also be used for relatively high frequencies of the order of 8 cycles per day with significant lowering of the peak load.

4.2 Using the mass to reduce diurnal load fluctuations

One of the most widely used strategies for energy conservation is the simple night set-back (fig. 4.1). This is a simple way to reduce energy expenditure by simply reducing the temperature setpoint during unoccupied periods and returning it to comfort level in time for the occupants' arrival. The main problem faced when this strategy is used, is the inability of the system to maintain comfort conditions throughout the occupied period of the day. This deficiency is related to the so-called optimum start-up and stop, two keywords used by HVAC engineers that are somewhat misleading since, in many cases, the system is not turned off

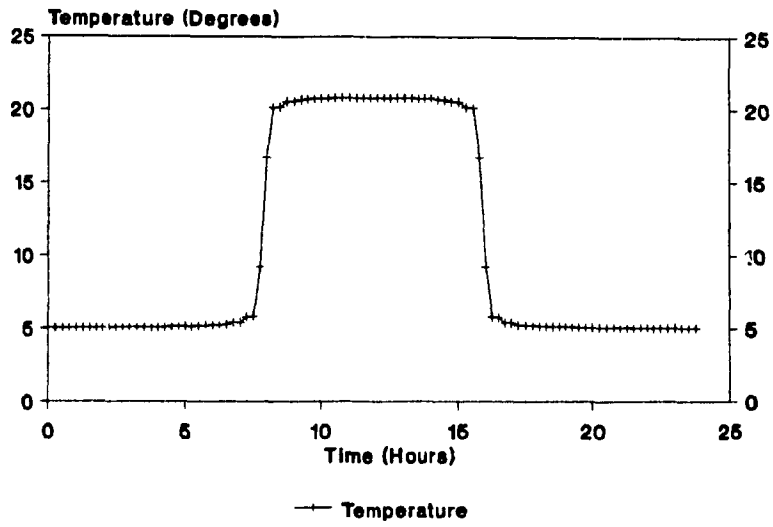


Figure 4.1 Simple setback

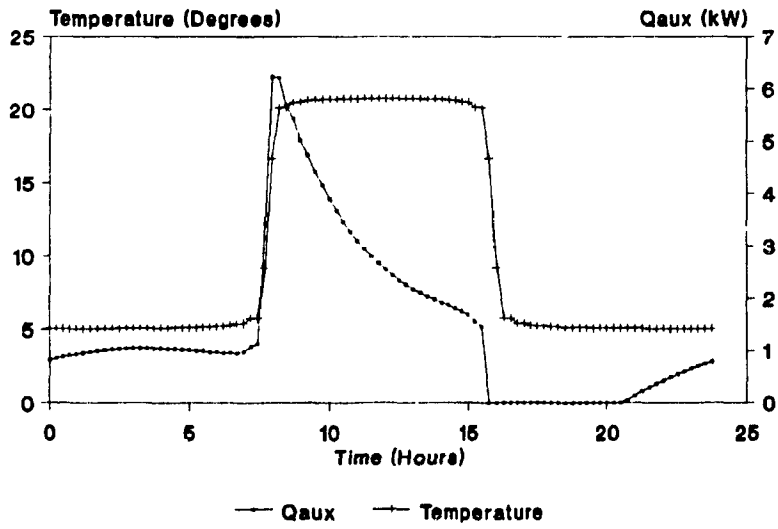


Figure 4.2 Auxiliary energy requirements for the square profile

completely during unoccupied periods of time or else the setback would not be maintained. Instead of optimum start up/stop strategies, the discussion, therefore, should centre on optimum setpoint profiles. This ensures that thermal comfort will be achieved without compromising energy use. These two goals will be attained using optimum equipment sizes.

4.2.1 Problems associated with square set-back profile and possible solutions

The most important problem associated with the square setback profile is the fact that the conditions reached at the time of occupancy may not be within comfort levels. This may be either because the equipment sizes could not handle the pick-up demand, or the building warm-up was not started early enough; both are caused by the lack of knowledge of the building's thermal dynamics. The former problem arises at the design phase and the latter at the operation phase. Since a system is sized based on design outdoor temperatures, this consideration allows for sizes that are large enough to respond to steady state heat losses but not to compensate for the energy losses from the mass of the building during the unoccupied periods when setback is used.

To demonstrate this problem, model 3_c (the room model described in chapter 3) was used to calculate the auxiliary heat required to produce a square setpoint profile. The setback was intentionally large, namely 15°C, to clearly show the effect of the pick-up demand. The only load considered was due to the outside temperature variation $T_o(s)$ whose mean was -5°C and had a range of 20°C. Figure 4.2 clearly shows the magnitude of the demand when the setpoint is brought up to comfort conditions. The

problem related to the inability of the system to respond to the high peak load may be solved by either:

1. Allowing the last few degrees to be achieved by internal gains, such as people and equipment,
- or
2. Using no night set back

These two options represent extremes: one compromises thermal comfort, while the other compromises energy consumption. The optimum solution, therefore, has to be somewhere in between these two extremes i.e. an alternative that would produce thermal comfort for reasonable energy consumption and equipment sizes.

Athienitis (1988), by assuming advance approximate predictions of the weather and using a detailed program, tested different setback profiles to reduce the peak demand (and therefore equipment sizes) and still conserve energy over the no-setback option. The results showed that a ramp increase of the setpoint, which produced a reduction of the peak demand, was a possible solution. The approach, although considering the predicted weather patterns for the choice of the setpoint profile, did not consider in an explicit manner the building characteristics. It also relied on a trial and error approach to determine the best rate of setpoint change.

4.2.2 Setpoint temperature variation for frequencies of 1 cycle/day

The effectiveness of the algorithm described below depends, on apart from weather prediction, on knowledge of the building characteristics. The algorithm, by its nature, is based on balancing the effect of the load with the effect of the auxiliary energy on the room air temperature and is developed using frequency domain methods.

4.2.2.1 The discrete frequency domain approach and discrete Fourier transforms

The use of the discrete frequency domain method for simulation and analysis of HVAC systems presents advantages that are lacking in time domain methods; the primary advantage of this method is its flexibility in the analysis of systems. While time domain methods require simulation as a tool for the analysis of systems, the discrete frequency domain method can be used to perform analysis without simulation (Athienitis et al 1987). In addition, it can be used to study the performance of systems whose models are described by transcendental functions as is the case with distributed parameter systems. In general, time domain methods would require the approximation of these systems as lumped parameter systems (Athienitis 1985). Using the DFT, the response of the system can simply be determined from the product of the forcing and system transfer functions. If the time domain response is required, the Inverse Discrete Fourier Transform (IDFT) of this product can be found directly from the frequency domain response.

The modelling and formulation methodology as described by Athienitis et al (1987) is as follows.

" (1) Decide the number N of harmonics to be analyzed for. If n represents a harmonic number and P is the time length of the simulation or analysis (e.g. a day or a week etc.), then a harmonic's frequency ω_n is equal to $2\pi n/P$.

(2) Obtain the appropriate Discrete Fourier series representation for the sources. An arbitrary source $M(t)$ is represented by a Fourier series of the form

$$M(t) = \sum_{n=-N}^N m_n(j\omega_n) \exp(j\omega_n t) \quad (1a)$$

the complex coefficients $m_n(j\omega_n)$ being determined numerically by

$$m_n = \left[\sum_{k=1}^K M(t_k) \exp(-j\omega_n t_k) \right] / P \quad (1b)$$

where $M(t_k)$ is the value of M at time t_k corresponding to point k (for a total of K values over the time length P)

(3) Determine the discrete frequency response $H(j\omega_n)$ of the output of interest to unit input at each node. The periodic response to each source is obtained by superposition of the output harmonics using complex (phasor) multiplication. For example, for an output temperature $T(t)$ we have

$$T(t) = \sum_{n=-N}^N H(j\omega_n) m_n(j\omega_n) \exp(j\omega_n t) \quad (1c)$$

Both the Discrete Fourier Transform (equation 1b) and its inverse (equation 1a) can easily be implemented in a computer program in the form of a subroutine. One shortcoming of such an approach is the distortion

known as Gibb's phenomenon which occurs at discontinuities of functions, such as the edges of a pulse waveform. This was overcome by the inclusion of the Fejer approximation in the subroutine calculating the DFT and the IDFT (Ley et al, 1959).

The transfer functions describing the HVAC system components as well as those describing the room model, can easily be used to study their frequency responses by simply substituting s with $j\omega$ and can be combined to produce the system's overall transfer function if needed, or can be studied individually or in sub-systems in both the frequency and time domain.

4.2.2.2 The Algorithm

Consider figure 4.3, displaying the block diagram of the system considered. $Z(1,1)$ is the impedance relating the auxiliary heat input $Q_{aux}(s)$ to $T_{ai}(s)$ the room air temperature. In addition, the transfer function $U_0Z(1,1)$ relates the load $T_0(s)$ to the room air temperature.

The algorithm is described in detail in figure 4.4 and is based on frequency analysis using the Discrete Fourier Transform and its inverse. Although this algorithm only considers variations in ambient temperature, it can be generalized with further work to include other disturbances using the principle of superposition.

To generate the profile that will subsequently be used to vary T_{SP} in an optimal manner, the following steps have to be taken:

1. The model must be subjected to a disturbance that is of the same phase as the predicted disturbance but whose range is increased steadily until it produces a room air temperature

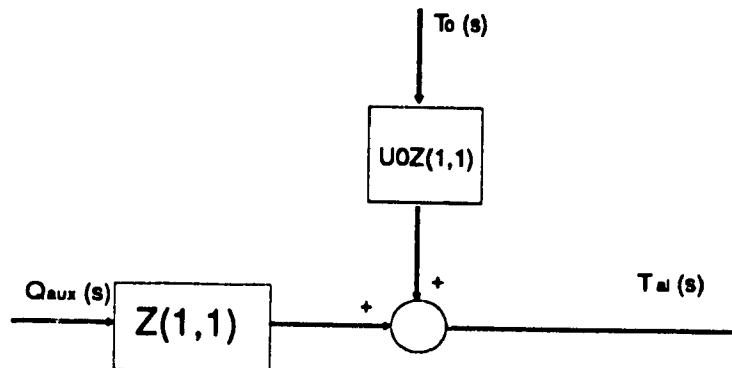


Figure 4.3 The system block diagram

variation, the range of which is equivalent to the setback required. This, in effect, is the passive response of the model and in the absence of any auxiliary heat input, the rate of change of the room air temperature is indicative of the charging and discharging rates the building characteristics dictate.

2. The profile's mean must be shifted up so that the temperature range coincides with the required setpoint range.
3. Since this will produce the temperature required for occupation late in the afternoon, the profile's phase must be shifted so that the maximum temperature, which is the temperature required to satisfy thermal comfort, is attained at a predetermined time.

```

                                F(T0(t))=T0(jω)
STEP 1.....TSP(jω)=T0(jω)*U0Z(1,1)
                                F-1(TSP(jω))=TSP(t)
STEP 2.....
                                IF (Range(TSP(t)) = Max(TSP(t))-Min(TSP(t)))THEN
                                    increase Range(T0(t))
                                    F(T0(t))=T0(jω)
                                    TSP(jω)=T0(jω)*U0Z(1,1)
                                    F-1(TSP(jω))=TSP(t)
                                ENDIF
                                IF (Range(TSP(t)) > Required) THEN
                                    decrease Range(T0(t))
                                    F(T0(t))=T0(jω)
                                    TSP(jω)=T0(jω)*U0Z(1,1)
                                    F-1(TSP(jω))=TSP(t)
                                ENDIF
STEP 3.....
                                IF( tMAX(TSP) ≠ predetermined time) THEN
                                    shift TSP(t) until
                                        tMAX(TSP) = predetermined time
                                ENDIF
STEP 4.....
                                IF( MAX(TSP(t))≠ Required) THEN
                                    TSP(t)=TSP(t)+(Required-MAX(TSP))
                                ENDIF
                                DO 20 t=ON, OFF
                                TSP(t)=TSP(t)+(COMFORT(TSP)-TSP(t))
                                Continue
20

```

Figure 4.4 Algorithm for generating setpoint profiles

4. The profile is then kept at the desired temperature throughout the occupied period, while on either side of this period the setpoint is allowed to vary at rates established in step 1.

The predetermined time mentioned in step 3 is the pivotal point on which optimization of the profile is balanced. To demonstrate the importance of this time the algorithm is implemented as a subroutine in a computer program and is used to produce two setpoint profiles and the auxiliary heat input required to maintain them.

Figure 4.5 shows the setpoint profile generated when the maximum temperature mentioned in step 3 is attained at the time of occupation which was considered to be 8 a.m.. Profile 1 completely eliminates the peak demand associated with the boost of the system, as shown in figure 4.2 for the square profile. Instead, the peak energy requirement occurs much earlier and is in response to the energy affinity of the building mass i.e at this point in the cycle the building has the lowest energy content and therefore the greatest storage capability. As a result, the algorithm, by increasing the setpoint at a rate compatible with the building characteristics, charges the mass accordingly so that by 8 am the building mass is completely charged and only steady state heat losses need to be countered by the heating system.

A profile that resembles those tested by Athienitis (1988), Profile 2, is shown in figure 4.6 together with the required auxiliary heat input. In this case, the maximum temperature mentioned in step 3 is attained at noon, the mid-point of the working day.

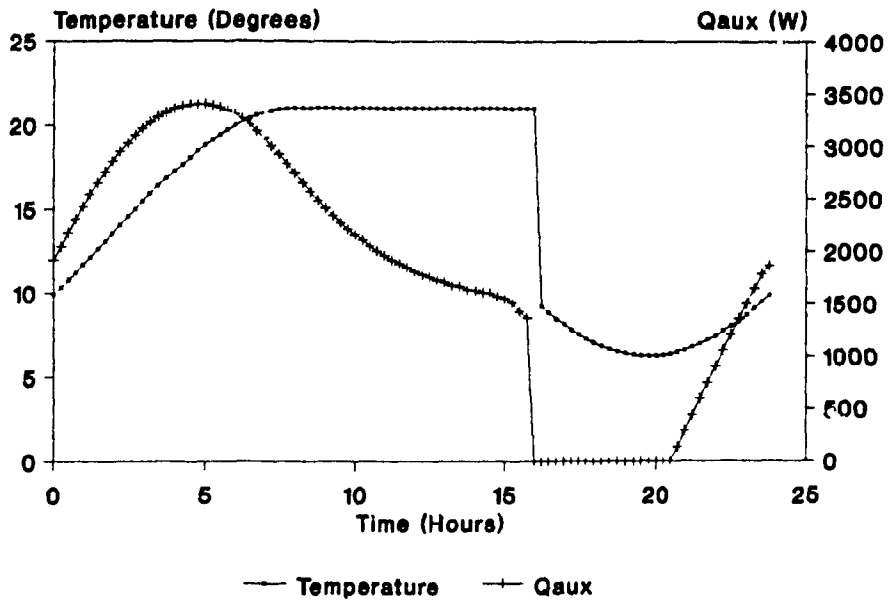


Figure 4.5 Profile 1

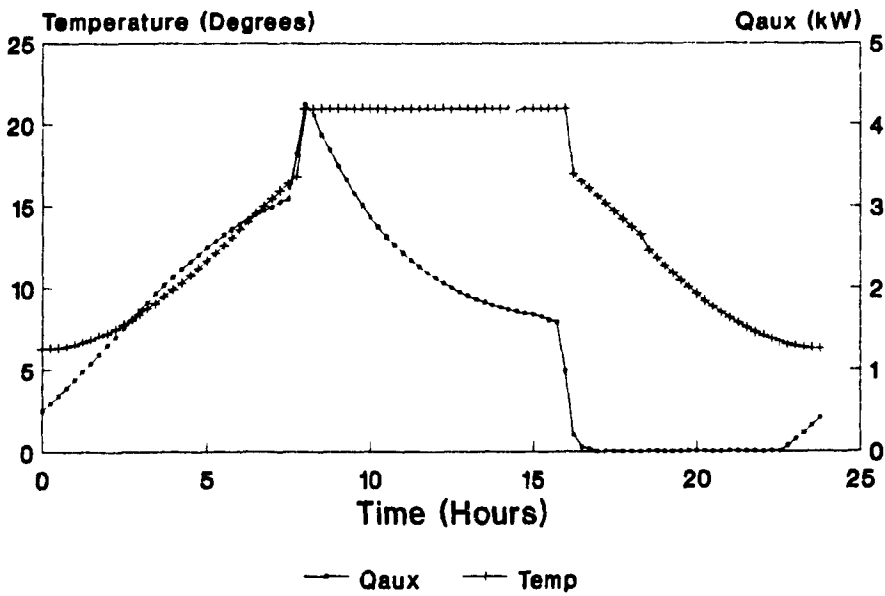


Figure 4.6 Profile 2

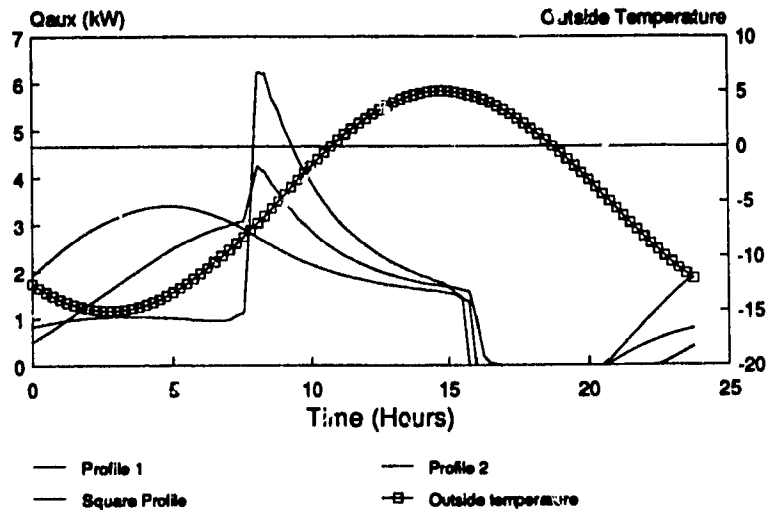


Figure 4.7 Comparison of the different profiles and energy requirements

The peak that appears at 8 am is an indication that the building mass's affinity for energy is not compensated for until this time and therefore a boost is necessary to achieve the desired conditions. The magnitude of the peak demand, however, is significantly lower than the one produced by the square setpoint profile, but slightly higher than the one produced by Profile 1 (figure 4.6).

From the above discussion it is evident that setpoint profiles required to achieve the optimization of all the parameters involved in building operation, are specific to a building, its heating system and the weather predicted for each day.

4.2.3 Discussion

Figure 4.7 clearly shows why different profiles will produce such a range of peak demand and energy requirements. Profile 1 takes full advantage of the mass thermal storage capability, with Profile 2 using it

somewhat less and the square profile working against it. It is also evident that energy consumption is inversely proportional to the peak demand and therefore larger sized equipment is required for energy conserving profiles if the system is to attain comfort levels at the time of occupancy. This is somewhat of a paradox since oversized system components are known to waste energy due to the inefficiencies associated with part-load performance. Although energy waste due to oversizing of equipment is difficult to quantify, it is generally accepted that part load operation may often increase inefficiencies, compromise in many cases thermal comfort and shorten the life of system components. It is preferable to size a system in accordance with the normal conditions rather than the exceptional ones and use the building's mass as a reservoir for extra energy requirements both for long term strategies, such as the setpoint profile generation and for short term strategies, which will be described shortly.

4.3 Utilizing the mass to reduce peak loads for frequencies higher than 1 cycle per day

Temperature setpoint variation for periods of less than 3 hours are now possible with the increasing use of programmable controllers and thermostats. This ability to vary the setpoint, which, in effect, is equivalent to controlled temperature swings, is what enables the storage and release of thermal energy from the mass of the building. To demonstrate the validity of the above statement, a computer study was performed using one harmonic representation of the loads and the setpoint variation.

4.3.1 Methodology

The study performed dealt with the cyclic load variation occurring in a theatre. The load was assumed to be the result of the total sensible contribution of the 500 people present. Of this sensible load, 70% was assumed to be convective while 30% radiative. Of the radiative load, the fraction assumed absorbed by the floor (the massive element) was proportional to the fraction of the floor area over the total surface area of the theatre (fig 4.8). The floor was considered to be cold while the cooling was provided by air supplied to the centre of the enclosure. The supply air was assumed to be instantaneously and perfectly mixed with the room air.

The study compared the cooling energy variation for the same load but with

1. A constant set-point and
2. A varying set-point.

The variation in the setpoint was calculated based on thermal comfort criteria and the capacitive nature of the thermal mass present. Thermal comfort considerations were based on the work of Sprague and McNall (1970). Their efforts in determining the effect of drifts in temperature on comfort, acceptability and health concluded that no serious occupancy complaints occur in air conditioned spaces for temperature fluctuations which obey the following expression: $\Delta T^2 * f_h < 4.63$, where ΔT is the peak to peak amplitude of the temperature fluctuation and f_h is the cyclic frequency in cycles per hour (Sprague and McNall 1970).

Based on these considerations and the fact that the period for the load was 7800 sec, the set point variation had an amplitude of 1.6°C (or $\Delta T = 3.7^{\circ}\text{C}$).

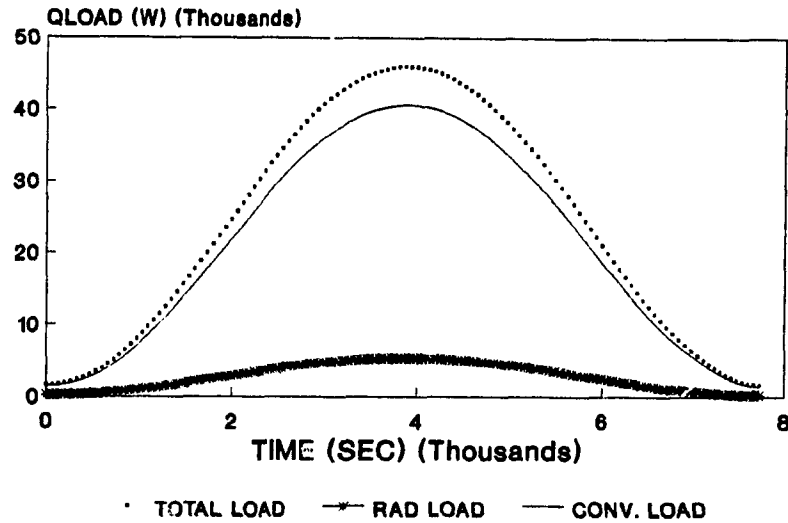


Figure 4.8 Convective, Radiative and total load variation

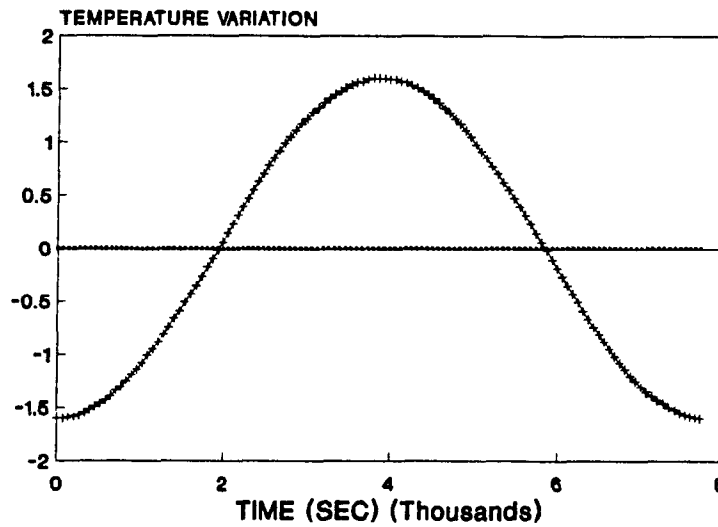


Figure 4.9 Temperature setpoint variation

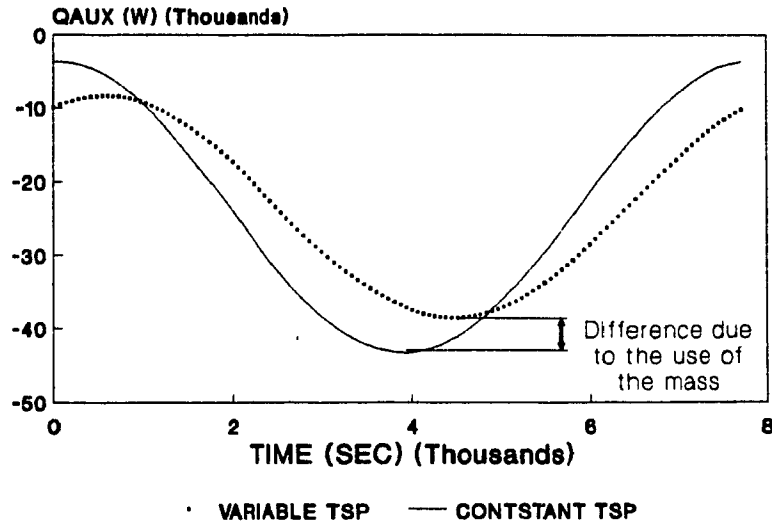


Figure 4.10 Cooling energy required for constant and varying setpoint

The mean of the temperature setpoint fluctuation as well as the constant setpoint were considered to be around the optimum comfort temperature. Since, however, the study deals with changes rather than absolute values, figure 4.9 represents the setpoint variation. In a similar manner, figure 4.8 displays the change in the load rather than its absolute value.

4.3.2 Discussion of results

Figure 4.10 shows the cooling energy required to counteract the load variation of figure 4.8. It is evident that a significant lowering of the peak demand occurs, a fact that can only be attributed to the use of the mass in the air conditioning process.

The shape, or phase, of the setpoint variation was chosen such that full use was made of the capacitive effect of the mass. The lowest temperature was reached when the lowest load occurred, and therefore when the walls were at their highest affinity for "coolness". As the load was

increasing, the setpoint was allowed to rise which in turn allowed the massive element to release its "coolness". Once the load reached its peak at which time the mass discharged the allowable "coolness", the setpoint started decreasing, allowing the mass to be charged again.

4.4 Conclusions

The studies outlined here are comparative ones and therefore experimental validation has not been attempted. However, the results are in general agreement with those described by Athienitis (1988). In both cases it is evident that the use of the thermal mass can lead to improved operating conditions. This capability, however, is not imparted to conventional HVAC systems by virtue of their lack of a control system that would integrate the HVAC system and the building. Instead, a conventional HVAC system seeks to maintain the indoor conditions with hardly any reference to the enclosure and with only minimal use of information from the outside, or load generating conditions.

For improved HVAC system operation it is therefore necessary to incorporate some elements that are related to the enclosure's behaviour, an approach that can not be done to any significant degree using conventional feedback controllers. Strategies, such as the ones described here, can thus be incorporated in a "performance based" control system that can make full use of the capabilities of microprocessor based control.

CHAPTER 5

A THEORETICAL STUDY OF INTEGRATED BUILDING - HVAC SYSTEM DYNAMIC CONTROL

5.1 Introduction

Conventional control systems tend to ignore the dynamic interaction between the HVAC system and the building mass resulting sometimes in discomfort due to large temperature fluctuations, energy waste and instabilities (Hartman 1988). This is particularly evident in cases where high radiative gain fluctuations are present. By its nature, the building mass introduces high thermal lags which the feedback controllers may be unable to compensate for effectively without introducing high temperature swings. In addition to this problem, the part load performance of the HVAC system poses serious problems in the operation and control of the HVAC system. In cases where the load on the system is reduced to less than the design conditions, serious instabilities may result (Hamilton et al 1974), unless action is taken to avoid them before they are manifested. Such action may require the reduction of set-points and/or increase of flow rates that will result not only in the continued stability of the system, but also in improved thermal comfort and reduced energy expenditure. Finally, another case where effective manipulation of the HVAC system will produce tangible benefits is the use of the mass of the building as a heat storage to be used by the HVAC system resulting in reduced equipment sizes, as has been discussed in chapter 4.

Dynamic control strategies are based on the knowledge of the building's thermal behaviour. Such knowledge, however, whether acquired through modelling or experimental measurements, can only be useful if it can be used to achieve improved thermal comfort and reduced energy consumption. As Hartman (1988) states, many Energy Management and Control Systems combine conventional control with "add-on" energy reduction strategies that frequently work counter to each other resulting in the achievement of neither thermal comfort nor reduced energy consumption. A control system that would be able to achieve the desirable performance is clearly one with (a) supervisory capabilities, to manipulate and orchestrate setpoints, flow rates etc., and (b) an anticipatory nature to enable it to anticipate the effect of disturbances on the room air temperature (Hartman, 1988). This system would allow the integration of HVAC system and building dynamics and would be able to anticipate the effects of load changes on comfort, energy consumption and stability considerations. The anticipatory nature of such a control system would require a computing machine that would predict the effect of a disturbance on the system and which would take corrective action to counteract it. It is apparent, therefore, that such a system would rely heavily on feedforward control algorithms. The concept of feedforward control has been developed by the process control industry (Stephanopoulos, 1984) but its application to HVAC systems has not been examined in a rigorous manner. Following is a discussion of the advantages and disadvantages of feedforward control as well as its comparison and subsequent combination with the feedback control approach.

5.2 Control system design approaches

Figure 5.1 shows the basic differences between feedforward (fig. 5.1a) and feedback (fig. 5.1b) control loops. From these two figures it is obvious that, whereas the feedback controller reacts in a compensatory manner after the disturbance has produced a deviation from the desired output, the feedforward controller senses the disturbance before it produces the deviation in an anticipatory manner.

To demonstrate the steps that have to be taken for the design of a feedforward controller, the simple room model, model 3, is used. For simplicity, only one disturbance, the ambient temperature $T_0(s)$, is used,

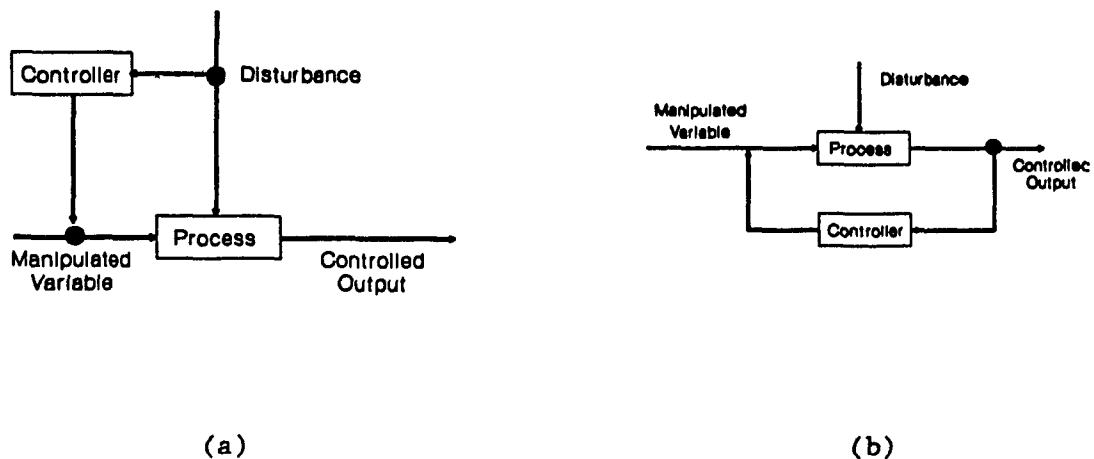


FIGURE 5.1 Structure of (a) feedforward and (b) feedback control loops

while the HVAC system is represented with the auxiliary heating (or cooling) $Q_{aux}(s)$ as its final manipulated variable. $T_{a1}(s)$, the room air

temperature, is the output of the system. $G_0(s)$ and $G_q(s)$ are the transfer functions that relate the effect of the disturbance $T_0(s)$ and $Q_{aux}(s)$ respectively on the room air temperature. $G_0(s)$ is therefore the ratio of the impedance of the room air node to the envelope resistance, while $G_q(s)$ is the product of the transfer function of a heat extracting or adding element (such as an electric heater) and the impedance at the room air node .

Consider the block diagram of the process in figure 5.2a. From this diagram the energy balance is :

$$T_{ai} = Q_{aux}G_q + T_0G_0 \quad (5.1)$$

If T_{ai} is set equal to T_{aisp} (the desired set-point temperature), then equation 5.1 becomes:

$$T_{aisp} = Q_{aux}G_q + T_0G_0 \quad (5.2)$$

Therefore, in terms of the manipulated variable, Q_{aux} , equation 5.2 becomes:

$$Q_{aux} = \left[\frac{1}{G_0} T_{aisp} - T_0 \right] \frac{G_0}{G_q} \quad (5.3)$$

which determines the nature of the feedforward control system. Figure 5.2b shows the transfer functions that form the feedforward controller:

$G_c = G_0/G_q$ being the transfer function of the main feedforward controller while

$G_{SP} = 1/G_0$ is the set point element transfer function that governs the steady state and transient characteristics for changes in the set-point.

Inclusion of the sensor (or measuring device) transfer function G_m and of the final control element (such as an SCR or a valve) transfer function G_f modifies the block diagram somewhat (figure 5.2c). Both G_c and G_{SP} are also modified, as will be shown. From figure 5.2c the room air temperature T_{ai} is defined as follows:

$$T_{ai} = G_q G_f G_c G_{SP} T_{ai,sp} + [G_0 - G_q G_f G_c G_m] T_0 \quad (5.4)$$

Based on this equation, two important aspects of feedforward control can be defined:

1. Disturbance elimination, i.e. the reduction of the coefficient of T_0 to zero i.e.:

$$G_0 - G_q G_f G_c G_m = 0 \quad (5.5)$$

which results in the new feedforward controller transfer function:

$$G_c = G_0 / G_q G_f G_m \quad (5.6)$$

2. Set-point tracking, that is keeping the coefficients of $T_{ai,sp}$ to one so that T_{ai} is kept identical to $T_{ai,sp}$. This is achieved as follows:

$$G_q G_f G_c G_{SP} = 1 \quad (5.7)$$

Substituting G_c from equation (5.6)

$$G_q G_f G_{SP} (G_0 / G_q G_f G_c G_m) = 1 \quad (5.8)$$

therefore

$$G_{SP} = G_m / G_q \quad (5.9)$$

If G_m and G_f are equal to unity, then both G_c and G_{SP} are reduced to the definitions in equation (5.3).

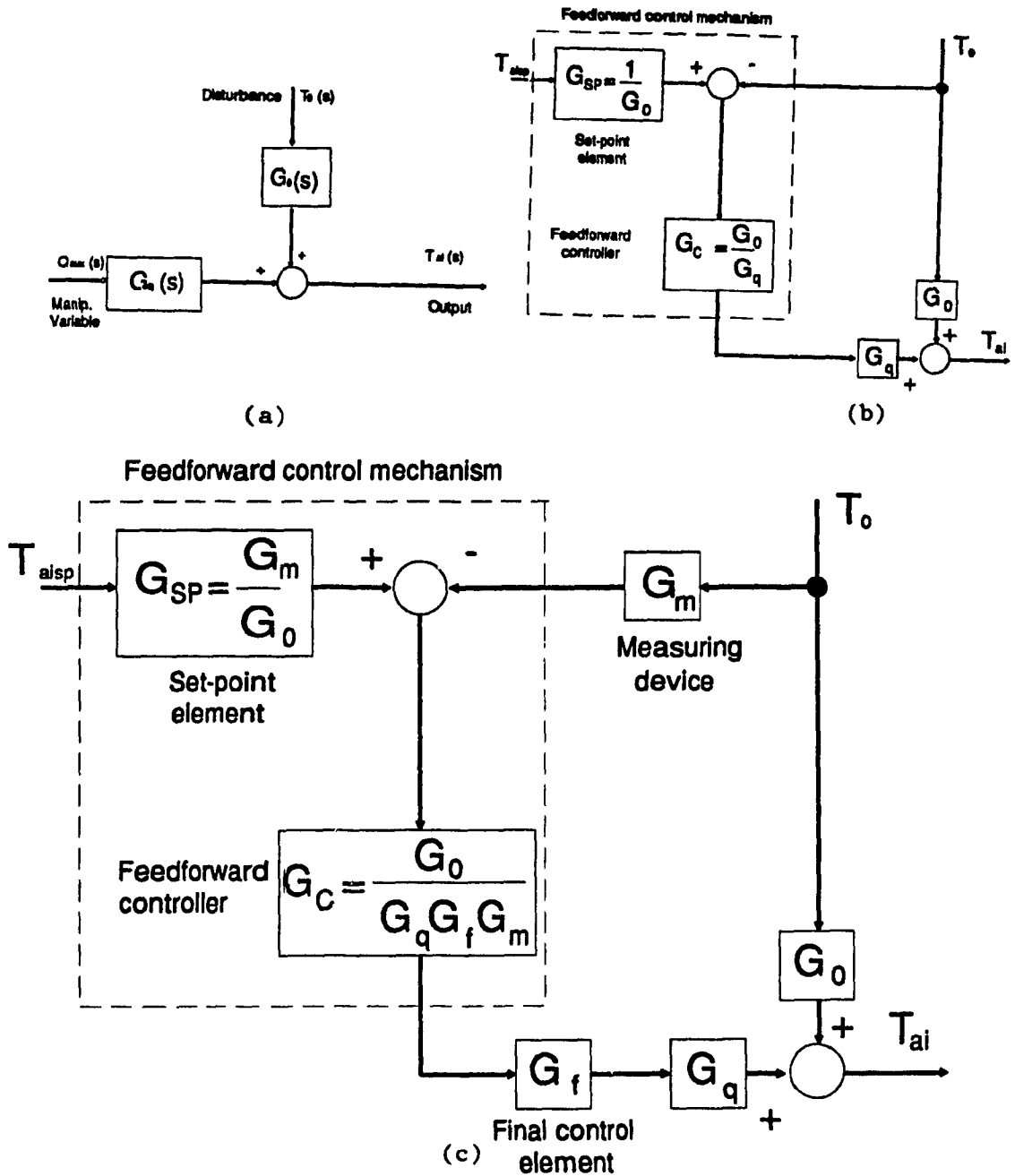


Figure 5. 2 Block diagrams for (a) process (b) feedforward loop
 (c) feedforward loop with measuring device and final control element

It should be noted that if the block diagram in figure 5.2c (or 5.2b) is reduced we obtain:

$$T_{ai} = T_{aisp} - T_0 G_0 + T_0 G_0 = T_{aisp} \quad (5.10)$$

i.e. we have perfect control since we anticipate the effect of T_0 on the air temperature.

5.2.1 Comparison of feedforward and feedback control systems

From the preceding discussion, several observations can be made. The feedforward control loop retains most of the external characteristics of a feedback loop, such as a measurement which is compared to a setpoint signal with the resulting signal being the actuating one. The similarities, however, stop here and two important differences are evident:

1. The feedforward controller cannot be a conventional feedback controller (P, PI, PID) but rather is an algorithm implemented using a digital interface.
2. The feedforward loop strives to maintain perfect control by cancelling the disturbance before it is manifested in the output, while the feedback loop senses the error in the output and then attempts to correct it.

The effectiveness, however, of a feedforward control loop depends on an exact knowledge of the system transfer functions and a correct measurement of all possible disturbances. This is a serious drawback especially since a feedforward is an open loop with no recourse of action after the introduction of an error to the output introduced by, say, model oversimplification.

5.2.2 Feedforward-feedback control

To overcome these shortcomings of the feedforward control loop, a feedback loop is included (figure 5.3) which compensates for most of the weaknesses of the feedforward control loop, specifically where errors are introduced through modelling inaccuracies or unaccounted for disturbances. When dealing with thermal lag effects and time delays associated with heat storage, this hybrid control system combines the good performance of the feedforward control with the relative insensitivity of the feedback control loop to errors in modelling and identification/measurement of disturbances.

To demonstrate the approach to be taken for the design of such a system, figure 5.3, which includes the transfer functions introduced in the earlier sections, has been constructed. From the previous discussion:

$$T_{ai} = Q_{aux}G_q + T_0G_0 \quad (5.11)$$

Therefore from figure 5.3 the value for Q_{aux} is given by:

$$Q_{aux} = C_f c = G_f(c_1 + c_2) = G_f G_{c1} \epsilon_1 + G_f G_{c2} \epsilon_2 \quad (5.12)$$

Rearranging and substituting for ϵ_1 and ϵ_2

$$Q_{aux} = G_f G_{c1} (T_{aisp} - G_{m1} T_{ai}) + G_f G_{c2} (G_{SP} T_{aisp} - G_{m2} T_0) \quad (5.13)$$

Replacing Q_{aux} in equation 11 by equation 13 and rearranging:

$$T_{ai} = \frac{G_q G_f (G_{c1} + G_{c2} G_{SP})}{1 + G_q G_f G_{c1} G_{m1}} T_{aisp} + \frac{G_0 - G_q G_f G_{c2} G_{m2}}{1 + G_q G_f G_{c1} G_{m1}} T_0 \quad (5.14)$$

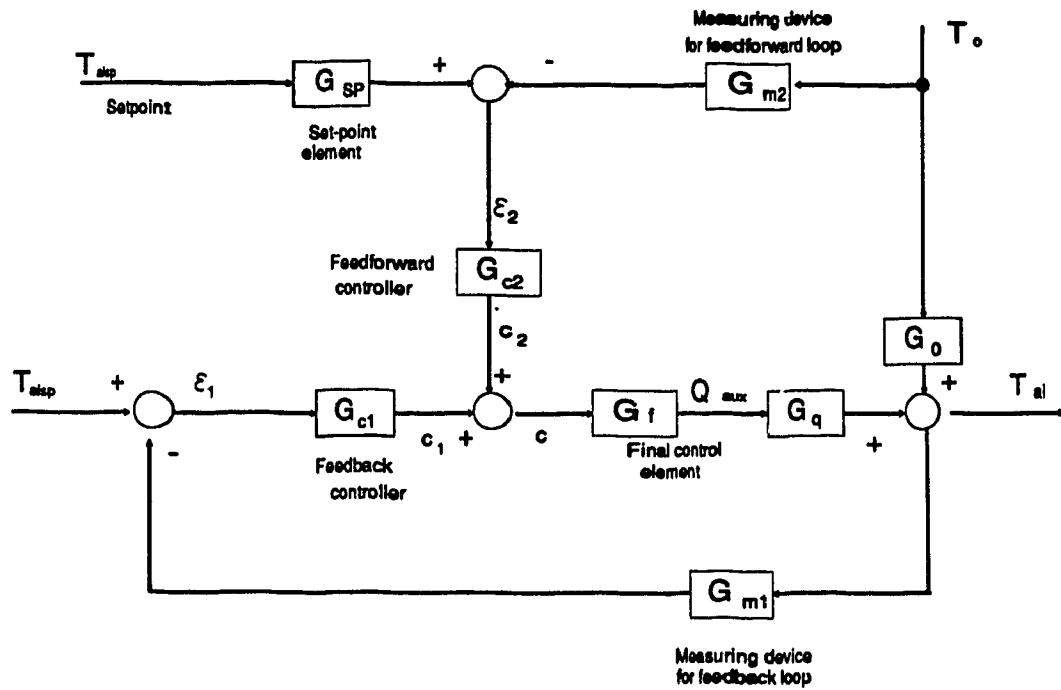


Figure 5.3 Diagram for feedforward-feedback control loop

This equation displays the characteristics of the hybrid control system:

1. Since the stability of the closed loop response depends on the following characteristic equation:

$$1 + G_q G_f G_{c1} G_{m1} = 0 \quad (5.15)$$

it is evident that the addition of a feedforward loop does not change the stability characteristics of the feedback loop.

2. If the transfer functions of the feedforward loop are known exactly, ϵ_1 remains zero since all disturbances are anticipated and compensated for before they have an effect on T_{ai} .
3. If any of the feedforward loop transfer functions are only known approximately, then:

$$G_0 - G_q G_f G_{c2} G_{m2} \neq 0 \quad (5.16)$$

and

$$G_q G_f G_{c2} G_{SP} \neq 1 \quad (5.17)$$

which results in imperfect control producing an error which causes $\epsilon_1 \neq 0$ and $T_{ai} \neq T_{aisp}$. In this case the feedback loop is activated and compensates for ϵ_1 .

Although the properties of the feedforward and the combined feedforward-feedback control systems have been compared to the simple feedback loop and described extensively here, it would be instructive to study their relative behaviour in dealing with a simulated condition.

5.3 A comparative study of feedback and feedforward control

In order to demonstrate the differences, advantages and disadvantages of the different control system design approaches, a constant volume system is considered that serves the theatre described in appendix A. Since, however, it is desirable to study the transient time responses of the system, the discrete frequency approach that has been used in chapter 4 is not appropriate. It is therefore necessary to use a

numerical approach to invert the transfer function representing the system.

5.3.1 Numerical inversion of Laplace transforms

The transfer functions describing the HVAC system components as well as the transfer functions describing the room model can easily be used to study their frequency responses by simply substituting s with $j\omega$ and can be combined to produce the system's overall transfer function if needed, or can be studied individually or in sub-systems in both the frequency and time domain.

One shortcoming that cannot be overcome using the DFT is the response of the system to a step or a ramp forcing function. Since studies involving the responses of systems to forcing functions of this nature can reveal further characteristics on the behaviour of the system, it is desirable to incorporate an additional mathematical approach to the study of the HVAC system-building envelope interaction that would allow the numerical inversion of the system transfer function and which would use the symbolic representation used by the DFT directly. Such an approach would therefore be required to numerically invert the transfer functions which in effect are Laplace transforms of each model's describing differential equations.

Different numerical methods for Laplace transform inversion are available, but in general, they require the determination of poles and residues which might be computationally prohibitive if multiple poles occur. The method for the numerical inversion of the Laplace transforms developed by Vlach (1969) and improved by Singhal et al (1975,1976,1981)

provides an efficient way to calculate the time response of systems without determining poles or residues. In addition, the method can easily be incorporated in programs dealing with the frequency response analysis of systems with very few changes in the program. It is applicable to stiff systems, those with multiple poles and also those with distributed parameter elements.

By definition, the inverse Laplace transform $v(t)$ of a transfer function $V(s)$ is found through the use of the formula

$$v(t) = \frac{1}{2\pi j} \int_{c-j\infty}^{c+j\infty} V(s) e^{st} ds \quad (5.18)$$

The exact inversion, however, is only possible if the poles of $V(s)$ are known. To avoid root finding, Vlach and Singhal proposed the substitution of st with z thus arriving at the formula

$$v(t) = \frac{1}{2\pi j} \int_{c'-j\infty}^{c'+j\infty} V(z/t) e^z dz \quad (5.19)$$

and subsequently approximating e^z by a Padé rational function

$$R_{N,M}(z) = \frac{P_N(z)}{Q_M(z)} = \frac{\sum_{i=0}^N (M+N-i)! \binom{N}{i} z^i}{\sum_{i=0}^M (-1)^i (M+N-i)! \binom{M}{i} z^i} \quad (5.20)$$

where $P_N(z)$ and $Q_M(z)$ are polynomials of orders N and M respectively.

The first $M+N+1$ terms of this function's Taylor expansion are equal to those of the Taylor expansion of e^z and when (5.20) is inserted in (5.19), the approximation $v'(t)$ to $v(t)$ becomes

$$v'(t) = \frac{1}{2\pi j} \int_{c'-j\infty}^{c'+j\infty} V(z/t) R_{M,N}(z) dz \quad (5.21)$$

This integral can then be evaluated using the residual theorem by closing the path of integration along an infinite arc either to the left (counterclockwise) or to the right (clockwise). To eliminate any contribution from the path along the infinite arc, M and N are chosen such that the function

$$F(z) = V(z/t) R_{N,M}(z) \quad (5.22)$$

has at least two more poles than zeros. Then

$$\int F(z) dz = \pm 2\pi j (\text{sum of the residue of } (z) \text{ at its poles in the closed path})$$

the sign being dependent on the direction the path is closed. If N and M are chosen such that $N < M$ then

$$R_{N,M}(z) = \sum_{i=1}^M \frac{K_i}{z-z_i} \quad (5.23)$$

where K_i are the residues and z_i the poles of $R_{N,M}$. Closing the path of integration around the poles of $R_{N,M}$ in the right half plane Singhal and Vlach arrived at

$$R_{N,M}(z) = - \frac{1}{t} \sum_{i=1}^M K_i V(z_i/t) \quad (5.24)$$

which is the basic inversion formula.

Real time functions can now be evaluated by using only the poles z_i in the upper half plane, thus reducing the computations to one half.

If M is even and the bar denotes complex conjugate

$$v'(t) = - \frac{1}{t} \sum_{i=1}^{M'} K_i V(z_i/t) - \frac{1}{t} \sum_{i=1}^{M'} K_i \bar{V}(\bar{z}_i/t) \quad (5.25)$$

$$= - \frac{1}{t} \sum_{i=1}^{M'} 2\text{Re}[K_i V(z_i/t)] \quad (5.26)$$

$$= - \frac{1}{t} \sum_{i=1}^{M'} \text{Re}[K'_i V(z_i/t)] \quad (5.27)$$

where $M' = M/2$ and $K'_i = 2K_i$

Values for K'_i and z_i for different M and N were calculated and tabulated by Singhal et al (1976).

This method was particularly useful for the study that will be described in this chapter since it does not require discretization of distributed elements such as a massive floor slab. It also allows the use of dead times (time lags) without any artificial manipulation of the constants present, as is required if other numerical methods are used (Clark 1985). Further, it can be readily incorporated within a program for frequency response analysis because the transfer functions are already determined as functions of s ($= j\omega$)

5.3.2 DYCON: A program for time and frequency domain studies of building - HVAC system dynamics

DYCON is a program that was developed as part of this thesis and incorporates both frequency and time domain capabilities in the study of HVAC system dynamics.

The structure of DYCON is shown in figure 5.4. The main feature of this program is its capacity for the user to specify one of three venues to study the dynamics of HVAC systems:

1. Simulation using the numerical inversion of Laplace transforms.
2. Analysis of the dynamics through the study of the system's response at discrete frequencies, and
3. Analysis of the system dynamics through the study of the periodic response of the system using the inverse discrete Fourier transform.

The models used by DYCON are all described in the s domain and can therefore be used for simulation purposes by the numerical inversion of Laplace transforms. As well, by simply substituting $j\omega$ for s , frequency response studies, such as those described in chapter 3, can be performed. In addition, through the use of the discrete Fourier transform and its inverse, the response of the system to periodic forcing functions can also be studied. The room models available to the user have already been described in chapter 3, while the system components are described below. Following this, the study of the possibilities offered in integrating the HVAC system with the room for improved system performance will be discussed.

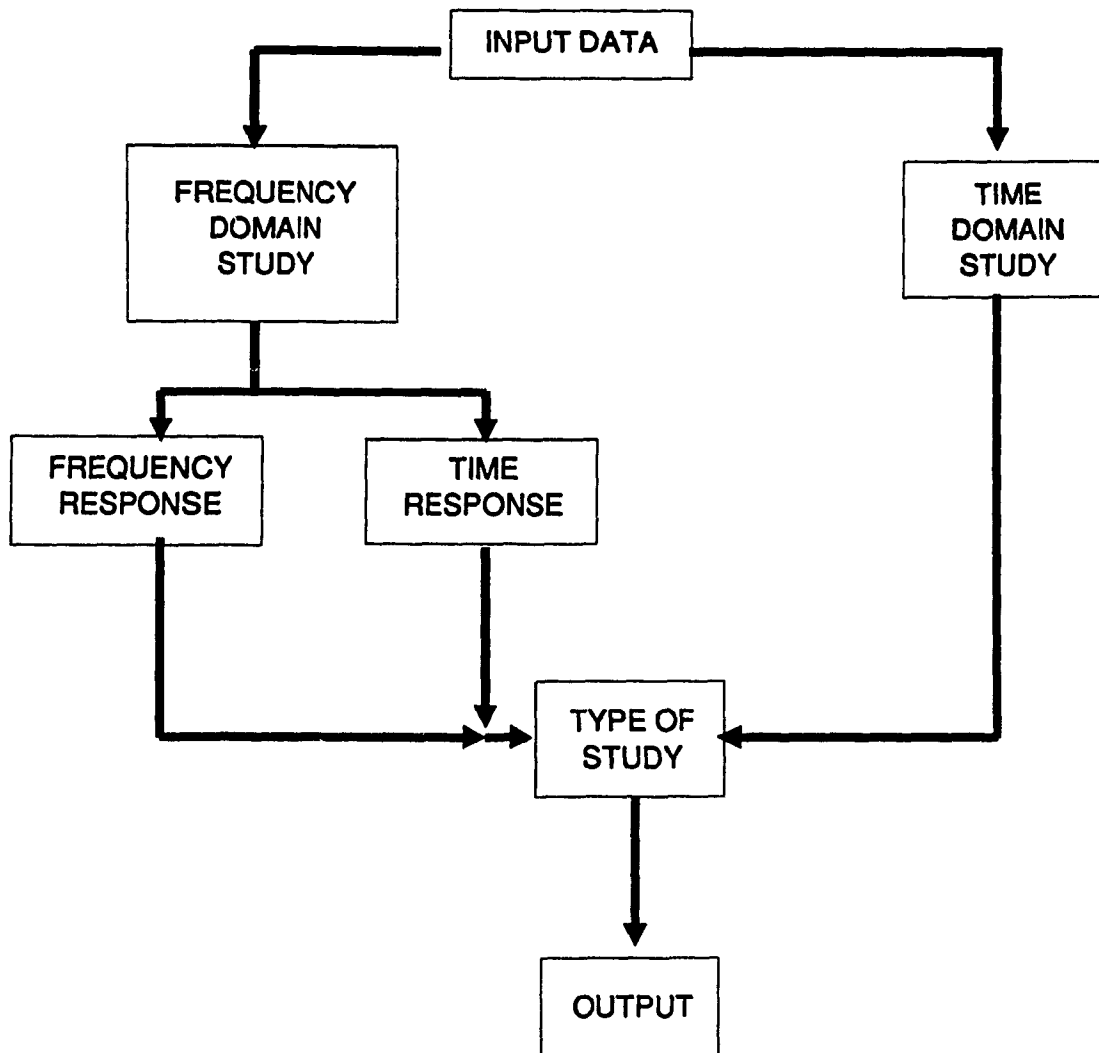


Figure 5.4 The structure of DYCON

5.3.2.1 Air ducts

The object of the HVAC air distribution system is to provide the proper combination of temperature, humidity and air motion in the occupied space. A complete model for the air distribution system should account for the effect that changes in the above conditions at the outlet of the heat exchanger will have on the thermal comfort of the occupants of the conditioned space.

The model used by DYCON was developed by Tobias (1973) and deals with only the temperature response of air flowing through the duct. The model development assumes constant and uniform temperature of the air surrounding the duct and describes the temperature of air flowing through the duct at any distance based on the following equations:

$$\rho_a \cdot A_d \cdot c_{pa} \cdot \frac{\delta T_{d,a}}{\delta t} + m_a \cdot c_{pa} \cdot \frac{\delta T_{d,a}}{\delta y} + h_{i,d} \cdot (T_{d,a} - T_d) = 0 \quad (5.28)$$

and

$$dd \cdot c_{pd} \cdot \frac{\delta T_d}{\delta t} + (h_{i,d} + h_{o,d}) \cdot T_d - h_{i,d} \cdot T_{d,a} = 0 \quad (5.29)$$

Taking the Laplace transform of the two partial differential equations:

$$\frac{m_a \cdot c_{pa}}{h_i} \cdot \frac{\delta T_{d,a}}{\delta y} + T_{d,a} \left(\frac{\rho_a \cdot A_d}{m_a} - \frac{m_a \cdot c_{pa}}{h_i} s + 1 \right) = T_d \quad (5.30)$$

$$T_{d,a} \left(\frac{dd \cdot cp_d}{h_i + h_o} \cdot s + 1 \right) = \frac{h_i}{h_i + h_o} T_{d,a} \quad (5.31)$$

Solving for $T_{d,a}$ the following equation is obtained:

$$\begin{aligned} \frac{T_{d,a}(y,s)}{T_{d,a}(0,s)} &= \exp\left(-\frac{y}{V} \cdot s\right) \cdot \exp\left(-\frac{y}{L} \cdot \left(1 - \frac{K}{r \cdot s + 1}\right)\right) \\ &= \exp\left(-\frac{y}{V} \cdot s\right) \cdot \exp\left(-\frac{(1-K) \cdot y}{L}\right) \cdot \exp\left(-\frac{K \cdot y}{L} \cdot \frac{r \cdot s}{r \cdot s + 1}\right) \end{aligned} \quad (5.32)$$

where:

$$K = \frac{h_i}{h_i + h_o}$$

$$r = \frac{dd \cdot cp_d}{h_o + h_i}$$

$$L = \frac{m_a \cdot cp_a}{h_i}$$

$$V = \frac{m_a}{A_d}$$

Each exponential has its own contribution to the overall transfer function. The first exponential i.e. $\exp(-(y/V) \cdot s)$ is the transport delay, namely, the time it takes to travel y meters at V m/s. The second exponential is the attenuation of the temperature rise of the air above the ambient air temperature at any location in the duct when the heat exchanger air outlet temperature is constant. Finally, the third exponential represents the additional attenuation and phase shift in the

duct air temperature due to changing heat exchanger air outlet temperature.

5.3.2.2 Heat exchangers

Although the user has the choice of entering the gain and time constant describing the heat exchanger, DYCON provides a model for the calculation of these parameters.

In order to choose a model from the large number of heat exchangers models available in literature, three criteria were established which would have to be satisfied if the model were to be included:

1. The behaviour of particular interest is the response of the discharge air temperature to step change in water flow rate.
2. The thermal properties of the fin should be included in the model.
3. A criterion by which the validity of the model for the heat exchanger under consideration can be ascertained.

The model fulfilling all three criteria is a first order model of a serpentine cross-flow heat exchanger developed by Boot et al (1977) which was based on an earlier work by Pearson et al (1974). Details of the derivation of the algebraic expressions for the gain and the time constant of the coil are given in appendix C.

5.3.2.3 Control valves

Control valves are designed to maintain any of a number of mathematical relations between the valve stroke and the effective port

area known as the "flow characteristic" of the valve. The actuator thus moves the valve stem, either sliding or rotary, to establish the desired port area through the valve.

The flow characteristic of a valve defines the flow behaviour as the valve plug stem moves in response to controller signals. This definition allows for consideration from two points of view:

1. The installed flow characteristic which is the actual relationship between the valve stroke and the flow rate, and
2. The inherent flow characteristic which is based on a constant pressure drop across the valve body throughout the stroke and which is the one presented in the industry's catalogues.

As was mentioned in chapter 2, the two types of valves widely used are those having a linear and those having an equal percentage inherent flow characteristic. Although equal percentage valves offer an apparently non-linear relationship between the stroke and the increase in flow, the combined response of an equal percentage valve and the associated pipe circuit often approaches linearity. It should therefore be stressed here that the valve is assumed to have a linear installed characteristic.

The model used by DYCON is described by equation

$$\frac{\Delta m_w(s)}{\Delta y} = \frac{K_v}{1 + \tau_v s} \quad (5.33)$$

where $\Delta m_v(s)$ - mass flow rate variation in s-domain
 Δy - change in valve stroke
 K_v - valve gain (input)
 τ_v - valve time constant (input)

5.3.2.4 Sensors

Sensors are generally described by a first order transfer function. In addition, DYCON allows for entering a time delay to account for any positioning delays between the sensing element and the comparator.

$$G_s(s) = \frac{e^{-\tau s}}{1 + \tau_s s} \quad (5.34)$$

where τ - time lag (input)

τ_s - sensor time constant (input)

5.3.2.5 Controller

DYCON allows the user to describe a P, PI or PID controller the most often used being a PI controller which is described by the equation:

$$G_{\text{control}}(s) = K_p \left(1 + \frac{1}{\tau_i s} \right) \quad (5.35)$$

where K_p - proportional gain

τ_i - integral time

In addition to the components described above, the program allows for the introduction of a time delay within the system to allow for inclusion of considerations for mixing of the supply with the room air.

The user can exclude any, some, or all, of the components described above depending on the type of system he wishes to study.

5.3.3 Feedback control of the system

The block diagram for the basic system used for the study is shown in figure 5.4 while the parameters describing it and those describing the room model are in appendix A in the format of DYCON input screens.

The room is assumed to be a theatre which is $20 \times 25 \times 7 \text{ m}^3$. The load, equivalent to about 160 people entering over a period of 15 minutes, is 60 kW of which 10% or 6 kW is radiative, the rest being convective.

The transfer functions relating the radiative and convective loads as well as temperature setpoint changes to the room air temperature can be derived from figure 5.4:

$$T_{a11} = T_{a1sp} * \frac{G_c G_x}{1 + G_c G_x G_s} \quad (5.36)$$

$$T_{a12} = Q_{rad} * \frac{Z17}{1 + G_c G_x G_s} \quad (5.37)$$

$$T_{a13} = Q_{conv} * \frac{Z11}{1 + G_c G_x G_s} \quad (5.38)$$

where $G_x = G_{valve} G_{coil} G'_{duct} Z11$

$$G'_{duct} = G_{duct} c p_a m_a$$

therefore their combined effect is

$$T_{ai} = T_{a11} + T_{a12} + T_{a13} \quad (5.39)$$

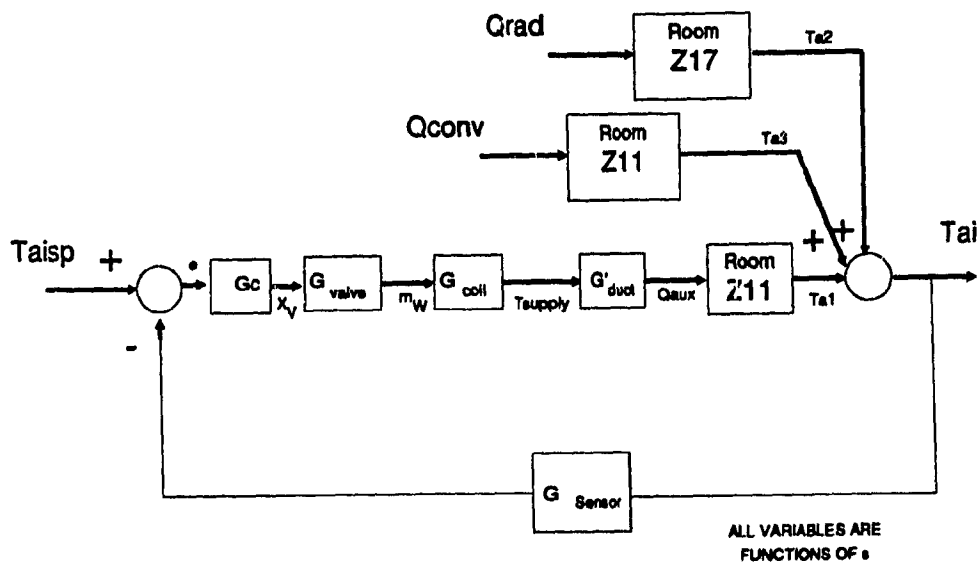
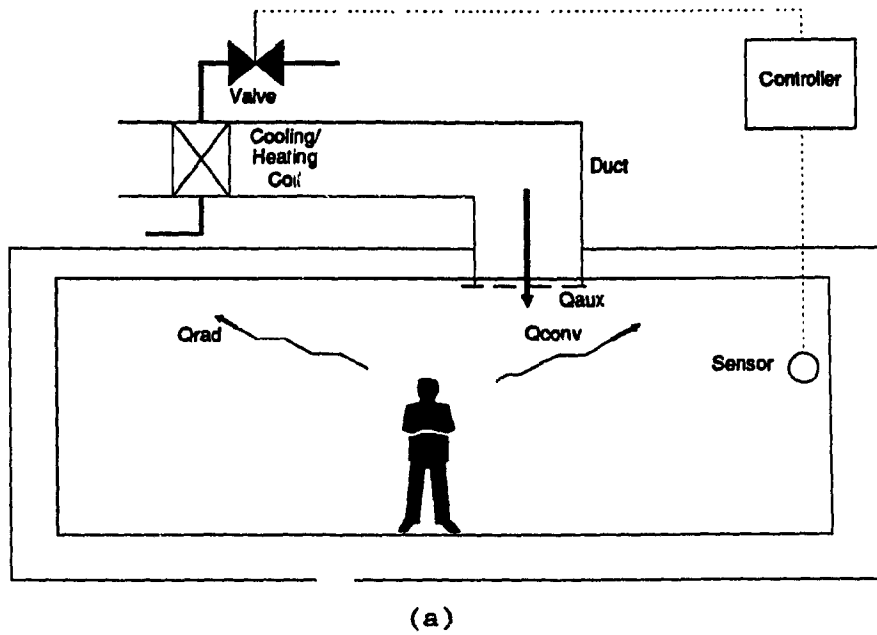


Figure 5.5 (a) Schematic of room and HVAC system, (b) Block diagram of the system

Since the room air temperature is controlled by a PI controller, it was desired to estimate the proportional gain and integral time which will produce a stable operation of the system. DYCON provides the capability to the user to study the response of a system in both frequency and time domains.

To establish these controller constants, the Ziegler-Nichols tuning approach was taken (Stephanopoulos 1984). Using only proportional control action, and with the feedback loop closed, a unit setpoint change was introduced and the proportional constant was varied until the system oscillated continuously. The gain at which this occurs, is called the ultimate gain and the period of the oscillation is known as the ultimate period.

This procedure was carried out using the simulation capabilities of DYCON for two systems; one for the system described by figure 5.4 and shown in figure 5.5, and the other for a system with the same properties as the previous one but which included a delay of 300 seconds to account for poor supply air distribution design (fig. 5.6).

The ultimate gain for the first case was 55 control units/°C, while the ultimate period was 600 seconds. The open loop frequency analysis, carried out using the frequency domain capabilities of DYCON, produced results that agree with the time domain response of the system (figure 5.7). As was expected, the ultimate gain for the case that included the delay was much lower (15 c.u./°C), while the period of oscillation was much higher (1800 sec.). The frequency response of this system also agreed with the time domain response (fig. 5.8). The second cross-over point of the frequency response at a period of about 600 seconds, was of no consequence to the

stability considerations. If only frequency domain analysis were used in this study, there would be no way of determining if this period were related to the stability of the system or not. In effect, this points to the fact that for a thorough study of the dynamics of systems, both frequency and time domain methods should be used.

The controller constants were calculated according to the Ziegler-Nichols tuning technique; the ultimate gain was divided by 2.2 to result in the proportional gain of the PI controller, while the integral time was calculated by dividing the ultimate period by 1.2.

Due, however to the high overshoot produced by the system that incorporated the 300 seconds delay, the controller constants were adjusted so that the overshoot was reduced by increasing the integral time of the PI controller and decreasing the proportional gain, thus producing a more sluggish response, but one with a lower overshoot (figure 5.9).

In both cases the responses (fig. 5.9, 5.10) were typical of feedback systems. As expected, the system with the delay produced a higher overshoot than the base case which was the result of the controller constants required for stability considerations.

These two studies show the significant shortcomings that are inherent in feedback control systems. Regardless of the care taken in designing a feedback control system, any significant delays that may be present (whether due to high radiative loads or otherwise) will have a detrimental effect on the behaviour of the system, primarily because feedback control design approaches cannot account for them and require that low gains be used to protect the system from instabilities.

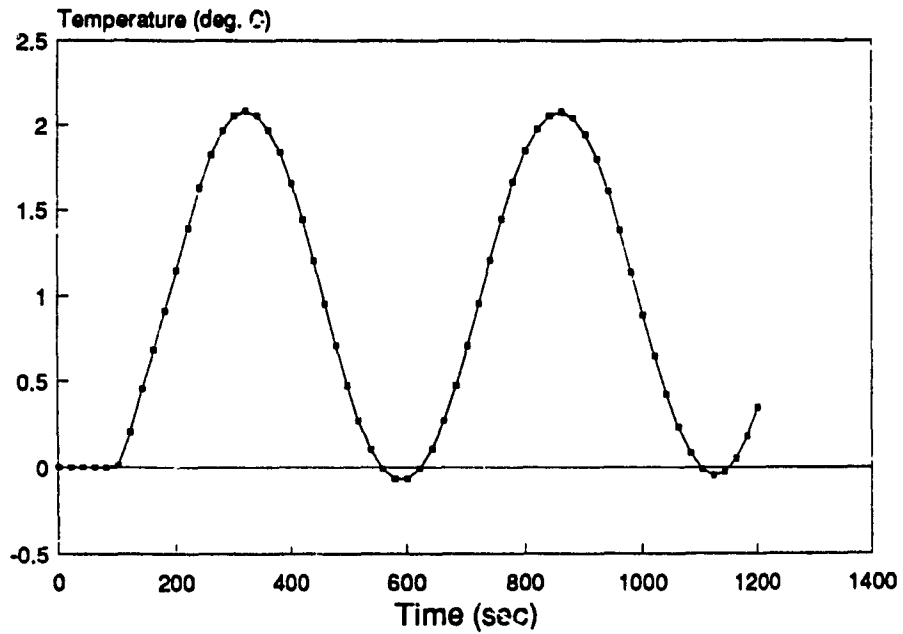


Figure 5.6 Time response at the stability limit for calculation of K_p and τ_1 for feedback loop: Base case

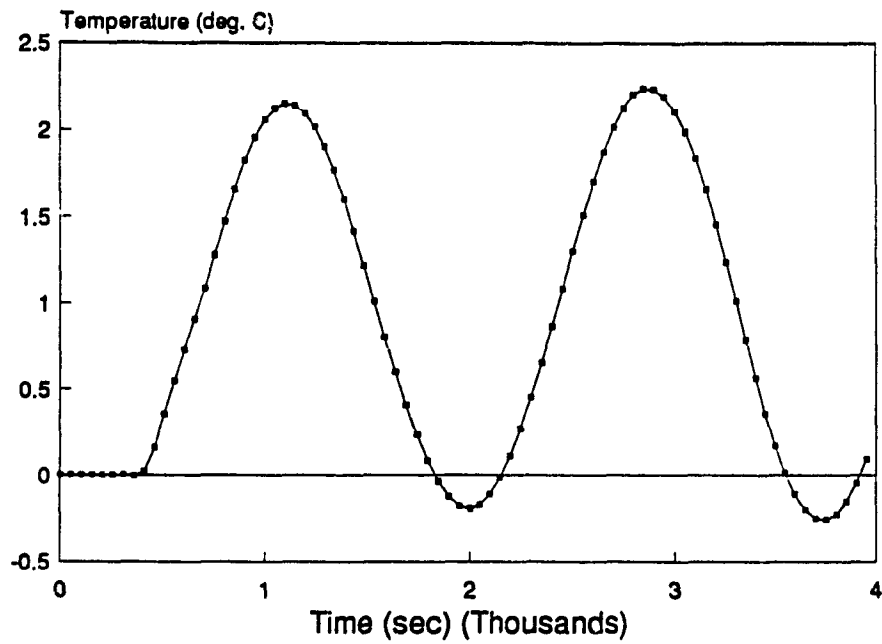
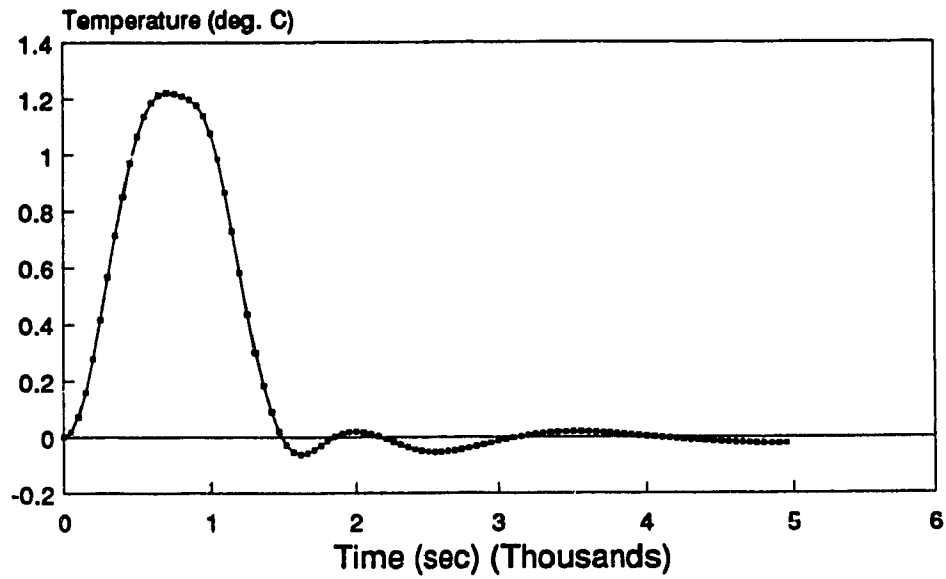
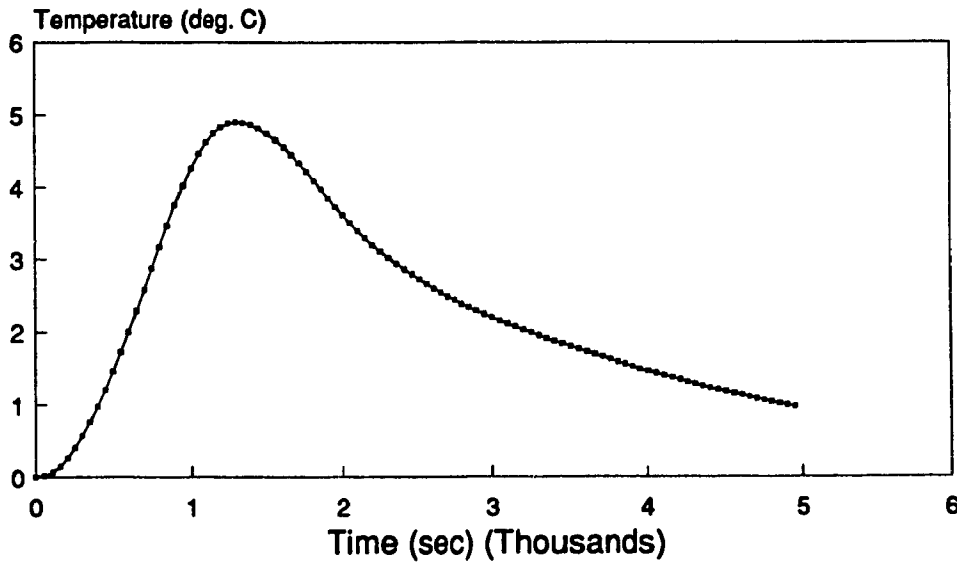


Figure 5.7 Time response at the stability limit for calculation of K_p and τ_1 for feedback loop: System with 300 sec delay



— $K_p=25, T_i=500$

Figure 5.8 Time response of system : Base case



— $K_p=6, T_i=1600$

Figure 5.9 Time response of system : System with 300 sec delay

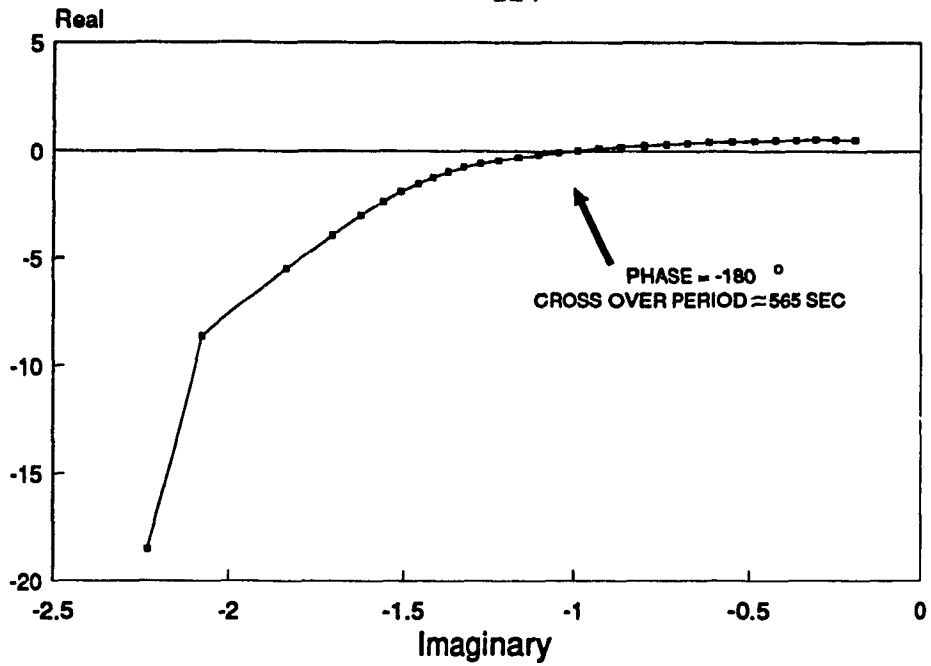


Figure 5.10 Frequency response of the system : Base case

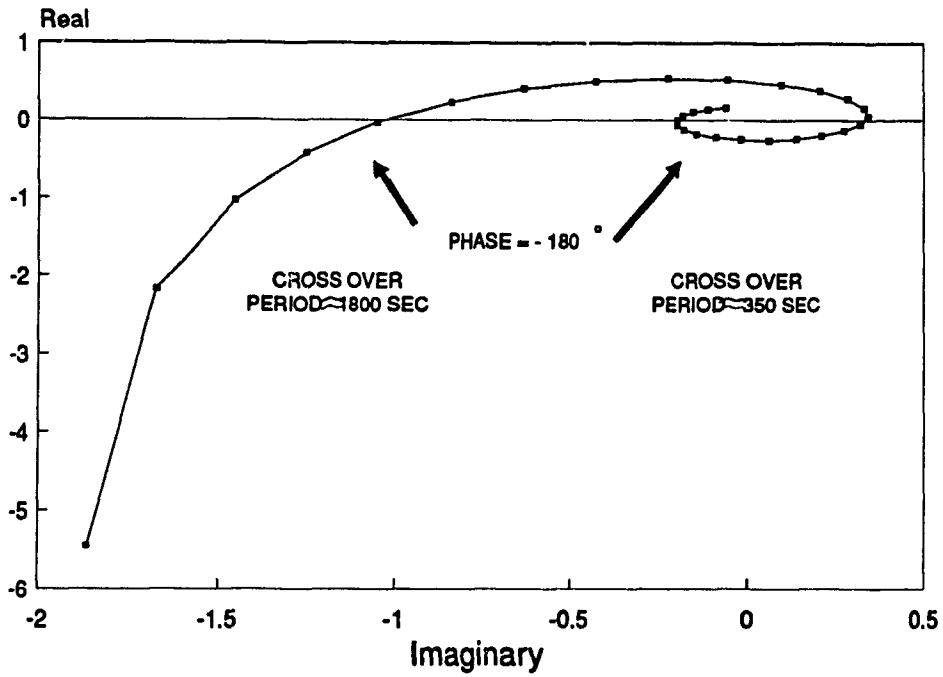


Figure 5.11 Frequency response of the system : System with 300 sec. delay

In effect, the feedback control system's inability to respond well to the presence of delays, renders it an inappropriate system for enclosures with high radiative loads and precludes any consideration of integrating the enclosure mass influences on room air temperature variations.

5.3.4 Feedforward control system

Since the conventional building control system design approach, namely, feedback control, does not have capabilities to combine the characteristics of both HVAC system and building enclosure into an effective unit, a new approach is needed. This new approach, namely, feedforward control, is based on the knowledge of the system which is composed of both the HVAC system and the building enclosure. If the system can be accurately modelled and the disturbances precisely measured, then perfect control is possible. This property of the feedforward control differentiates it from predictive control which, by definition, is based on probabilistic projections. Predictive control may, however, be part of feedforward control as a tool to describe optimum setpoint profiles or in cases where disturbances either cannot be measured accurately or their effect is not well known.

To describe the development of the feedforward control loop it is necessary to start from the fundamental energy balance (see fig.5.5b):

$$T_{ai} = Q_{aux}Z11 + Q_{conv}Z11 + Q_{rad}Z17 \quad (5.40)$$

Since the objective of the feedforward control loop is to maintain the room temperature at the desired setpoint:

$$T_{ai} = T_{aisp} = Q_{aux}Z11 + Q_{conv}Z11 + Q_{rad}Z17 \quad (5.41)$$

Therefore, if the disturbance is known beforehand or it is measured as it occurs, and the enclosure's transfer functions are known, then the auxiliary energy required can be supplied as needed completely counteracting the disturbances and producing perfect control. This can be expressed as follows:

$$Q_{aux} = \frac{T_{aisp}}{Z_{11}} - Q_{conv} - Q_{rad} \frac{Z_{17}}{Z_{11}} \quad (5.42)$$

Equation 5.42 can be used to arrive at the movement of the valve stem required to produce the Q_{aux} needed for perfect control, provided the HVAC system's component transfer functions are known.

Thus if x is the valve stem movement then:

$$Q_{aux} = x*(G_{valve}G_{coil}G'_{duct}) \quad (5.43)$$

Therefore equation 5.42 can be expressed as:

$$x = \frac{T_{aisp}}{G_x} - \frac{Q_{conv}Z_{11}}{G_x} - \frac{Q_{rad}Z_{17}}{G_x} \quad (5.44)$$

Where $G_x = G_{valve}G_{coil}G'_{duct}Z_{11}$

Therefore, provided the disturbances and the transfer functions of the system are exactly known, then T_{ai} can be maintained at T_{aisp} by moving the valve stem accordingly .

It must be noted that the feedforward control loop (fig. 5.12) is a computational machine that accepts as inputs the measured (or expected) disturbances. Using an algorithm, it computes the loads on the system and dictates to the final control element (the valve) the response required to offset the effect of the loads before they manifest themselves as temperature fluctuations.

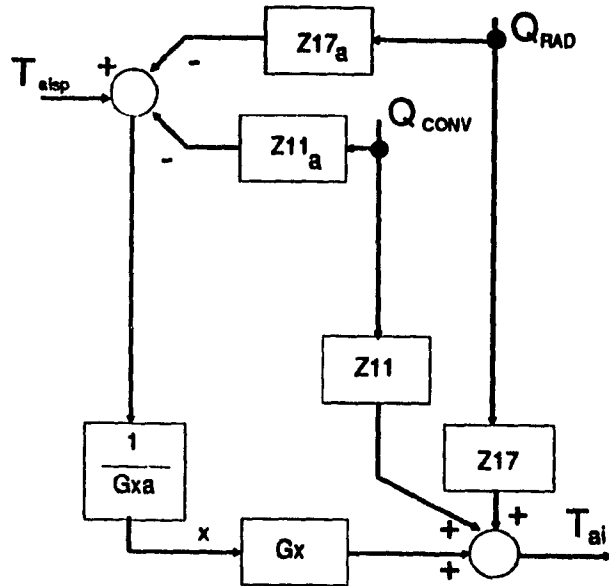


Figure 5.12 Feedforward loop

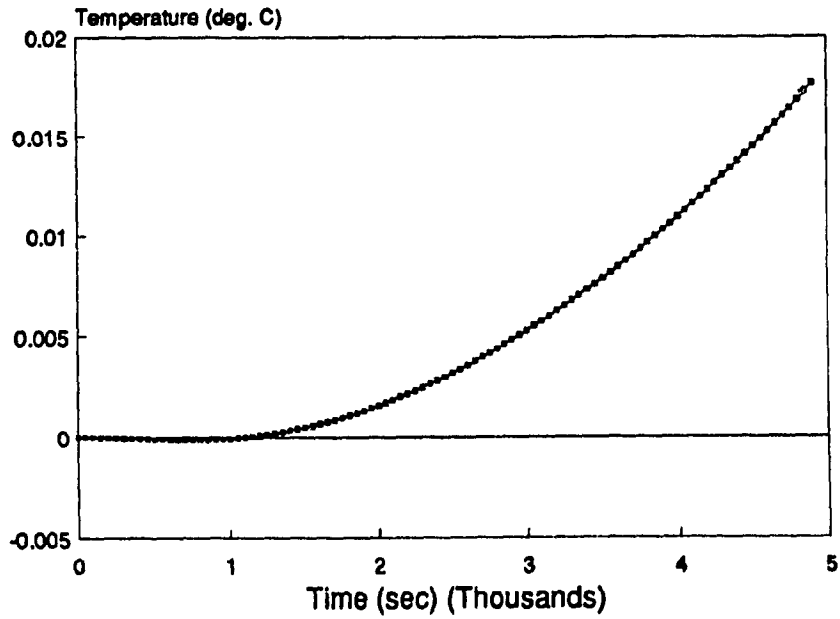


Figure 5.13 Feedforward loop time response

The block diagram of the feedforward control loop is shown in figure 5.12 where the subscript *a* denotes approximate as opposed to actual transfer functions. The resulting transfer functions describing each input's contribution to the room air temperature T_{ai} is therefore:

$$T'_{ai1} = T_{aisp} \frac{G_x}{G_{xa}} - Q_{rad} Z17_a - Q_{conv} Z11_a \quad (5.45)$$

$$T'_{ai2} = Q_{rad} Z17$$

$$T'_{ai3} = Q_{conv} Z11$$

Therefore, using the superposition principle:

$$T_{ai} = T'_{ai1} + T'_{ai2} + T'_{ai3} \quad (5.46)$$

DYCON allows the user to choose the degree of approximation of the feedforward system transfer function by selecting from the three room models already described in chapter 3. The rest of the transfer function is identical to the one representing the simulated system. The response of the system can be seen in fig 5.12. It is evident that this control system provides excellent control initially. Due to the modelling inaccuracies, however, the error increases monotonically. Since there is no way to check this increase (feedforward control is an open loop control system) the system would be destabilized and any gains initially made would be lost.

It is apparent that this control system design approach does not have the same stability considerations as feedback control. Therefore, if a process can be modelled accurately, any delays present will not make any difference to the response of the system. Modelling approximation errors,

however, can evidently cause destabilization with no recourse for correction available to the system.

5.3.5 Feedforward-feedback control system

Both feedback and feedforward control systems have advantages that can be complementary to the other's disadvantages. Feedback is insensitive to modelling approximation but is adversely affected by the presence of significant dead times resulting in high overshoots and sluggish responses to disturbances. Feedforward control, on the other hand, takes care of these dead times making them part of the feedforward controller algorithm and acts before the effect of a disturbance is felt by the system. However, it requires identification and measurement of all disturbances and, if the system is not perfectly modelled, has no recourse in correcting errors. It is therefore evident that the combination of both systems would produce a hybrid system that provides for effective indoor climate control.

The block diagram representing this hybrid system can be seen in figure 5.13. It is evident from the block diagram that the combination of the contributions of the feedforward algorithm (c_2) and the feedback loop (c_1) will dictate the required movement x to the valve stem. This is in order to counteract the disturbances or the variations of T_{airsp} prescribed by methods similar to the one described in chapter 4. Perfect control is feasible provided the feedforward algorithm contains an exact representation of the system. Should this not be the case, then the feedback loop is called upon to correct the deviation by introducing additional movement c_1 to the valve stem.

The transfer functions describing the contribution of each input are a combination of the feedforward and feedback components of the control system:

$$T_{a1} = T_{aisp} * \frac{G_c G_x}{1 + G_c G_x G_s} + \frac{(T_{aisp}/G_{xa}) * G_x}{1 + G_c G_x G_s} \quad (5.47)$$

$$T_{a2} = Q_{rad} * \frac{Z17}{1 + G_c G_x G_s} - \frac{(Q_{rad} * Z17_a / G_{xa}) * G_x}{1 + G_c G_x G_s} \quad (5.48)$$

$$T_{a3} = Q_{conv} * \frac{Z11}{1 + G_c G_x G_s} - \frac{(Q_{conv} * Z11_a / G_{xa}) * G_x}{1 + G_c G_x G_s} \quad (5.49)$$

Where $G_x = G_{valve} G_{coil} G'_{duct} Z11$

Therefore by virtue of the superposition principle :

$$T_{a1} = T_{a1} + T_{a2} + T_{a3} \quad (5.50)$$

The first observation that can be made from the above equations is that the stability considerations of the feedback loop are not affected, since the characteristic equation of the system is not affected by the addition of the feedforward loop. Figures 5.15 and 5.16 show the response of this system to the loads described in the previous sections and for the same systems used by the feedback control studies. The overshoot was reduced significantly in both cases and the responses of the feedback-feedforward system were as stable as the feedback loop.

Since this was the case, i.e. the same characteristic equation for both the feedback and the hybrid system, anything that would affect the stability of the feedback loop, such as delays in the sensing element,

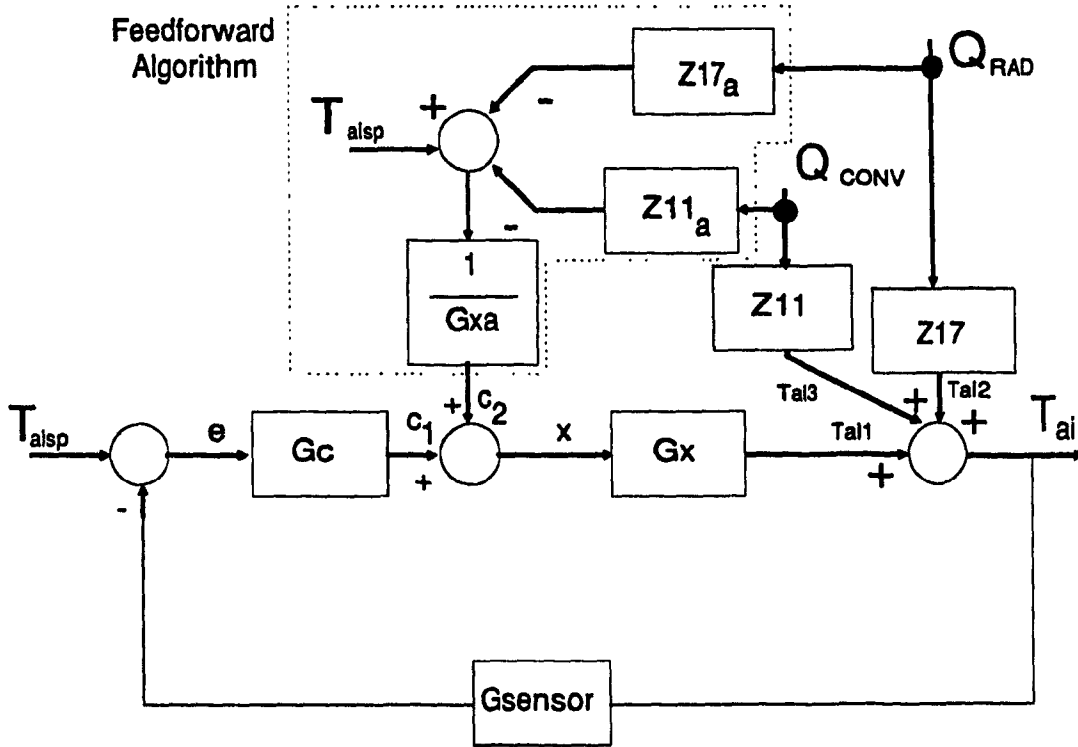


Figure 5.14 Block diagram for feedforward-feedback control

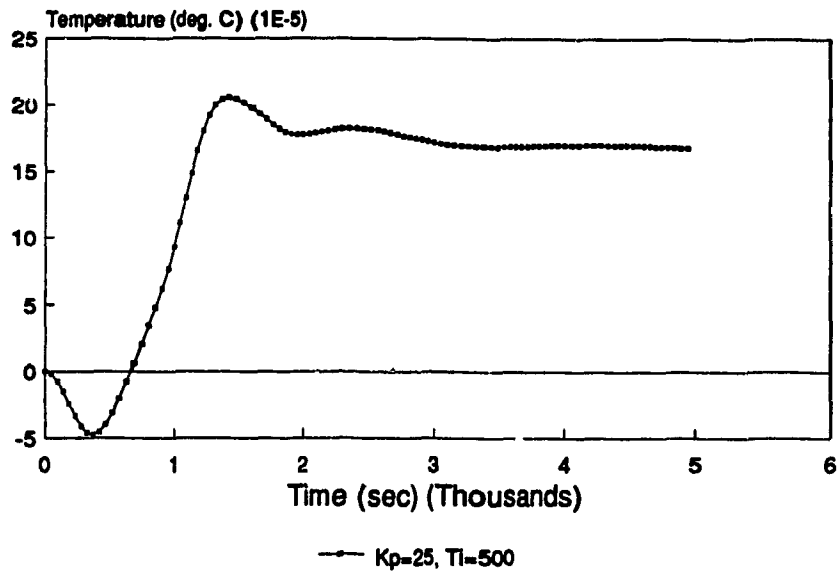


Figure 5.15 Response of feedforward-feedback : Base case

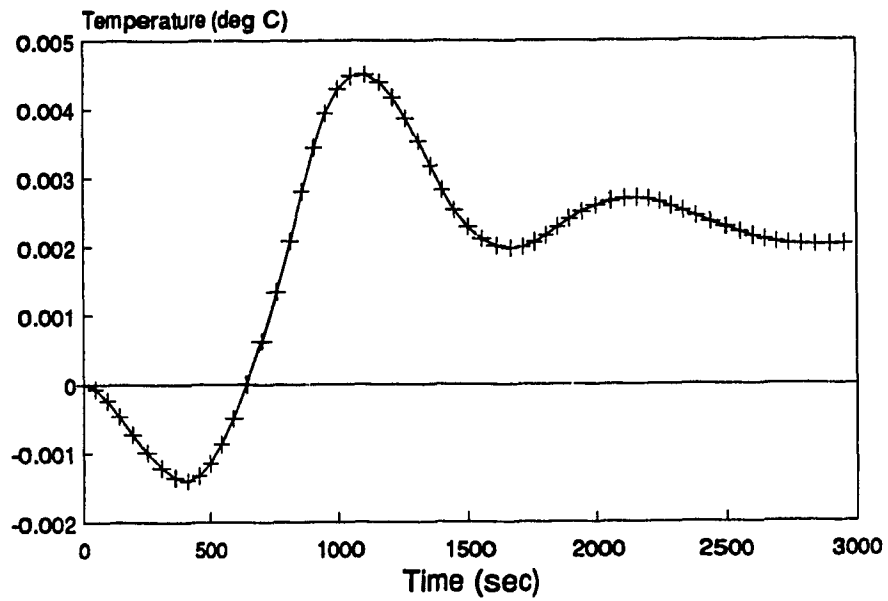


Figure 5.16 Response of the combined feedforward-feedback control loop:
System with 300 sec delay

would have the same effect on the feedback-feedforward loop. Therefore, the low values of the proportional gain and high values of the integral time would have to be maintained.

The main benefit of this system however, is not one of improved stability, but rather one of improved performance. Where the feedback control loop produces high overshoots and is sluggish and an imperfect feedforward loop will be inherently unstable, their combination results in a hybrid system with the stability characteristics of the feedback loop and the response of a feedforward loop.

In effect, the feedforward-feedback control system is a system that can be effectively designed only if the HVAC system and the building enclosure are integrated into a single system and their interaction is well understood and used for the purpose of improved system performance.

5.4 Conclusion

The integration of building and HVAC system dynamic characteristics into the feedforward-feedback control system offers the capability to exploit their interaction so that problems related to thermal comfort and energy conservation can be effectively addressed.

It is apparent that this approach requires extensive knowledge of the system and the associated heat transfer processes, but the balancing of any modelling approximations with the feedback loop provides the warranty that the system will have the characteristics and behaviour of the simple feedback. Depending on the modelling approximation used and the accuracy

of the measuring devices, however, the improvement in the response of the system will cause significant progress in thermal comfort and energy conservation considerations.

CHAPTER 6

CONCLUSIONS AND EXTENSIONS OF WORK

The comparison of room models in chapter 3 demonstrates the importance of the modelling complexity. It is evident that studies of frequency responses of models offer significant information about the behaviour of each model without resorting to simulation, an approach that would necessitate the introduction of variables that may influence the behaviour of the individual models. In addition, the study of the models with different thermal mass provided insights into the behaviour of the coupled and individual effects of the air and massive element behaviour. It was shown that short and long term effects were the result of the combined effect of the thermal behaviour of the room air and the enclosure's thermal mass. In addition, it was determined that, especially with respect to massive buildings, for convective loads there is a relatively clear separation between short and long term dynamics at an approximate frequency of 36 cycles/day (periods of about 40 min.). However, for radiative loads no such separation exists, which implies that feedback control cannot properly limit the room temperature swings imposed by such loads.

The use of dynamic control strategies in chapter 4 for the use of the thermal mass as a thermal storage showed that knowledge of the enclosure's thermal characteristics can be used to achieve lower peak demands and that such dynamic control strategies were not necessarily restricted to frequencies of 1 cycle per day but were applicable to higher

frequencies. This is in accordance with the findings of chapter 3 related to the relative influences of air and thermal masses.

Finally, chapter 5 presents comparative studies of the feedforward-feedback control system with respect to the conventional feedback control system. It can be concluded from this comparison that significant improvement in the system behaviour can be achieved by the hybrid system. This stems directly from the fact that this system treats the HVAC system and the building enclosure as one integrated system and possesses the capability to react to disturbances that are in the region where neither short nor long term dynamic strategies can be applied.

6.1 Extensions of the current work

Although extensive work has been done by others for both system component and building modelling, the focal point has not been the study of the system and building interaction. The dynamics of this interaction need to be studied and exploited extensively, if strategies such as optimizing the setpoint profile of the room temperature, or alternate control systems such as the feedforward-feedback system are to be successful.

The inclusion of knowledge acquired about the interaction of the air and mass of the enclosure into a control system would improve both energy conservation and thermal comfort, since this would allow the HVAC system to behave as a part of the building in a manner that complements the building's thermal behaviour.

In order for the effective feedforward-feedback control system to be studied in detail, it is necessary that subsequent work :

1. Develop methods for defining the "as built" dynamic models of HVAC system components.
2. Develop methods for defining the "as built" dynamic models of enclosures.
3. Perform experimental studies with models derived in stages 1 and 2 implementing feedforward control strategies.

The models for both HVAC system components and rooms exist in literature. However, it may be desirable to find the individual model's unique parameters. This would entail frequency response studies and the fitting of results obtained to a second order system with a time delay, since such a system could be reliably used to represent the majority of real systems.

Finally, one possible experimental study would be the control of radiant heating, a process that is very hard to control using conventional control approaches because of its slow response. This would allow the study of modelling detail required for effective control of the process and would conclusively demonstrate the advantages and disadvantages of the feedforward-feedback system.

A control system, such as the feedback-feedforward control system, with the capability to integrate the HVAC system and the building dynamics, would have implications on both energy conservation and thermal comfort. The stability of the feedback loop would not be affected by this "addition", but the behaviour of the whole system would improve significantly since it would greatly reduce the unavoidable temperature fluctuations associated with feedback control.

REFERENCES

ASHRAE, "ASHRAE Handbook 1986 Fundamentals", 1986.

Athienitis, A.K., "A Predictive Control Algorithm for Massive Buildings"
Ashrae Trans. Vol.94, pt.2,1988.

Athienitis, A.K., Sullivan, H.F. and Hollands K.G.T., "Analytical Model,
Sensitivity Analysis and Algorithm for Temperature Swings in Direct
Gain Rooms", Solar Energy, Vol. 36, pp.303-312, 1986

Athienitis, A.K., Sullivan, H.F. and Hollands K.G.T., "Discrete Fourier
Series Models for Building Auxiliary Energy Loads Based on Network
Formulation Techniques", Solar Energy, Vol. 39, No. 3, pp.203-210,
1987.

Athienitis, A.K., Sullivan, H.F. and Hollands K.G.T., "Passive Solar
Simulation for Multizone Buildings: A Frequency Domain Approach"
Proc. Solar Energy Society of Canada Conference pp.107-112, 1986.

Bhargava, S.C. , McQuiston, F.C. and Zirkle, L.D. , "Transfer Functions for
Crossflow Multirow Heat Exchangers" Ashrae Trans. pt.2, pp.294-314,
1975 .

Boot, J.L. , Pearson, J.T. and Leonard, R.G., "An Improved Dynamic
Response Model for Finned Serpentine Cross-Flow Heat Exchangers"
Ashrae Trans. pp.218-239, 1977 .

Borresen, B.A., "Thermal Room Models for Control Analysis" Ashrae Trans. pt.2, pp.251-261, 1981 .

CandaPlan Group Inc., "BESA: Technical Reference", 1987.

Carslow, H.S. and Jaeger, J.C., "Conduction in Solids" 2nd Ed. Oxford Univ. Press, 1959 .

Clapp, M.D., "Cost Savings Using Building Management and Control Systems", CLIMA 2000, Ed. P.O. Fanger, Vol. 3, Energy Management, pp 33-36, Copenhagen, 1985.

Clark, D.R. , Hurley, C.W. and Hill, C.R., "Dynamic Models for HVAC System Components" Ashrae Trans. pp.737-751, 1985 .

Clark, D.R.. "HVACSIM⁺ Building Systems and Equipment Simulation Program Reference Manual" National Information Service, NBSIR 84-2996, 1985.

Considine, D.M., "Process Instruments and Controls Handbook", 3rd Ed., McGraw-Hill Book Company, 1985

Curtis, R, et al, "The DOE2 Building Energy Use Analysis Program" Lawrence Berkley Laboratory, 1984 .

- Dumas, A., Sarti, E., " A New System for Automatic Control of Indoor Temperature", CLIMA 2000, Ed. P.O. Fanger, Vol. 3, Energy Management, pp 129-134, Copenhagen, 1985.
- Elmahdy, A.H. and Mitalas, G.P., "A Simple Model for Cooling and Dehumidifying Coils for Use in Calculating Energy Requirements for Buildings" Ashrae Trans. pt.1, pp.103-117, 1977.
- Eto, J.H. and Powell, G., "Implications of Office Building Thermal Mass and Multi-Day Temperature Profiles for Cooling Strategies", Heat Transfer in Building Structures, Proc. of the 23rd National Heat Transfer Conference, ASME, Denver, Colorado, 1985.
- Gardner, J.R., "Simplified Dynamic Relations for Finned-Coil Heat Exchangers" ASHRAE Trans, Vol. 78, Part II, pp 163-169, 1972
- Gartner, J.R. and Daane, L.E., "Dynamic Response Relations for a Serpentine Crossflow Heat Exchanger with Water Velocity Disturbance" ASHRAE Trans. pp.53-68, 1969.
- Gardner, J.R. and Harrison, H.L., "Dynamic Characteristics of Water-to-Air Crossflow Heat Exchangers" ASHRAE Trans. pp.212-224, 1965.
- Gondal, I.A. "Linear Analysis of an Air-Temperature Control Loop" Ashrae Trans. pp.736-751, 1987

Griffiths, I.D. and McIntyre, D.A., "Sensitivity to Temporal Conditions"
Ergonomics Vol. 17 p.499, 1974.

Haghighat, F. and Athienitis, A., "Comparison Between Time Domain and
Frequency Domain Computer Program for Building Energy Analysis",
Computer Aided Design, Vol 20, No. 9, November 1988, pp. 525-532

Hamilton, D.C. Leonard, R.G. and Pearson, J.T., "Dynamic Response
Characteristics of a Discharge Air Temperature Control System at
Near Full and Part Heating Load" ASHRAE Trans. pp. 181-194, 1974.

Hamilton, D.C. Leonard, R.G. and Pearson, J.T., "A System for a Discharge
Air Temperature Control System" ASHRAE Trans. pp. 251-268, 1977.

Hartman, T.B., "Dynamic Control: Fundamentals and Considerations" ASHRAE
Trans., pp. 599-609, 1988.

Hill, C.R., "Simulation of a Multizone Air Handler" ASHRAE Trans.
pp.752-765, 1985.

Hittle D.C., "The Building Loads Analysis System Thermodynamics (BLAST)
Program, Version 2.0: Users Manual", 1979.

Jacobsen, F.R., "Energy Signature and Energy Monitoring in Building Energy
Management Systems", CLIMA 2000, Ed. P.O. Fanger, Vol. 3, Energy
Management, pp. 25-30, Copenhagen, 1985.

Kimura K., "Scientific Basis for Air Conditioning", Applied Science Publishers, 1977.

Kmetzo, J.L., "Development of Control Strategies for the Individual Building", Proc. of Conf. on Improving Efficiency and Performance of HVAC equipment and Systems for Commercial and Industrial Buildings pp. 46-51, Purdue University, 1976.

Lay, Lutz, and Rehberg, "Linear Circuit Analysis", McGraw-Hill Co., 1959

Mackie, E.I., "The Effect of Building Heat Storage on HVAC Systems" Proc. 3rd International Symp. on the Use of Computers for environmental Engineering Related to Buildings pp.129-134, 1978.

Matsunawa, K., Shukuya, M., Nohara, F., "Energy Savings Effect of Zero Energy Band Control on Air-Conditioning Systems", CLIMA 2000, Ed. P.O. Fanger, Vol. 3, Energy Management, pp 209-213, Copenhagen, 1985.

Mehta, D.P., "Dynamic Performance of PI Controllers: Experimental Validation" Ashrae Trans. pp.1775-1793, 1987.

Miller, D.E., "A Simulation to Study HVAC Process Dynamics" ASHRAE Trans. pp.809-825, 1982.

- Ngan, T.H., "Predictive Control of a Simple HVAC System in a Test Hut", Masters Thesis, Concordia University, Center for Building Studies, March 1985.
- Park, C., Bushby, S.T., Kelly, G.E., "Simulation of a Large Office Building System Using the HVACSIM⁺ Program" ASHRAE Trans., 1989.
- Park, C. , Clark, D.R. and Kelly, G.E., "An Overview of HVACSIM⁺, a Dynamic Building / HVAC / Control Systems Simulation Program" Proc. of Building Energy Simulation Conf. pp.175-185, 1985.
- Patterson, N.R., Alwin, J.B., "The impact of ASHRAE Standard 90-75 on High Rise Office Building Energy and Economics", Handbook of Energy Conservation for Mechanical Systems Ed. Rose, R.W., Van Nostrand Reinhold Co., N.Y., pp.436-448, 1978.
- Pearson, J.T. , Leonard, R.G. and McCutchan, R.D., "Gain and Time Constant for Finned Serpentine Crossflow Heat Exchangers" Ashrae Trans. pt.2, pp.255-267, 1974.
- Persson, L., Strand, R., "Microprocessors for Automatic Control, Supervision and Energy Savings in HVAC Systems", CLIMA 2000, Ed. P.O. Fanger, Vol. 3, Energy Management, pp 123-127, Copenhagen, 1985.
- Pratt, A.W., , "Heat Transmission in Buildings", John Wiley and Sons Ltd., 1981.

Sander, D., Dumouchel, P., "Room Simulation Algorithms for Use in HVAC Systems Simulation Computer Program", Proc. 3rd International Symp. on the Use of Computers for Environmental Engineering Related to Buildings pp.31-42, Banff 1978.

Schwenk, D.M., "Single-Loop Digital Controllers in HVAC ", ASHRAE Transactions, 1988

Shavit, G. and Brandt, S.G., "The Dynamic Performance of a Discharge Air-Temperature System with a P-I Controller" Ashrae Trans. pp.826-838, 1982.

Shekar, S.C. and Green, G.H., "Dynamic Study of a Chill water Cooling and Dehumidifying Coil" Ashrae Trans. pp.36-51, 1970.

Shih, J.Y., "Energy Conservation Methods through the use of Building Automation Systems", Proc. of Conf. on Improving Efficiency and Performance of HVAC Equipment and Systems for Commercial and Industrial Buildings pp. 61-69, Purdue University, 1976.

Singhal, K. and Vlach, J., "Computation of Time Domain Response by Numerical Inversion of the Laplace Transform" Journal of the Franklin Institute Vol. 299 pp.109-126, 1975.

Singhal, K., Vlach J., Nakhla M., "Absolutely Stable, High Order Method for Time Domain Solution of Networks" Archiv für Elektronik und Uebertragungstechnik Vol. 30 pp.157-166, 1976.

Singhal, K. and Vlach, J., "Method for Computing Time Response of Systems described by Transfer Functions" Journal of the Franklin Institute Vol. 311 pp.123-130, 1981.

Sinnamohideen, K. and Janisse N., "Energy Conservation through Improved Control Strategies" Proc. of Conf. on Improving Efficiency and Performance of HVAC equipment and Systems for Commercial and Industrial Buildings pp. 361-369, Purdue University, 1976.

Sprague, C.H. and McNall, P.E., "The Effects of Fluctuating Temperature and Relative Humidity on Thermal Sensation (Thermal Comfort) of Sedentary Subject" ASHRAE Trans. Vol 79, p.34, 1970.

Stephanopoulos, G., "Chemical Process Control, An Introduction to Theory and Practice" Prentice-Hall, 1984.

Stoecker, W.F. and Daber R.P., "Conserving Energy in Dual-Duct Systems by Reducing the Throttling Ranges of Air-Temperature Controllers" ASHRAE Trans. pp.23-34, 1978.

Stoecker, W.F. et al, "Stability of an Air-Temperature Control Loop" ASHRAE Trans. pp.35-53, 1978.

Stoecker, W.F. et al., "Reducing the Peaks of Internal Air - Conditioning Loads by Use of Temperature Swings" Ashrae Trans. pt.2, pp. 599-608, 1981.

Thompson, J.G., "The Effect of Room and Control Systems Dynamics on Energy Consumption" Ashrae Trans. pp.883-896, 1981.

Tobias, I.R., "Simplified Transfer Function for Temperature Response of Fluids Flowing Through Coils, Pipes or Ducts" Ashrae Trans. pp.19-22, 1973.

Vlach, J., "Numerical Method for Transient Responses of Linear Networks with Lumped, Distributed or Mixed Parameters" Journal of the Franklin Institute Vol 288 pp.99-113, 1969.

Xunchang, W., "A Precise Computation Method of the Energy Saving Effect on the Regular Floating Variations of the Room-Temperature Setpoint with Outdoor Temperature", CLIMA 2000, Ed. P.O. Fanger, Vol. 3, Energy Management, pp 33-36, Copenhagen, 1985.

Zhang, X. and Warren, M.L., "Use of a General Control Simulation Program" ASHRAE Trans., 1988.

Zmeureanu, R., Fazio, P. Haghghat, F., " Analytical and Interprogram Validation of a Building Thermal Model" Energy and Buildings pp.121-133, 1987.

Zvolner, S.M., "Energy Conservation Opportunities through use of a Computerized Building Management System", Proc. 3rd International Symp. on the Use of Computers for Environmental Engineering Related to Buildings pp.31-42, Banff 1978.

APPENDIX A
DESCRIPTION OF ROOM AND SYSTEM PARAMETERS USED IN
CHAPTER 5

ROOM DATA

	Y	(Y/N)
Are Z11 AND Z1N calculated by DYCON.....		
General Room Data		
Depth of room.....	25.00	(m)
Height of room.....	7.00	(m)
Width of room.....	20.00	(m)
Window height.....	1.93	(m)
Window width.....	5.74	(m)
Wall resistance.....	3.500	(m ² K/W)
Ceiling resistance.....	7.350	(m ² K/W)
Window resistance.....	.400	(m ² K/W)
Combined heat transfer coef. (Horizontal heat flow).....	8.00	(W/m ² K)
Combined heat transfer coef. (Vertical heat flow).....	9.00	(W/m ² K)
Infiltration.....	.50	(ACH)
Floor Data		
Thickness.....	.042	(m)
Density.....	2100.0	(kg/m ³)
Specific heat capacity.....	800.0	(J/kg.K)
Conductivity..	1.70	(W/m.K)
Co ductance....	1.00	(W/m ² K)
ACCEPT DATA ? (Y/N)		

SYSTEM DATA

Controller data			
Do you want to include a controller in the system..	Y	(Y/N)	
Proportional gain.....	0.00	(/°C)	
Integral time	0.0	(sec)	
Derivative time	0.0	(sec)	
Final control element data (e.g. valve)			
Do you want to include a valve in the system.....	Y	(Y/N)	
Gain.....	5.0	(kg/s)	
Time constant	3.0	(sec)	
Time lag.....	0.0	(sec)	
Heat exchanger data			
Do you want to include a heat exch. in the system..	Y	(Y/N)	
Do you want to input the gain and time constant....	Y	(Y/N)	
Gain.....	109.3	(°C/kg/sec)	
Time Constant.....	20.0	(sec)	

ACCEPT DATA ? Y (Y/N)

SYSTEM DATA			
Duct data		Y	(Y/N)
Do you want to include a duct in the system.....			(W/m ² K)
Inside heat transfer coef.....	10.0		(W/m ² K)
Outside heat transfer coef.....	4.0		(J/kg.K)
Specific heat capacity (air).....	1007.0		(J/kg.K)
Specific heat capacity (duct material).....	800.0		(kg)
Weight per meter of duct.....	10.00		(m)
Duct length.....	20.0		(m/s)
Air Velocity.....	.20		(kg/s)
Air mass flow rate.....	.25		
Sensor data		Y	(Y/N)
Do you want to include a sensor in the system			(/°C)
Gain.....	1.0		(sec)
Time constant.....	0.0		(sec)
Time delay.....	30.0		
			ACCEPT DATA ? Y (Y/N)

TYPE OF STUDY TO BE PERFORMED

- 1. Frequency domain study
- 2. Time domain study

ENTER 1 OR 2 DEPENDING ON THE TYPE OF STUDY 2

Z11 AND Z1N ARE ROOM IMPEDANCES - N IS THE ROOM SURFACE NODE CONSIDERED

Do you want to use approximate Z11 and Z1N	N	(Y/N)
Enter Gain for Z11.....	0.00	
Enter time delay for Z11.....	0.0	(sec)
Enter first time constant for Z11.....	0.0	(sec)
Enter second time constant for Z11.....	0.0	(sec)
Enter Gain for Z1N.....	0.00	
Enter time delay for Z1N.....	0.0	(sec)
Enter first time constant for Z1N.....	0.0	(sec)
Enter second time constant for Z1N.....	0.0	(sec)

ACCEPT DATA ? Y (Y/N)

TIME DOMAIN STUDIES	
General data	
Start time.....	1.00000(sec)
Time step.....	50.00 (sec)
Stop time.....	5000 (sec)
Type of Study	
1. Setpoint unit step response	
2. Feedback control loop	
3. Feedforward control loop	
4. Feedback-Feedforward control	
	3
	ENTER YOUR CHOICE
Load and setpoint changes (Ramp or step)	
Setpoint change.....	0.0 (°C)
Time over which setpoint increases (Enter 0 if step)..	0.00 (sec)
Load change.....	60.0 (kW)
Fraction of load which is radiative.....	10.0 (%)
Time over which load increases (Enter 0 if step).....	900.0 (sec)
	ACCEPT DATA ? Y (Y/N)

APPROXIMATE MODEL CHOICE
ENTER CHOICE OF MODEL FOR USE IN FEEDFORWARD CONTROLLER 3
1. Detailed Model 2. Lumped Mass Model 3. Air Only Model 4. Model fitted to second order T.F.
ACCEPT DATA ? Y (Y/N)

APPENDIX B
LISTING OF DYCONFOR.FOR
THE FORTRAN PROGRAM FOR DYCON

```

***** DYCONFOR*****
*
*   DYCON IS A PROGRAM THAT CAN BE USED TO STUDY DYNAMIC CONTROL
*   STRATEGIES AS WELL AS THE INTERACTION OF THE BUILDING
*   AND ITS MECHANICAL SYSTEM.
*   DIFFERENT SYSTEMS CAN BE ANALYSED BY CHANGING ONE OR BOTH OF THE
*   FINAL SUBROUTINES: ILT FOR TIME DOMAIN ANALYSIS USING THE
*   NUMERICAL INVERSION OF LAPLACE TRANSFORMS AND FREQ FOR
*   FREQUENCY DOMAIN ANALYSIS.

```

```

*****

```

```

    IMPLICIT REAL*8 (A-H,O-Z)
    REAL*8 KF,KSENS,KVLV,KCOIL
    REAL*8 TAMB(51),QLDR(51),QLDC(51),TSP(51),MSP
    REAL*8 MVR(51),SPR(51),TIME(51),T,STIME,AMD
    COMPLEX*16 CQLDR(25),CQLDC(25),CTSP(25)
    COMMON/RES/UFA,UFT,UO,CA,AFC,Z11SS1,Z1NSS1,TF,DF,CPF,KF,UF
    COMMON/RES1/RFL,Z11SS2,Z1NSS2,RFK
    COMMON/DCT/HID,HOD,CPAD,CPDD,DD,V,Y,AMD,INCLD
    COMMON/CONTR/TAUI,PRK,CTAUD,I CLC
    COMMON/SNS/KSENS,TAUS,TAUD,INCLS
    COMMON/VLV/KVLV,TAUV,INCLV,TAUDV
    COMMON/CL/KCOIL,TAUC,INCLCL
    COMMON/ILT/AM,CPA,ILF,IFQ
    COMMON/ZAPPR/IM
    COMMON/INPROF/TUP,QRUP,QCUP,TTA,TTSP

```

```

***** I N P U T *****

```

```

    OPEN(30,FILE='ROOM.DAT',STATUS='OLD')
    READ(30,*)IRCZ,DPR,HR,WR,WH,WW
    CLOSE(30,STATUS='KEEP')

```

```

    OPEN(31,FILE='RESIST.DAT',STATUS='OLD')
    READ(31,*)RW,RC,HCR,HCR1,RWIND
    CLOSE(31,STATUS='KEEP')

```

```

    RCR=1.d0/HCR
    RCR1=1.DO/HCR1

```

```

    OPEN(32,FILE='FLOOR.DAT',STATUS='OLD')
    READ(32,*)TF,DF,CPF,KF,UF
    CLOSE(32,STATUS='KEEP')

```

```

    OPEN(33,FILE='AIR.DAT',STATUS='OLD')
    READ(33,*)ACH,DA,CPA
    CLOSE(33,STATUS='KEEP')

```

```

    OPEN(34,FILE='DUCT.DAT',STATUS='OLD')
    READ(34,*)INCLD,HID,HOD,CPAD,CPDD,DD,Y,V,AMD
    AM=AMD
    CLOSE(34,STATUS='KEEP')

```

```

OPEN(35, FILE='CONTR.DAT', STATUS='OLD')
READ(35, *) ICLC, PRK, TAUI, CTAUD
CLOSE(35, STATUS='KEEP')

```

```

OPEN(36, FILE='VLV.DAT', STATUS='OLD')
READ(36, *) INCLV, KVLV, TAUV, TAUDV
CLOSE(36, STATUS='KEEP')

```

```

OPEN(37, FILE='SNSOR.DAT', STATUS='OLD')
READ(37, *) INCLS, KSENS, TAUS, TAUD
CLOSE(37, STATUS='KEEP')

```

```

OPEN(38, FILE='HEXCH.DAT', STATUS='OLD')
READ(38, *) IHE, ICL, KCOIL, TAUC
CLOSE(38, STATUS='KEEP')

```

```

IF(ICL.EQ.2) THEN

```

```

*****
***** CALCULATE DYNAMIC PROPERTIES OF COIL
*****
      CALL COIL(KCOIL, TAUC)

```

```

ENDIF

```

```

OPEN(39, FILE='TYPESTDY.DAT', STATUS='OLD')
READ(39, *) ILTF
CLOSE(39, STATUS='KEEP')

```

```

OPEN(41, FILE='TYPMDL.INP', STATUS='OLD')
READ(41, *) IM
CLOSE(41, STATUS='KEEP')

```

```

IF(IM.EQ.4) THEN

```

```

      WRITE(*,*)
      WRITE(*,*)
      WRITE(*,*)
      WRITE(*,*)

```

```

      WRITE(*,*) ' USE OF APPROXIMATED IMPEDANCES NOT YET AVAILABLE '
      STOP

```

```

ENDIF

```

```

OPEN(42, FILE='APPRZ11.DAT', STATUS='OLD')
READ(42, *) APPR, ZIG, ZITD, ZITC1, ZITC2
CLOSE(42, STATUS='KEEP')

```

```

IF(APPR.EQ.1) THEN

```

```

      WRITE(*,*)
      WRITE(*,*)
      WRITE(*,*)
      WRITE(*,*)

```

```

      WRITE(*,*) ' USE OF APPROXIMATED IMPEDANCES NOT YET AVAILABLE '
      STOP

```

```

ENDIF

```

```

*
```

* TO INCORPORATE APPROXIMATE IMPEDANCES A THIRD PARAMETER SHOULD BE
 * ADDED TO THE FUNCTIONS Z11F AND Z1NF TO SIGNIFY IF APPROXIMATED
 * IMPEDANCES ARE TO BE USED AND ALSO FOR Z1NF TO INDICATE WHAT THE N
 * STANDS FOR
 *

PI=3.141592654

***** CALCULATE PROPERTIES OF ROOM

CALL RESCAP(ACH,DA,CPA,TF,KF,UF,RW,RC,RCR
 +,RWIND,DPR,HR,WR,WH,WW,UFA,UFT,UO,CA,AFC,Z11SS1,Z1NSS1,Z11SS2,
 +Z1NSS2,RFL,RFK,RCR1)

IF(ILTF.EQ.2) THEN

***** * PERFORM NUMERICAL INVERSION OF THE LAPLACE TRANSFORMS
 ***** IN ILT

WRITE(*,*)

WRITE(*,*)

WRITE(*,*)

WRITE(*,*)

WRITE(*,*)' NUMERICAL INVERSION OF LAPLACE TRANSFORM FOR'

OPEN(11,FILE='ILT.DAT',STATUS='OLD')

READ(11,*)STIME,DELTAT,TEND,ILF

CLOSE(11,STATUS='KEEP')

OPEN(12,FILE='ILTSP.DAT',STATUS='OLD')

READ(12,*)TUP,TIMSP

CLOSE(12,STATUS='KEEP')

OPEN(13,FILE='ILQLD.DAT',STATUS='OLD')

READ(13,*)QUP,FRTIO,TTA

CLOSE(13,STATUS='KEEP')

FRTIO=FRTIO/100.DO

QUP=QUP*1000.DO

QRUP=QUP*FRTIO

QCUP=QUP-QRUP

CALL INVLT(STIME,DELTAT,TEND)

ENDIF

IF(ILTF.EQ.1) THEN

WRITE(*,*)

WRITE(*,*)

WRITE(*,*)


```

WRITE(*,*)
WRITE(*,*)'          DISCRETE FREQUENCY ANALYSIS AND/OR SIMULATION'

WRITE(*,*)'          IN PROGRESS

```

```

*** ONLY DISCRETE FOURIER IS' REQUIRED
      OPEN(13,FILE='PERIOD.DAT',STATUS='OLD')
      READ(13,*) NDT,NHARM,PERIOD,I1,ISIM
      CLOSE(13,STATUS='KEEP')
* GENERATE ONE HARMONIC REPRESENTATION OF TSP
*
      OPEN(15,FILE='TSP.INP',STATUS='OLD')
      READ(15,*)ISP,IRDSP,MSP,TSPX,TSPN,TOM,PHI
      CLOSE(15,STATUS='KEEP')
      IF(TOM.NE.(2.DO*PI/PERIOD))THEN
        WRITE(*,*)
        WRITE(*,*)'PERIOD FOR TSP >PERIOD BY',((2.DO*PI/TOM)-PERIOD)
      ENDIF

      IF(IRDSP.EQ.1)THEN
*
*       READ TSP AND CHECK IF THE TIME STEP AGREES WITH
*       THE ONE USED BY THE PROGRAM
*
        OPEN(52,FILE='TSP.DAT',STATUS='UNKNOWN')
        READ(52,*)(TIME(I),TSP(I),I=1,NDT)
        CLOSE(52,STATUS='KEEP')
        DELTAT=PERIOD/NDT
        IF((TIME(5)-TIME(4)).NE.DELTAT)THEN
          WRITE(*,*)
          WRITE(*,*)'          ERROR IN TSP INPUT FILE'
          WRITE(*,*)'          TIME STEP USED INCORRECT'
        ENDIF
        CALL FOURIE(TSP,CTSP,NHARM,TIME,NDT,1,PERIOD,1)
      ENDIF
      IF(MSP.NE.0.DO) THEN
        CALL TSPG(TSPX,TSPN,TOM,PHI,NHARM,NDT,PERIOD,ISP,MSP,CTSP,
+TSP)
      ENDIF

```

```

*****
*** CTSP IS THE COMPLEX ARRAY CONTAINING THE SETPOINT VARIATION ***
*****

```

```

*
*   READ QLOAD AND CHECK IF THE TIME STEP AGREES WITH
*   THE ONE USED BY THE PROGRAM
*
      OPEN(14,FILE='QLD.INP',STATUS='OLD')

```

```

      READ(14,*)ILD,IRDL,LMSP,QMAX,QMIN,QOM,THETA,RADTIO,IFQ
      CLOSE(14,STATUS='KEEP')
      IF(IFQ.NE.1)THEN
      IF(QOM.NE.(2.DO*PI/PERIOD))THEN
      WRITE(*,*)'PERIOD FOR QLD >PERIOD BY',((2.DO*PI/QOM)-PERIOD)
      ENDIF
      IF(IRDL.EQ.1)THEN

      OPEN(51,FILE='LOAD.DAT',STATUS='UNKNOWN')
      READ(51,*)(TIME(I),QLDR(I),QLDC(I),I-1,NDT)
      CLOSE(51,STATUS='KEEP')
      DELTAT=PERIOD/NDT
      IF((TIME(5)-TIME(4)).NE.DELTAT)THEN
      WRITE(*,*)'                ERROR IN LOAD INPUT FILE'
      WRITE(*,*)'                TIME STEP USED INCORRECT'
      ENDIF
      CALL FOURIE(QLDR,CQLDR,NHARM,TIME,NDT,1,PERIOD,1)
      CALL FOURIE(QLDC,CQLDC,NHARM,TIME,NDT,1,PERIOD,1)
      ENDIF
      IF(LMSP.NE.ZERO) THEN
*
*       GENERATE LOAD PROFILE

      CALL QLOAD(QMAX,QMIN,RADTIO,NHARM,PERIOD
+,NDT,CQLDR,CQLDC,THETA,QOM,ILD,LMSP)

      ENDIF
      ENDIF
*****
***  QLD IS THE COMPLEX ARRAY CONTAINING THE LOAD VARIATION ***
*****
      CALL FREQ(IRCZ,ISIM,NDT,NHARM,PERIOD,CQLDR,CQLDC,CTSP)
      WRITE(*,*)
      WRITE(*,*)

      ENDIF

      WRITE(*,*)
      WRITE(*,*)

      STOP
      END

```

```
*****
```

```

*****
**
** SUBROUTINE FOR NUMERICAL LAPLACE TRANSFORM INVERSION
** OF SYSTEM TRANSFER FUNCTION
*   T - START TIME (CANNOT BE 0)
*   H - TIME STEP
*   TEND - LAST TIME INCREMENT CONDITION
*   ILTF - SYSTEM TRANSFER FUNCTION
*   TDR - TIME DOMAIN RESPONSE USING LOWER INTEGRATION ORDER
*   TDR1 - TIME DOMAIN RESPONSE USING HIGHER INTEGRATION ORDER
*   DIFFERENCE BETWEEN TDR1 AND TDR PROVIDES INDICATION TO THE
*   ERROR INTRODUCED DURING INTEGRATION
*****
SUBROUTINE INVLT(T,H,TEND)

IMPLICIT REAL*8 (A-H,O-Z)
REAL*8 TDR,TDR1, TI
COMPLEX*16 Z(5),KPRIM(5),S,Z1(5),KPRIME1(5),FDF1,FDF2,ILTF
COMMON/ILT/AM,CPA,ILF,IFQ

OPEN(15,FILE='M_2MEQ10.ILT',STATUS='OLD')
OPEN(16,FILE='M_1MEQ10.ILT',STATUS='OLD')

IF(ILF.EQ.1) THEN
WRITE(*,*)'                               STEP FEEDBACK RESPONSE IN PROGRESS'
WRITE(*,*)
WRITE(*,*)
WRITE(*,*)
WRITE(*,*)
WRITE(*,*)
WRITE(*,*)'                               OUTPUT IN FILE >>ILTSFBR.PRN<<'
OPEN(80,FILE='ILTSFBR.PRN',STATUS='UNKNOWN')
WRITE(80,*)TEND/H,3
WRITE(80,900)
ENDIF
IF(ILF.EQ.2) THEN
WRITE(*,*)'                               FEEDBACK RESPONSE IN PROGRESS'
WRITE(*,*)
WRITE(*,*)
WRITE(*,*)
WRITE(*,*)
WRITE(*,*)
WRITE(*,*)'                               OUTPUT IN FILE >>ILTFB.PRN<<'
OPEN(81,FILE='ILTFB.PRN',STATUS='UNKNOWN')
WRITE(81,*)TEND/H,3
WRITE(81,900)
ENDIF

```

```

IF(ILF.EQ.3) THEN
WRITE(*,*)'                                FEEDFORWARD RESPONSE IN PROGRESS'
WRITE(*,*)
WRITE(*,*)
WRITE(*,*)
WRITE(*,*)
WRITE(*,*)
WRITE(*,*)
WRITE(*,*)'                                OUTPUT IN FILE >>ILTF.PRN<<'
OPEN(82, FILE='ILTF.PRN', STATUS='UNKNOWN')
WRITE(82,*)TEND/H,3
WRITE(82,900)
ENDIF
IF(ILF.EQ.4) THEN
WRITE(*,*)'                                FEEDBACK-FEEDFORWARD RESPONSE IN PROGRESS'

WRITE(*,*)
WRITE(*,*)
WRITE(*,*)
WRITE(*,*)
WRITE(*,*)
WRITE(*,*)'                                OUTPUT IN FILE >>ILTFFB.PRN<<'
OPEN(83, FILE='ILTFFB.PRN', STATUS='UNKNOWN')
WRITE(83,*)TEND/H,3
WRITE(83,900)
ENDIF

**** INITIALIZE ZI, K', M', FOR M=10,N=8 AND FOR M=10,N=9 *****

READ(15,*)(Z(I),I=1,5)
READ(15,*)(KPRIM(I),I=1,5)
READ(15,*)MPRIME

READ(16,*)(Z1(I),I=1,5)
READ(16,*)(KPRIME1(I),I=1,5)
READ(16,*)MPRIME1

***** THE MAIN PART OF THE NUMERICAL INVERSION IS DONE BY *****
***** SUBSTITUTING THE LAPLACE OPERATOR "S" WITH ZI/H *****

10 IF (T.GT.TEND) RETURN

TDR=0.DO
TDR1=0.DO

DO ?0 I=1,MPRIME
TDR=TDR-DREAL(ILTF(Z(I)/T)*KPRIM(I))
TDR1=TDR1-DREAL(ILTF(Z1(I)/T)*KPRIME1(I))
20 CONTINUE
TDR=TDR/T
TDR1=TDR1/T

IF(ILF.EQ.1) THEN

```

```

WRITE(80,801)T,TDR,(TDR-TDR1)

ENDIF
IF(ILF.EQ.2) THEN
WRITE(81,801)T,TDR,(TDR-TDR1)

ENDIF
IF(ILF.EQ.3) THEN
WRITE(82,801)T,TDR,(TDR-TDR1)

ENDIF
IF(ILF.EQ.4) THEN
WRITE(83,801)T,TDR,(TDR-TDR1)

ENDIF

T=T+H
GOTO 10
801 FORMAT(2X,F15.5,2X,F15.10,2X,F15.5)
900 FORMAT(12X,"TIME",',',6X,"TEMPERATURE VARN",',',6X,"ERROR,"')
RETURN
END

```

```

*****
***

```

```

COMPLEX*16 FUNCTION ILTF(S)

```

```

IMPLICIT REAL*8(A-H,O-Z)
COMPLEX*16 S,IL1,IL2,CCOIL,GC,VALVE,DUCT,Z11F,SENS,IL3
COMPLEX*16 IL4,IL5,IL6,TSPF,QRAD,QCONF,Z1NF,G,GX,GXA,ZZ1,ZZ7
COMPLEX*16 ZZ1A,ZZ7A,TSP,QCON,QRAD,T1,T2,GCX,GSCX
COMPLEX*16 G1,X,TAI1,TAI2,TAI3,CHEO,TA1,TA2,TA3
REAL*8 AM,CPA,M,K,TH
COMMON/ILT/AM,CPA,ILF,IFQ
COMMON/ZAPPR/IM

```

```

ZZ1=Z11F(1,S)
ZZ7=Z1NF(1,S)
TSP=TSPF(S)
QRAD=QRADF(S)

```

```

IF(ILF.EQ.1)THEN

```

```

***** UNIT STEP RESPONSE OF FEEDBACK TRANSFER FUNCTION*****

```

```

IL1=GC(S)*VALVE(S)*CCOIL(S)*DUCT(S)*ZZ1*AM*CPA
IL2=IL1/(1+(IL1*SENS(S)))
ILTF=(1.00/S)*IL2
ENDIF

```

```

IF(ILF.EQ.3) THEN
**** FEEDFORWARD CONTROL
      G=VALVE(S)*CCOIL(S)*DUCT(S)*CPA*AM

      IF(G.EQ.(0.DO,0.DO))THEN
        G=(1.D-32,0.DO)
      ENDIF

      GX=G*ZZ1
      GXA=G*Z11F(IM,S)
      TAI1=QRAD*ZZ7
      TAI2=QCONF(S)*ZZ1
      T1=(TSP/Z1NF(IM,S))-(QRAD)
      T2=T1*Z1NF(IM,S)/Z11F(IM,S)
      TAI3=GX*(T2-(QCONF(S)))*Z11F(IM,S)/GXA

      ILTF=TAI1+TAI2+TAI3

```

```

      ENDIF
      IF(ILF.EQ.2) THEN
**** FEEDBACK CONTROL
      GX=VALVE(S)*CCOIL(S)*DUCT(S)*CPA*AM*ZZ1
      GCX=GX*GC(S)
      GSCX=GCX*SENS(S)
      CHEQ=1+GSCX
      TAI1=TSP*GCX/CHEQ
      TAI2=QRAD*ZZ7/CHEQ
      TAI3=QCONF(S)*ZZ1/CHEQ

```

```

      ILTF=TAI1+TAI2+TAI3
      ENDIF

```

```

      IF(ILF.EQ.4) THEN
*** PERFORM FEEDFORWARD-FEEDBACK CONTROL
      G=VALVE(S)*CCOIL(S)*DUCT(S)*CPA*AM
      IF(G.EQ.(0.DO,0.DO))THEN
        G=(1.D-32,0.DO)
      ENDIF

```

```

      GX=G*ZZ1
      GXA=G*Z11F(IM,S)
      GCX=GX*GC(S)
      GSCX=GCX*SENS(S)
      CHEQ=1+GSCX
      TAI1=TSP*GCX/CHEQ
      TAI2=QRAD*ZZ7/CHEQ
      TAI3=QCONF(S)*ZZ1/CHEQ
      TAI= TSP*(GX*(GC(S)+(1/GXA)))/CHEQ

```

```

*      TA1=TAI1+(((TSP/GXA)*GX)/CHEQ)
      TA2=TAI2-(((QRAD*Z1NF(IM,S)/GXA)*GX)/CHEQ)
      TA3=TAI3-(((QCONF(S)*Z11F(IM,S)/GXA)*GX)/CHEQ)
      ILTF=TA1+TA2+TA3
      ENDIF

```

```

      RETURN
      END

```

```

*****

```

```

*      FUNCTION DESCRIBING THE SETPOINT VARIATION

```

```

*****

```

```

      COMPLEX*16 FUNCTION TSPF(S)
      COMPLEX*16 S
      REAL*8 TUP,QRUP,QCUP,TTA,TTSP
      COMMON/INPROF/TUP,QRUP,QCUP,TTA,TTSP

```

```

      IF(TTSP.EQ.0.DO) THEN
        TSPF=TUP/S
      ELSE
        M=TUP/TTSP
        TSPF=M*((1.DO-CDEXP(-TTSP*S))/(S**2))
      ENDIF
      RETURN
      END

```

```

*****

```

```

*      FUNCTION DESCRIBING THE RADIATIVE LOAD VARIATION VARIATION

```

```

*****

```

```

      COMPLEX*16 FUNCTION QRADF(S)
      COMPLEX*16 S
      REAL*8 QRUP,M,TUP,QCUP,TTA,TTSP
      COMMON INPROF/TUP,QRUP,QCUP,TTA,TTSP

```

```

      IF(TTA.EQ.0.DO) THEN
        QRADF=QRUP/S
      ELSE
        M=QRUP/TTA
        QRADF=M*((1.DO-CDEXP(-TTA*S))/(S**2))
      ENDIF

```

```

      RETURN
      END

```

```

*****

```

```

*      FUNCTION DESCRIBING THE CONVECTIVE LOAD VARIATION

```

```

COMPLEX*16 FUNCTION QCONF(S)
COMPLEX*16 S
REAL*8 QCUP,TUP,QRUP,TTA,M,TTSP
COMMON/INPROF/TUP,QRUP,QCUP,TTA,TTSP

IF(TTA.EQ.0.DO)THEN
  QCONF=QCUP/S
ELSE
  M=QCUP/TTA
  QCONF=M*((1-CDEXP(-TTA*S))/(S**2))
ENDIF
RETURN
END

```

SUBROUTINE COIL(KCOIL,TAUC)

```

C   THIS PROGRAM'S PURPOSE IS TO CALCULATE THE TIME CONSTANT
C   AND GAIN FOR A SINGLE ROW, FINNED, SERPANTINE, CROSS FLOW
C   HEAT EXCHANGER FOR CHANGES IN WATER FLOW RATE
C
C
C
C   NOMECAULTURE
C
C   M - WATERSIDE HEAT TRANSFER VELOCITY EXPONENT(=0.83)
C
C   KH - GAIN OF HEAT EXCH.
C   TAU= TIME CONSTANT FOR HEAT EXCH.
C   FT=FLUSH TIME
C
C   HEAT EXCHANGER DESCRIPTION
C
C   H - HEIGHT
C   W - WIDTH
C   TS - TUBE SPACING
C   N - NUMBER OF PASSES
C   LF - LENGTH OF FINNED TUBE (N*W)
C
C   TUBE DATA
C   OD - OUTSIDE DIAMETER
C   DI - INSIDE DIAMETER

```


C TL - TOTAL LENGTH OF TUBE
 C
 C MATERIAL PROPERTIES OF TUBE
 C
 C TCP - SPECIFIC HEAT CAPACITY
 C TD - TUBE DENSITY
 C
 C FIN DATA
 C
 C FT - FIN THICKNESS
 C FP - FIN PITCH
 C FDP - FIN DEPTH
 C ETAF- FIN EFFECTIVENESS
 C
 C MATERIAL PROPERTIES OF FIN
 C
 C FCP - SPECIFIC HEAT CAPACITY
 C FD - FIN DENSITY
 C FK - FIN CONDUCTIVITY
 C
 C WATER FLOW DATA
 C
 C WM - WATER MASS FLOW RATE
 C WV - WATER VELOCITY
 C TWI - INLET WATER TEMPERATURE
 C WK - WATER CONDUCTIVITY
 C WCP - WATER SPECIFIC HEAT CAPACITY
 C WD - WATER DENSITY
 C WVIS - WATER VISCOCITY
 C REW - REYNOLD'S # FOR WATER FLOW

 C PRW - PRANTL # FOR WATER FLOW
 C HW - WATER HT. TRANSF. COEF.
 C
 C AIR FLOW DATA
 C
 C AM - AIR MASS FLOW RATE

 C AV - AIR VELOCITY
 C TAI - INLET AIR TEMPERATURE
 C AK - AIR CONDUCTIVITY
 C ACP - AIR HEAT CAPACITY
 C AD - AIR DENSITY
 C AVIS - AIR VISCOCITY
 C SIG - RATIO OF FREE FLOW TO FRONTAL AREA OF EXCHANGER
 C ALPHA- RATIO OF TOTAL TRANSFER AREA OF AIR SIDE TO TOTAL
 C EXCHANGER VOLUME
 C DHA - HYDRAULIC DIAMETER OF AIR SIDE
 C REA - REYNOLD'S # FOR AIR FLOW
 C ETAHA- OVERALL FIN EFF.* HEAT TRANSFER COEFF. FOR AIR

REAL*8 M, KH, TAU, H, W, TS, LTF, OD, DI, TL, TCP, TD, FP, FDP, ETAF, FCP, FD, FK

REAL*8 WM, WV, TWI, WK, WCP, WD, WVIS, REW, PRW, HW, AM, AV, TAI, AK, ACP, AD
 REAL*8 ALPHA, DHA, REA, ETAHA, FTH, PI, AVIS, SIG, KCOIL, TAUC

OPEN(12, FILE='HEXDES.DAT', STATUS='OLD')
 READ(12, *)H, W, TS, N
 CLOSE(12, STATUS='KEEP')

OPEN(13, FILE='HEXTUB.DAT', STATUS='OLD')
 READ(13, *)OD, DI, LTF, TL, TCP, TD
 CLOSE(13, STATUS='KEEP')

OPEN(14, FILE='HEXFIN1.DAT', STATUS='OLD')
 READ(14, *)FTH, FP, FDP
 CLOSE(14, STATUS='KEEP')

OPEN(15, FILE='HEXFIN2.DAT', STATUS='OLD')
 READ(15, *)FCP, FD, FK
 CLOSE(15, STATUS='KEEP')

OPEN(16, FILE='HEXWAT.DAT', STATUS='OLD')
 READ(16, *)PT, WD, WK, WVIS1, EWVIS, WCP, WV, TWI
 CLOSE(16, STATUS='KEEP')

OPEN(17, FILE='HEXAIR.DAT', STATUS='OLD')
 READ(17, *)APRH, PAIRH, AD1, EAD, AK1, EAK, AVIS1, EAVIS, ACP, AV
 CLOSE(17, STATUS='KEEP')

OPEN(18, FILE='VARIAB.DAT', STATUS='OLD')
 READ(18, *)ETAF, TAI, TWI
 CLOSE(18, STATUS='KEEP')

M=0.83
 PI=3.14159265D0
 WVIS=WVIS1*(10**EWVIS)
 AK=AK1*(10**EAK)
 AVIS=AVIS1*(10**EAVIS)
 AD=AD1*(10**EAD)
 LTF=N*W

C THERMAL CAPACITANCE OF METAL PER UNIT LENGTH OF FINNED TUBE

C TUBE

LTF=N*W
 $TCAP=(PI/4)*TL*((OD**2)-(DI**2))*TD*TCP/LTF$

C FIN

VOLF1=PI*(OD+FTH)
 VOLF2=FDP*TS

$$\begin{aligned} \text{VOLF3} &= ((\text{OD} + (2 * \text{FTH})) ** 2) * (\text{PI} / 4) \\ \text{VOLF} &= (\text{VOLF1} + (\text{FP} * (\text{VOLF2} - \text{VOLF3}))) * \text{FTH} \\ \text{FCAP} &= \text{VOLF} * \text{FD} * \text{FCP} \end{aligned}$$

C TOTAL CAPACITANCE
TFCAP=TCAP+FCAP

C FLUID CONTACT AREA PER UNIT LENGTH OF FINNED TUBE

C WATER SIDE
AW=PI*DI

C AIR SIDE

$$\begin{aligned} \text{AA1} &= (\text{PI} / 4) * ((\text{OD} + (2 * \text{FTH})) ** 2) \\ \text{AA2} &= 2 * ((\text{FDP} * \text{TS}) - \text{AA1}) \\ \text{AA3} &= \text{PI} * (\text{OD} + (2 * \text{FTH})) * ((1 / \text{FP}) - \text{FTH}) \\ \text{AA} &= (\text{AA3} + \text{AA2}) * \text{FP} \end{aligned}$$

C FLUSH TIME
F1=TL/WV

C CONVECTION COEFFICIENTS

C WATER SIDE
REW=(WD*WV*DI)/WVIS
PRW=(WCP*WVIS)/WK
HW=0.0155*(REW**0.83)*(PRW**0.5)*WK/DI

C AIR SIDE
SIG=(TS-OD-(2*FTH))*((1/FP)-FTH)*(FP/TS)

$$\text{ALPHA} = \text{AA} / (\text{TS} * \text{FDP})$$

$$\text{DHA} = 4 * \text{SIG} / \text{ALPHA}$$

$$\begin{aligned} \text{REA} &= (\text{AD} * \text{AV} * \text{DHA}) / (\text{SIG} * \text{AVIS}) \\ \text{ETAJA} &= 1.44 * (\text{REA} ** (-0.813)) \end{aligned}$$

$$\text{ETAHA} = (\text{ETAJA} * \text{AD} * \text{AV} * \text{ACP}) / (\text{SIG} * ((\text{ACP} * \text{AVIS} / \text{AK}) ** (2/3)))$$

C MASS FLOW RATES

$$\begin{aligned} \text{UM} &= \text{WD} * \text{WV} * \text{PI} * (\text{DI} ** 2) / 4 \\ \text{AM} &= \text{AD} * \text{AV} * \text{TS} \end{aligned}$$

C DIMENSIONLESS PARAMETERS

$$\text{B1} = (\text{WM} * \text{WCP}) / (\text{LTF} * \text{AM} * \text{ACP})$$

```

B2=(AW*HW)/(AM*ACP)
B3=TFCAP/(AM*ACP*FT)
B4=(ETAHA*AA)/(AM*ACP)
C4=1-EXP(-B4)
C=1/((1/B2)+(1/C4))
BB=C/B1

```

C GAIN CALCULATION

```
KH=((TWI-TAI)/WM)*B1*(1-(1+BB-(M*C*BB/B2))*EXP(-BB))
```

C TIME CONSTANT CALCULATION

```

TAU1=B1*FT*(TWI-TAI)/(KH*WM)
TAU2=M*B3*(C**2)*(1-EXP(-BB))/(C4*(B2**2))
TAU3=(1-(M*C/B2))*(1+(B3/B1))
TAU4=(1-((1+BB)*EXP(-BB)))**2
TAU5=BB*(1-EXP(-BB))
TAU=TAU1*(TAU2+((TAU3*TAU4)/TAU5))

```

C TESTING FOR CONDITIONS UNDER WHICH THE MODEL IS NO LONGER VALID

```

RF=(FDP+TS-(2*OD))/(8*PI*FK*OD*FTH)
CF=ETAF*FD*FCP*FTH*((FDP*TS)-(PI*(DO**2)/4))
TAUF=RF*CF
IF(TAUF.GT.TAU)THEN
  WRITE(*,*)'MODEL NOT VALID'
ELSE
  KCOIL=KH
  TAUC=TAU
ENDIF
RETURN
END

```

```

*****' *****
***

```

```

COMPLEX*16 FUNCTION CCOIL(S)
REAL *8 KCOIL, TAUC
COMPLEX*16 S
COMMON/CL/KCOIL, TAUC, INCLCL

```

```
IF(INCLCL.EQ.1)THEN
```

```

      CCOIL=KCOIL/(1+(TAUC*S))
    ELSE
      CCOIL=(1.D0,0.D0)
    RETURN
  ENDIF
END

```

```

*****
***

```

```

*
*   THE PURPOSE OF THIS FUNCTION IS TO CALCULATE THE TRANSFER FUNCTION
*
*   FOR A DUCT IN THE FREQUENCY DOMAIN
*
*   NOMECAUTURE
*   V - AIR VELOCITY
*   Y - DISTANCE FROM INLET OF CONDUIT
*   AMD - MASS FLOW RATE OF AIR
*   A - CROSS-SECTIONAL AREA OF DUCT
*   HI - INSIDE HEAT TRANSFER COEFFICIENT OF DUCT
*   HO - OUTSIDE HEAT TRANSFER COEFFICIENT OF DUCT
*   CPA - HEAT CAPACITY OF AIR
*   CPD - HEAT CAPACITY OF DUCT
*   DD - WEIGHT OF DUCT PER METER
*   K - DIMENTIONLESS RATIO OF HEAT TR. COEFF.
*   L - LENGTH CONSTANT
*   TAU - TIME CONSTANT
*   DUCT - THE VARIATION OF THE AIR TEMP IN DUCT

```

```

*****
***

```

```

      COMPLEX*16 FUNCTION DUCT(S)
      IMPLICIT REAL*8 (A-H,O-Z)
      REAL*8 K,L
      COMPLEX*16 S,A1,A2,A3
      COMMON/DCT/HID,HOD,CPAD,CPDD,DD,V,Y,AMD,INCLD

```

C CALCULATION OF PARAMETERS

```

      K=HID/(HID+HOD)
      L=AMD*CPAD/HID
      TAU=DD*CPDD/(HOD+HID)
      A1=-Y*S/V
      A2=-((1-K)*Y)/L
      A3=-((K*Y/L)*(TAU*S/(TAU*S+1)))

```

C CALCULATION OF EFFECT OF DUCT ON AIR TEMP

IF(INCLD.EQ.1)THEN

```

      DUCT=CDEXP(A1)*CDEXP(A2)*CDEXP(A3)

```

```

ELSE
  DUCT=(1.D0,0.D0)
ENDIF
RETURN
END

```

```
*****
```

```

COMPLEX*16 FUNCTION GC(S)
IMPLICIT REAL*8 (A-H,O-Z)
COMPLEX*16 S
COMMON/CONTR/TAUI, PRK,CTAUD, ICLC
IF(ICLC.EQ.1) THEN
  IF(TAUI.EQ.0.D0)THEN
    GC=PRK
  ELSE
    IF(CTAUD.EQ.0.D0) THEN

      GC=PRK*(1+(1/(TAUI*S)))
    ELSE
      GC=PRK*(1.D0+(1.D0/(TAUI*S)))+(CTAUD*S)
    ENDIF
  ENDIF
ELSE
  GC=(1.D0,0.D0)
ENDIF
RETURN
END

```

```
*****
```

```

COMPLEX*16 FUNCTION SENS(S)
REAL*8 KSENS,TAUS,TAUD
COMPLEX*16 S
COMMON/SNS/KSENS,TAUS,TAUD,INCLS

IF(INCLS.EQ.1)THEN

  SENS=(KSENS*CDEXP(-TAUD*S))/(1+(TAUS*S))
ELSE
  SENS=(1.D0,0.D0)
ENDIF
RETURN
END

```

```
*****
```

```

COMPLEX*16 FUNCTION VALVE(S)
COMPLEX*16 S
REAL*8 KVLV,TAUV,TAUDV
COMMON/VLV/KVLV,TAUV,INCLV,TAUDV

IF(INCLV.EQ.1)THEN
  VALVE=(KVLV*CDEXP(-TAUDV*S))/(1+(TAUV*S))

```

```

ELSE
      VALVE=(1.D0,0.D0)
ENDIF
RETURN
END

```

```

**      FUNCTION FOR CALCULATION OF THE TRANSFER FUNCTION FOR
**      THE Z(1,1) IMPEDANCE
*      CA - AIR HEAT CAP.
*      UFA-OVERAL CONDUCTANCE BETWEEN FLOOR AND AIR NODE
*      UFT-UFA INCLUDING CONDUCTIVITY OF FLOOR
*      UO-OVERALL CONDUCTANCE OF AIR NODE TO OUTSIDE
*      AFC-FLOOR AREA
*      IF IA-1 THEN DISTRIBUTED MODEL IS USED
*      IF IA-2 THEN LUMPED MODEL IS USED
*      IF IA-3 THEN ONLY AIR MASS CONSIDERED
**

```

```

      COMPLEX*16 FUNCTION Z11F(IA,S)

```

```

      IMPLICIT REAL*8 (A-H,O-Z)

```

```

      REAL*8 KF

```

```

      COMPLEX*16 S,CAS,Y11,Y,DET,Y11L,Y11A

```

```

      COMMON/RES/UFA,UFT,UO,CA,AFC,Z11SS1,Z1NSS1,TF,DF,CPF,KF,UF
      COMMON/RES1/RFL,Z11SS2,Z1NSS2,RFK

```

**** READ PROPERTIES OF ROOM SUCH AS CAPACITANCES AND RESISTANCES

```

      CAS=(CA*S)+UO+UFA

```

```

      IF(IA.EQ.1)THEN

```

```

**      DISTIRBYTED MODEL *****

```

```

      Y-Y11(S)+UFA

```

```

      ENDIF

```

```

      IF(IA.EQ.2)THEN

```

```

**      LUMPED MODEL ****

```

```

      Y-Y11L(S)+UFA

```

```

      ENDIF

```

```

      IF(IA.EQ.3)THEN

```

```

**      AIR ONLY MODEL ***

```

```

      Y-Y11A(RFL)+UFA

```

```

      ENDIF

```

```

      DET=(Y*CAS)-(UFA**2)

```

```

      Z11F=Y/DET

```

RETURN
END

**
** FUNCTION FOR CALCULATION OF THE TRANSFER FUNCTION FOR
** THE Z(1,N) IMPEDANCE

* UFA-OVERAL CONDUCTANCE BETWEEN FLOOR AND AIR NODE
* UFT-UFA INCLUDING CONDUCTIVITY OF FLOOR
* UO-OVERALL CONDUCTANCE OF AIR NODE TO OUTSIDE
* AFC-FLOOR AREA
**

COMPLEX*16 FUNCTION Z1NF(IA,S)

IMPLICIT REAL*8 (A-H,O-Z)
REAL*8 KF
COMPLEX*16 DET,S,CAS,Y11,Y,Y11L,Y11A

COMMON/RES/UFA,UFT,UO,CA,AFC,Z11SS1,Z1NSS1,TF,DF,CPF,KF,UF
COMMON/RES1/RFL,Z11SS2,Z1NSS2,RFK

**** READ PROPERTIES OF ROOM SUCH AS CAPACITANCES AND RESISTANCES

CAS=(CA*S)+UO+UFA
IF(IA.EQ.1)THEN
** DISTRIBYTED MODEL *****
Y=Y11(S)+UFA
ENDIF
IF(IA.EQ.2)THEN
** LUMPED MODEL ****
Y=Y11L(S)+UFA
ENDIF
IF(IA.EQ.3)THEN
** AIR ONLY MODEL ***
RFL=RFQ
Y=Y11A(RFQ)+UFA
ENDIF
DET=(Y*CAS)-(UFA**2)
Z1NF=UFA/DET

RETURN
END

**
** FUNCTION FOR CALCULATION OF THE SELF ADMITTANCE Y11


```

**   FOR THE MASSIVE ELEMENT
*     TF=THICKNESS OF THE FLOOR
*     DF=DENSITY OF THE FLOOR
*     CPF= SP.HT. OF FLOOR
*     UF=CONDUCTANCE OF FLOOR
*     AFC=FLOOR AREA
**

```

```

*****

```

```

COMPLEX*16 FUNCTION Y11(S)

```

```

IMPLICIT REAL*8 (A-H,O-Z)

```

```

REAL*8 KF

```

```

COMPLEX*16 S, GATMA, GALPHA, CTANH, Y11A, Y11B

```

```

COMMON/RES/UFA, UFT, UO, CA, AFC, Z11SS1, Z1NSS1, TF, DF, CPF, KF, UF
COMMON/RES1/RFL, Z11SS2, Z1NSS2, RFK

```

```

AR=AFC

```

```

U=UF

```

```

ALPHA=KF/(DF*CPF)

```

```

GALPHA=CDSQRT(S/ALPHA)

```

```

GATMA=GALPHA*TF

```

```

Y11A=AR*((U/AR)+(KF*GALPHA*CTANH(GATMA)))

```

```

Y11B=(U/(KF*GALPHA*AR))*CTANH(GATMA)+1

```

```

Y11=(Y11A/Y11B)

```

```

RETURN

```

```

END

```

```

*****

```

```

COMPLEX*16 FUNCTION Y11L(S)

```

```

IMPLICIT REAL*8(A-H,O-Z)

```

```

REAL*8 KF

```

```

COMPLEX*16 S, Z1, Z2, Z3, Z

```

```

COMMON/RES/UFA, UFT, UO, CA, AFC, Z11SS1, Z1NSS1, TF, DF, CPF, KF, UF
COMMON/RES1/RFL, Z11SS2, Z1NSS2, RFK

```

```

CF=DF*CPF*TF*AFC

```

```

Z1=RFL

```

```

Z2=1.00/(CF*S)

```

```

Z3=0.500*RFK

```

```

Z=Z3+(1.00/((1.00/Z1)+(1.00/Z2)))

```

```

Y11L=1.00/Z

```

```

RETURN

```

```

END

```

```

*****

```

```

COMPLEX*16 FUNCTION Y11A(RFQ)
IMPLICIT REAL*8(A-H,O-Z)
REAL*8 KF
COMPLEX*16 S,Z1,Z2,Z3,Z

```

```

COMMON/RES/UFA,UFT,UO,CA,AFC,Z11SS1,Z1NSS1,TF,DF,CPF,KF,UF
COMMON/RES1/RFL,Z11SS2,Z1NSS2,RFK

```

```

RFQ=RFL
Z1=RFQ
Z3=0.5D0*RFK

```

```

Z=Z3+Z1
Y11A=1.D0/Z
RETURN
END

```

```

*****
**
** FUNCTION FOR CALCULATION OF THE TRANSFER ADMITTANCE Y12
** FOR THE MASSIVE ELEMENT

```

```

* TF-THICKNESS OF THE FLOOR
* DF-DENSITY OF THE FLOOR
* CPF- SP.HT. OF FLOOR
* UF-CONDUCTANCE OF FLOOR
* AFC-FLOOR AREA

```

```

*****

```

```

COMPLEX*16 FUNCTION Y12(S)

```

```

IMPLICIT REAL*8 (A-H,O-Z)
COMPLEX*16 CTANH,S,GATMA,GALPHA,Y11A,Y11B,CSINH,CCOSH
REAL*8 KF

```

```

COMMON/RES/UFA,UFT,UO,CA,AFC,Z11SS1,Z1NSS1,TF,DF,CPF,KF,UF
COMMON/RES1/RFL,Z11SS2,Z1NSS2,RFK
AR=AFC

```

```

U=UF
ALPHA=KF/(DF*CP)
GALPHA=CDSQRT(S/ALPHA)
GATMA=GALPHA*TF

```

```

Y12=-AR/(AR*CCOSH(GATMA)/U+CSINH(GATMA)/(KF*GALPHA))

```

```

RETURN
END

```

```

*****

```

```

*****
**
** SUBROUTINE FOR CALCULATION OF RESISTANCES AND AIR
** CAPACITANCE
*
* ACH-AIR CHANGE/H
* DA-AIR DENSITY
* CPA- SPECIFIC HEAT CAP. OF AIR
* TF-THICKNESS OF THE FLOOR
* DF-DENSITY OF THE FLOOR
* CPF- SP.HT. OF FLOOR
* UF-CONDUCTANCE OF FLOOR
* RW-RESISTANCE OF WALL
* RC-RESISTANCE OF CEILING
* RCR- COMBINED RAD.&CONV. RESISTANCE
* RWIND-RESISTANCE OF WINDOW
* DPR-ROOM DEPTH
* HR-ROOM HEIGHT
* WR-ROOM WIDTH
* WH-WINDOW HEIGHT
* WW-WINDOW WIDTH
*
* OUTPUTS
* UFA-OVERAL CONDUCTANCE BETWEEN FLOOR AND AIR NODE
* UFT-UFA INCLUDING CONDUCTIVITY OF FLOOR
* UO-OVERALL CONDUCTANCE OF AIR NODE TO OUTSIDE
* CA-AIR CAPACITY
* AFC-FLOOR AREA
* Z11SS-STEADYSTATE Z11
* Z1NSS-STEADY STATE Z1N
*****
SUBROUTINE RESCAP(ACH, DA, CPA, TF, KF, UF, RW, RC, RCR
+, RWIND, DPR, HR, WR, WH, WW, UFA, UFT, UO, CA, AFC, Z11SS1, Z1NSS1, Z11SS2,
+Z1NSS2, RFL, RFK, RCR1)

```

IMPLICIT REAL*8(A-H,O-Z)

REAL*8 KF

***** CALCULATION OF SURFACE AREAS AND ROOM VOLUME

```

AFC=DPR*WR
ALR=DPR*HR
AB=WR*HR
AWIN=WW*WH
AFW=AB-AWIN
VR=DPR*HR*WR

```

*** CALCULATION OF RESISTANCES

```

RFA=RCR1/AFC
RWLR=(RCR+RW)/ALR
RWB=(RCR+RW)/AB
RCL=(RCR+RC)/AFC
RWF=(RCR+RW)/AFW
RWIND=(RCR+RWIND)/AWIND
RINF=ACH*VR*DA*CPA/3600.DO

RR01=(1.DO/RWLR)+(1.DO/RWLR)+(1.DO/RWB)+(1.DO/RCL)+(1.DO/RWIND)
RR02=(1.DO/RINF)+(1.DO/RWF)
RR0=RR01+RR02
RO=1.DO/RR0
UO=1.DO/RO
UFA=1/RFA
UF=UF*AFC
RF=1.DO/UF
IF(TF.EQ.0.DO)THEN
  RFK=0.DO
ELSE
  UFK=KF*AFC/TF
  RFK=1.DO/UFK
ENDIF
RFT=RFK+RF
UFT=1.DO/RFT
RFL=(0.5DO*RFK)+RF
UFL=1.DO/RFL
RFR=RFA+(RFK*0.5DO)
UFR=1.DO/RFR

```

*** AIR CAPACITANCE

```

CA=DA*VR*CPA
*
* STEADY STATE IMPEDANCES
*
* FOR DISTRIBUTED MODEL
Z11SS1=(UFT+UFA)/(((UFT+UFA)*(UO+UFA))-(UFA**2))
Z1NSS1=UFA/(((UFT+UFA)*(UO+UFA))-(UFA**2))
*
* FOR LUMPED MODEL
Z11SS2=(UFL+UFR)/(((UFL+UFR)*(UO+UFR))-(UFR**2))
Z1NSS2=UFR/(((UFL+UFR)*(UO+UFR))-(UFR**2))

RETURN
END

```

```
*****
*   COMPLEX TAN HYPERBOLIC FUNCTION
*****
```

```
COMPLEX*16 FUNCTION CTANH(G)
COMPLEX*16 G

CTANH=(CDEXP(2.D0*G)-1)/(CDEXP(2.D0*G)+1)

RETURN
END
```

```
*****
*   COMPLEX COS HYPERBOLIC FUNCTION
*****
```

```
COMPLEX*16 FUNCTION CCOSH (G)
COMPLEX*16 G

CCOSH=(CDEXP(G)+CDEXP(-G))/2.D0

RETURN
END
```

```
*****
*   COMPLEX SIN HYPERBOLIC FUNCTION
*****
```

```
COMPLEX*16 FUNCTION CSINH(G)
COMPLEX*16 G

CSINH=(CDEXP(G)-CDEXP(-G))/2.D0

RETURN
END
```

```
*****
*****
```

```
*   MAGPHI CALCULATES THE PHASE PHI AND MAGNITUDE MAG
*   OF A COMPLEX NUMBER COMP
*****
```

```
SUBROUTINE MAGPHI(COMP, MAG, PHI)

REAL*8 MAG, PHI, B, ASQ, A, ATAN2
```

COMPLEX*16 COMP

*** A COMPLEX NUMBER " A + B*J " HAS A MAGNITUDE "MAG"
 *** AND A PHASE ANGLE "PHI" AS FOLLOWS

MAG=CABS(COMP)
 B=DIMAG(COMP)
 A=DREAL(COMP)
 PHI=ATAN2(B,A)

RETURN
 END

 C*****

SUBROUTINE FOURIE(F,C,NHARM,TIME,K,IOPTN,PERIOD,IFEJ)

C
 C FOURIE CALCULATES THE FORIER COEFFICIENTS C FOR A SERIES F
 C OR THE FOURIER SERIES F FROM COEFF. C
 C
 C IFEJ - IF EQUAL TO 0 FEJER APPROXIMATION IS DISABLED
 C IF EQUAL TO 1 FEJER APPROXIMATION IS ENABLED
 C IOPTN- IF EQUAL TO 1 FORIE COEFF ARE EVALUATED FROM F
 C IF EQUAL TO 2 FORIE SERIES IS EVALUATED FROM C
 C F- A REAL ARRAY THAT CONTAINS THE VALUES OF THE TIME
 C FUNCTION F(I) FOR K POINTS, THE TIME AT POINT I
 C BEING TIME(I), I=1..K
 C C- COMPLEX ARRAY CONTAINING FORIER COEFFICIENTS
 C FOR NHARMONICS (C(I), I=1..NHARM). C(1) IS THE MEAN TERM
 C C(2) THE FUNDAMENTAL, ETC
 C NHARM- THE NO OF TERMS IN THE FORIER SERIES. THIS NO
 C MUST BE ODD AND 2*NHARM.LE.K
 C
 C
 C

C*****
 C

INTEGER K,NHARM
 REAL*8 F(K),TIME(K),PERIOD
 COMPLEX*16 C(NHARM),W

* WRITE(*,*)'PERIOD',PERIOD,' NHARM ',NHARM,' K',K

PI=3.141593
 OM1=2.*PI/PERIOD

C
 C GOTO (5,6),IOPTN

C
 5 DT=(TIME(K)-TIME(1))/(K-1.)
 DO 1 J=1,NHARM

C
 C J TH COEFFICIENT IS STORED IN C(J+1), J=0,1,2 ,NHARM
 C

```

C(J)=(0.,0.)
C      LOOP FOR ALL POINTS
DO 2 L=1,K
  W=DCMPLX(0.DO,(J-1)*OM1*TIME(L)*1.DO)
2    C(J)=C(J)+F(L)*CDEXP(-W)

      IF(IFEJ.EQ.1)THEN
        C(J)=C(J)*DT/PERIOD*(NHARM-(J-1))/NHARM
      ENDIF
      IF(IFEJ.EQ.0)THEN
        C(J)=C(J)*DT/PERIOD
      ENDIF
1    CONTINUE

      GOTO 7

C
6    DT=PERIOD/K
C
      DO 8 L=1,K
        TIME(L)=(L-1)*DT

C COMPUTE VALUE OF F AT J-TH TIME POINT AND STORE IN F(J+1), J=0,1..K
C      FIRST SET EQUAL TO MEAN TERM
      F(L)=C(1)
C      LOOP FOR ALL HARM
DO 9 J=2,NHARM
C      ANOTHER POSSIBLE METHOD FOR FINDING W
C      W=DCMPLX(0.DO,2.*PI*(J-1)*(L-1)/K*1.DO)
      W=DCMPLX(0.DO,(J-1)*OM1*TIME(L)*1.DO)
9    F(L)=F(L)+(C(J)*CDEXP(W)+DCONJG(C(J)*CDEXP(W)))

8    CONTINUE

7    RETURN
      END

```

```

*****
*
*   FREQUENCY STUDIES
*
*****

```

```

SUBROUTINE FREQ(IRCZ,ISIM,NDT,NHARM,PERIOD,CQRAD,CQCONV,CTAISP)
IMPLICIT REAL*8 (A-H,O-Z)
INTEGER NH,NHARM,NDT
REAL*8 PERD(51),TIME(51),KF,FR(50),MAG
COMPLEX*16 Z11(25),Z12(25),Z13(25),Z14(25),Z15(25)
COMPLEX*16 Z16(25),Z17(25),Z18(25),COMP,FRQ1,CTAISP(NHARM)
COMPLEX*16 S,J,Z11F,Z11NF,FR0L,CQRAD(NHARM),CQCONV(NHARM)

```

```

COMPLEX*16 IL1,IL2,CCOIL,GC,VALVE,DUCT,SENS,FRQ2(25),Z11A(25)
COMPLEX*16 Z17A(25),TAI(25),G,GX,GXA,G1,X,GF,GCF,CHEQ,GFA,GSCF
COMPLEX*16 TAI1,TAI2,TAI3,TA1,TA2,TA3
REAL*8 AM,CPAI,MGFQ(51),PHFQ(51),TAIR(51)
COMMON/ILT/AM,CPA,ILF,IFQ
COMMON/RES/UFA,UFT,UO,CA,AFC,Z11SS1,Z1NSS1,TF,DF,CPF,KF,UF
COMMON/RES1/RFL,Z11SS2,Z1NSS2,RFK

```

```

PI=3.14157265DO
J=(0.DO,1.DO)
FOMEGA=2*PI/PERIOD

```

```

*** ESTABLISH WHETHER THE IMPEDANCES ARE TO BE READ OR CALCULATED

```

```

IF(IRCZ.EQ.1)THEN

```

```

** READ THE IMPEDANCES

```

```

WRITE(*,*)
WRITE(*,*)
WRITE(*,*)
WRITE(*,*)

```

```

WRITE(*,*)' READING THE IMPEDANCES'

```

```

OPEN(12,FILE='IMPED.BEP',STATUS='OLD')

```

```

READ(12,*) NDT,NM,P

```

```

IF(P.NE.PERIOD)THEN

```

```

WRITE(*,*)

```

```

WRITE(*,*)

```

```

WRITE(*,*)

```

```

WRITE(*,*)

```

```

WRITE(*,*)'

```

```

WARNING PERIOD USED BY IMPED.BEP'
NOT SAME AS THE ONE USED BY THIS PROGRAM'

```

```

WRITE(*,*)'

```

```

WRITE(*,*)'DISCREPANCY IS-',(P-PERIOD)

```

```

ENDIF

```

```

DO 10 I=1,NM

```

```

READ(12,*) PERD(I),Z11(I),Z12(I),Z13(I),Z14(I),Z15(I)

```

```

+,Z16(I),Z17(I),Z18(I)

```

```

10 CONTINUE
CLOSE(12,STATUS='KEEP')

```

```

ELSE

```

```

** CALCULATE THE IMPEDANCES

```

```

WRITE(*,*)

```

```

WRITE(*,*)

```

```

WRITE(*,*)

```

```

WRITE(*,*)

```

```

WRITE(*,*)'

```

```

CALCULATING THE IMPEDANCES'

```



```

Z11(1)-Z11SS1
Z17(1)-Z1NSS1
Z11A(1)-Z11SS2
Z17A(1)-Z11SS2
TAI(1)=(0.DO,0.DO)

DO 11 I=2,NHARM
  OMEGA=FOMEGA*DBLE(I-1)
  PPERIOD=2*PI/OMEGA
  S=I*OMEGA
  Z11(I)-Z11F(1,S)
  Z17(I)-Z1NF(1,S)
  Z11A(I)-Z11F(IM,S)
  Z17A(I)-Z1NF(IM,S)
11 CONTINUE
  ENDIF
  IF(IFQ.EQ.1) THEN
    WRITE(*,*)
    WRITE(*,*)
    WRITE(*,*)
    WRITE(*,*)

WRITE(*,*)'                PERFORMING OPEN LOOP RESPONSE'
WRITE(*,*)
WRITE(*,*)'                OUTPUT IN FILE >>OLOOP.PRN<< '
  OPEN(22,FILE='OLOOP.PRN',STATUS='UNKNOWN')
  WRITE(22,*)NHARM,5
  WRITE(22,500)
  WRITE(22,501)
**** PERFORM OPEN LOOP FREQUENCY RESPONSE ANALYSIS
  FRQ2(1)=(0.DO,0.DO)
  MGFQ(1)=0.DO
  PHFQ(1)=0.DO
  FR(1)=0.DO

  DO 12 I=2,NHARM
    OMEGA=FOMEGA*DBLE(I-1)
    PPERIOD=2*PI/OMEGA
    S=J*OMEGA

    FRQ1=GC(S)*CCOIL(S)*VALVE(S)*DUCT(S)*Z11(I)*CPA*AM
    FROL=FRQ1*SENS(S)

    CALL MAGPHI(FROL,FMAG,FPHI)

    WRITE(22,221)PPERIOD,FMAG,FPHI,FROL
12 CONTINUE
  ENDIF
  IF(IFQ.EQ.3) THEN

```

```

*** PERFORM DEMONSTRATION OF FEEDFORWARD CONTROL
WRITE(*,*)
WRITE(*,*)
WRITE(*,*)
WRITE(*,*)
WRITE(*,*)'FEEDFORWARD LOOP RESPONSE'
DO 13 I=2,NHARM
  OMEGA=FOMEGA*DBLE(I-1)
  PPERIOD=2*PI/OMEGA
  S=J*OMEGA

  G=VALVE(S)*CCOIL(S)*DUCT(S)*CPA*AM
  IF(G.EQ.(0.D0,0.D0))THEN
    G=(1.D-32,0.D0)
  ENDIF
  GX=G*Z11(I)
  GXA=G*Z11A(I)
  TAI1=CQRAD(I)*Z17(I)
  TAI2=CQCONV(I)*Z11(I)
  T1=(CTAISP(I)/Z17A(I))-CQRAD(I)
  T2=T1*Z17A(I)/Z11A(I)
  TAI3=GX*(T2-CQCONV(I))*Z11A(I)/GXA
  TAI(I)=TAI1+TAI2+TAI3
13 CONTINUE
IF(ISIM.EQ.2)THEN
  WRITE(*,*)
  WRITE(*,*)
  WRITE(*,*)
  WRITE(*,*)
WRITE(*,*)'          INVERTING DISCRETE FREQUENCY RESPONSE'

WRITE(*,*)'          OUTPUT IN FILE >>FFWRDT.PRN<<'
  CALI.FOURIE(TAIR,TAI,NHARM,TIME,NDT,2,PERIOD,0)
  OPEN(23,FILE='FFWRDT.PRN',STATUS='UNKNOWN')
  WRITE(23,*)NDT,2
  *   WRITE(23,502)
  *   WRITE(23,503)
  *   WRITE(23,231)(TIME(I),TAIR(I),I=1,NDT)
  ELSE
  WRITE(*,*)
  WRITE(*,*)
  WRITE(*,*)
  WRITE(*,*)
WRITE(*,*)'          OUTPUT: DISCRETE FREQUENCY RESPONSE'

WRITE(*,*)'          OUTPUT IN FILE >>FFWRDF.PRN<<'
  OPEN(24,FILE='FFWRDF.PRN',STATUS='UNKNOWN')
  WRITE(24,*)NHARM,3
  *   WRITE(24,504)
  *   WRITE(24,505)

  WRITE(24,241)PERIOD*40,TAI(1)

```

```

        WRITE(24,241)(PERIOD/DBLE(I),TAI(I),I-2,NHARM)
    ENDIF
    ENDIF

    IF(IFQ.EQ.2) THEN
**** PERFORM DEMONSTRATION OF FEEDBACK CONTROL
        WRITE(*,*)
        WRITE(*,*)
        WRITE(*,*)
        WRITE(*,*)
    WRITE(*,*) '                                FEEDBACK LOOP RESPONSE'

    DO 14 I=2,NHARM
        OMEGA=FOMEGA*DBLE(I-1)
        PPERIOD=2*PI/OMEGA
        S=J*OMEGA

        GX=VALVE(S)*CCOIL(S)*DUCT(S)*CPA*AM*Z11(I)
        IF(GF.EQ.(0.D0,0.D0))THEN
            GF=(1.D-32,0.D0)
        ENDIF
        GCX=GX*GC(S)
        GSCX=GCX*SENS(S)
        CHEQ=1+GSCF
        TAI1=CTAISP(I)*GCX/CHEQ
        TAI2=CQRAD(I)*Z17(I)/CHEQ
        TAI3=CQCONV(I)*Z11(I)/CHEQ
        TAI(I)=TAI1+TAI2+TAI3
14    CONTINUE
    IF(ISIM.EQ.2)THEN
        WRITE(*,*)
        WRITE(*,*)
        WRITE(*,*)
        WRITE(*,*)
    WRITE(*,*) '                                INVERTING DISCRETE FREQUENCY RESPONSE'

    WRITE(*,*) '                                OUTPUT IN FILE >>FBACKT.PRN<<'
        CALL FOURIE(TAIR,TAI,NHARM,TIME,NDT,2,PERIOD,0)
        OPEN(25,FILE='FBACKT.PRN',STATUS='UNKNOWN')
        WRITE(25,*)NDT,2
    *   WRITE(25,506)
        WRITE(25,507)
        WRITE(25,231)(TIME(I),TAIR(I),I-1,NDT)

    ELSE
        WRITE(*,*)
        WRITE(*,*)
        WRITE(*,*)

```

```

        WRITE(*,*)
WRITE(*,*)'                OUTPUT: DISCRETE FREQUENCY RESPONSE'

WRITE(*,*)'                OUTPUT IN FILE >>FBACKF.PRN<<'

        OPEN(26,FILE='FBACKF.PRN',STATUS='UNKNOWN')
        WRITE(26,*)NHARM,3
*       WRITE(26,508)
        WRITE(26,509)
        WRITE(26,241)PERIOD*40,TAI(1)
        WRITE(26,241)(PERIOD/DBLE(I),TAI(I),I=2,NHARM)
    ENDIF
ENDIF

    IF(IFQ.EQ.4) THEN
WRITE(*,*)
WRITE(*,*)
WRITE(*,*)
WRITE(*,*)
WRITE(*,*)'                FEEDFORWARD-FEEDBACK LOOP RESPONSE'

```

*** PERFORM FEEDFORWARD-FEEDBACK CONTROL

```

    DO 15 I=2,NHARM
        OMEGA=FOMEGA*DBLE(I-1)
        PPERIOD=2*PI/OMEGA
        S=J*OMEGA

        G=VALVE(S)*CCOIL(S)*DUCT(S)*CPA*AM
        IF(G.EQ.(0.D0,0.D0))THEN
            G=(1.D-32,0.D0)
        ENDIF
        GX=G*Z11(I)
        GXA=G*Z11A(I)
        GCX=GX*GC(S)
        GSCX=GCX*SENS(S)
        CHEQ=1+GSCX
        TAI1=CTAISP(I)*GCX/CHEQ
        TAI2=CQRAD(I)*Z17(I)/CHEQ
        TAI3=CQCONV(I)*Z11(I)/CHEQ
        TA1=TAI1+((CTAISP(I)*GX/GXA)/CHEQ)
        TA2=TAI2-(((CQRAD(I)*Z17A(I)/GXA)*GX)/CHEQ)
        TA3=TAI3-(((CQCONV(I)*Z11A(I)/GXA)*GX)/CHEQ)
        TAI(I)=TA1+TA2+TA3
15    CONTINUE

    IF(ISIM.EQ.2)THEN
        WRITE(*,*)

```

```

WRITE(*,*)
WRITE(*,*)
WRITE(*,*)

WRITE(*,*)'                               INVERTING DISCRETE FREQUENCY RESPONSE'

WRITE(*,*)'                               OUTPUT IN FILE >>FFFBT.PRN<<'

CALL FOURIE(TAIR,TAI,NHARM.TIME,NDT 2,PERIOD,0)
OPEN(27,FILE='FFFBT.PRN',STATUS='UNKNOWN')
WRITE(27,*)NDT,2
*   WRITE(27,510)
   WRITE(27,511)
   WRITE(27,231)(TIME(I),TAIR(I),I=1,NDT)

ELSE
   WRITE(*,*)
   WRITE(*,*)
   WRITE(*,*)
   WRITE(*,*)
WRITE(*,*)'                               OUTPUT: DISCRETE FREQUENCY RESPONSE'

WRITE(*,*)'                               OUTPUT IN FILE >>FFFBF.PRN<<'

OPEN(28,FILE='FFFBF.PRN',STATUS='UNKNOWN')
WRITE(28,*)NHARM,3
*   WRITE(28,512)
   WRITE(28,513)
   WRITE(28,241)PERIOD*40.TAI(1)
   WRITE(28,241)(PERIOD*DOUBLE(I),TAI(I),I=2,NHARM)
ENDIF

ENDIF

221  FORMAT(2X,F10.2,2X,F15.10,2X,F8.4,2X,F15.10,2X,F15.10)
231  FORMAT(2X,F10.2,2X,F20.4)
241  FORMAT(2X,F10.2,2X,F15.5,2X,F15.5)
500  FORMAT('***** OPEN LOOP FREQUENCY RESPONSE *****')
501  FORMAT(3X,' "PERIOD",',2X,' "MAGNITUDE",',2X,' "PHASE",',2X,
+ "REAL",',2X,' "IMAGINARY",')
* 502 FORMAT('*****FEEDFORWARD CONTROL (TIME RESPONSE)****')
503  FORMAT(3X,' "TIME",',2X,' "AIR TEMPERATURE",')
* 504 FORMAT('*****FEEDFORWARD CONTROL (FREQUENCY RESPONSE)****')
505  FORMAT(3X,' "PERIOD",',2X,' "TEMPERATURE-REAL",',2X,
+ "TEMPERATURE-IMAG",')
* 506 FORMAT('*****FEEDBACK CONTROL (TIME RESPONSE)****')
507  FORMAT(3X,' "TIME",',2X,' "AIR TEMPERATURE",')
* 508 FORMAT('*****FEEDBACK CONTROL (FREQUENCY RESPONSE)****')
509  FORMAT(3X,' "PERIOD",',2X,' "TEMPERATURE-REAL",',2X,

```

```

+ ' "TEMPERATURE-IMAG" ' )
* 510 FORMAT( ' ****FEEDBACK-FEEDFORWARD CONTROL (TIME RESPONSE)**** ' )
511   FORMAT( 3X, ' "TIME", ' , 2X, ' "AIR TEMPERATURE", ' )
* 512 FORMAT( ' ****FEEDBACK-FEEDFORWARD CONTROL (FREQUENCY RESPONSE)** ' )
513   FORMAT( 3X, ' "PERIOD", ' , 2X, ' "TEMPERATURE-REAL", ' , 2X,
+ ' "TEMPERATURE-IMAG" ' )
      RETURN
      END

```

```

*****
*
*   SUBROUTINE TSSPG PRODUCES CTSP(I), THE FREQUENCY COUNTERPART
*   TO TSP(I) THE SETPOINT VARIATION
*
*****

```

```

      SUBROUTINE TSPG(TSPX,TSPN,TOM,PHI,NHARM,NDT,PERIOD,ISP,MSP,
+CTSP,TSP)
      REAL*8 TSPX,ISPN,TSP(51),TOM,PERIOD,TIME(51),DELTAT,TSPM,TSPD
      REAL*8 PHI,TS(51),MSP
      COMPLEX*16 CTSP(NDT)

```

```

      DELTAT=PERIOD/NDT

```

```

      DO 21 I=1,NDT
          TIME(I)=DBLE(I-1)*DELTAT
          TSPM=(TSPX+TSPN)/2.DO
          TSPD=(TSPX-TSPN)/2.DO

```

```

          IF(ISP.EQ.1.AND.MSP.NE.0.DO)THEN

```

```

              TSP(I)=TSPM+(TSPD*COS((TOM*TIME(I))-PHI))
          ENDIF
          IF(ISP.EQ.2.AND.MSP.NE.0.DO)THEN
              TSP(I)=TSPM
          ENDIF

```

```

          IF(ISP.EQ.1.AND.MSP.EQ.0.DO)THEN
              TSP(I)=(TSPD*COS((TOM*TIME(I))-PHI))
          ENDIF
          IF(ISP.EQ.2.AND.MSP.EQ.0.DO)THEN
              TSP(I)=0.DO
          ENDIF

```

```

21   CONTINUE

```

```
CALL FOURIE(TSP,CTSP,NHARM,TIME,NDT,1,PERIOD,0)
CALL FOURIE(TS,CTSP,NHARM,TIME,NDT,2,PERIOD,0)
```

```
RETURN
END
```

```
*****
* SUBROUTINE QLOAD PRODUCES THE FREQUENCY ARRAYS REQUIRED
* FOR ACCOUNTING OF THE RADIANT AND CONVECTIVE INTERNAL GAINS
*****
```

```
SUBROUTINE QLOAD(QMAX,QMIN,RADTIO,NHARM,PERIOD
+,NDT,CQLDR,CQLDC,THETA,QOM,ILD,LDMSP)
IMPLICIT REAL*8 (A-H,O-Z)
REAL*8 QLD(51),QLDR(51)
REAL*8 QLDC(51),TIME(51),K1,K2
COMPLEX*16 CQLDR(25),CQLDC(25)
COMMON/RAD/FLA?TIO
```

```
DELTAT=PERIOD/NDT
```

```
DO 22 I=1,NDT
  TIME(I)=DELTAT*DBLE(I-1)
  IF(ILD.EQ.1.AND.LDMSP.NE.0.DO)THEN
    QLDM=(QMIN+QMAX)/2.DO
    QLDD=(QMAX-QMIN)/2.DO
    QLD(I)=QLDM+(QLDD*COS((QOM*TIME(I))-THETA))
  ENDIF

  IF(ILD.EQ.1.AND.LDMSP.EQ.0.DO)THEN
    QLDD=(QMAX-QMIN)/2.DO

    QLD(I)=(QLDD*COS((QOM*TIME(I))-THETA))
  ENDIF
  IF(ILD.EQ.2.AND.LDMSP.NE.0.DO)THEN
    QLD(I)=(QMIN+QMAX)/2.DO
  ENDIF
  IF(ILD.EQ.2.AND.LDMSP.EQ.0.DO)THEN
    QLD(I)=0.DO
  ENDIF
```

```
  QLDR(I)=QLD(I)*RADTIO
  QLDC(I)=QLD(I)*(1.DO-RADTIO)
```

```
22 CONTINUE
```

```
CALL FOURIE(QLDR,CQLDR,NHARM,TIME,NDT,1,PERIOD,1)
CALL FOURIE(QLDC,CQLDC,NHARM,TIME,NDT,1,PERIOD,1)
```

```
12? FORMAT(2X,F10.2,2X,F10.2,2X,F10.2,2X,F10.2)
```

```
RETURN
END
```

APPENDIX C
HEAT EXCHANGER MODEL USED
IN DYCON

The first order model for a finned serpentine cross flow heat exchanger used by DYCON was developed from a set of partial differential equations which was derived under the following assumptions (Pearson et al 1974):

1. The density and specific heat of the tube material and air were considered constant.
2. Negligible conductive resistance through the tube wall and between the tube and fins.
3. Negligible heat conduction in the water and tube in the direction of water flow.
4. Negligible row to row conduction through the fins.
5. Constant air temperature and velocity over the entrance cross-section to the heat exchanger.
6. Constant convective heat transfer coefficients on the air and water sides.
7. The heat capacitive effects of the water and metal contained in U-tube bends are accounted for by distributing the U-bend metal and water throughout the finned portion of the coil.
8. Fin effectiveness is constant.

Based on these assumptions, the heat exchanger can be modelled as a long finned-tube heat exchanger.

The system of dimensionless governing differential equations on which Boot et al (1977) based their model and which were developed by Pearson et al (1974) are:

$$\beta_1 \cdot \frac{\delta T_w^{xo}}{\delta x^*} + \beta_2 \left(T_w - \frac{T_a}{C_4} \right) + \beta_1 \frac{\delta T_w}{\delta t^*} = 0$$

$$T_a^{xo} - \beta_2 \left(T_w - \frac{T_a^{xo}}{C_4} \right) + \frac{\beta_3}{C_4} \cdot \frac{\delta T_a^{xo}}{\delta t^*} = 0$$

With initial and final air temperature distribution being:

$$T_a^{xo}(x^*, 0) = C_i \cdot \exp(-b_i \cdot x^*)$$

and

$$T_a^{xo}(x^*, \infty) = C_f \cdot \exp(-b_f \cdot x^*)$$

respectively.

With the exception of the β -parameters, the definitions of the parameters are in the nomenclature. The β -parameters have important physical meaning:

$$\beta_1 = \frac{m_w \cdot cp_w}{L_f \cdot m'_a \cdot cp_a} = \text{dimensionless heat capacity rate of water}$$

$$\beta_2 = \frac{A_w \cdot h_w}{m'_a \cdot cp_a} = \text{dimensionless water side conductance}$$

$$\beta_3 = \frac{C_m}{m'_a \cdot cp_a \cdot ft_{cc}} = \text{dimensionless heat capacity of tubes and fins divided by flush time}$$

$$\beta_4 = \frac{\eta_o \cdot h_a \cdot A_a}{m'_a \cdot cp_a} = \text{dimensionless air side conductance}$$

The two partial differential equations were subsequently combined in a second order partial differential equation whose solution was facilitated by dividing the response of this equation into two parts such that the two responses could be added to give the solution to the actual response. The final expressions for the gain and the time constant of a serpentine cross flow heat exchanger arrived at are:

$$K_{hc} = \frac{T_{wi} - T_{ai}}{m_w} \cdot \beta_1 \left(1 - \left(1 + b - \frac{mCb}{\beta_2} \right) \cdot \exp(-b) \right)$$

and

$$\tau_{hc} = \frac{\beta_1 \cdot ft \cdot (T_{wi} - T_{ai})}{m_w} \cdot \left(\frac{m \cdot \beta_3 C^2}{C_4 \cdot \beta_2^2} \cdot [1 - \exp(-b)] + \right.$$

$$\left. \frac{\left(1 - \frac{m \cdot C}{\beta_2} \right) \cdot \left(1 + \frac{\beta_3}{\beta_1} \right) \cdot [1 - (1+b) \cdot \exp(-b)]_2}{b \cdot [1 - \exp(-b)]} \right)$$

The criterion by which the model may be invalidated if it is breached is the magnitude of the fin time constant τ_f . To establish its magnitude, the thermal capacitance and resistance of the fin have to be found. The capacitance is described as follows:

$$C_f = \eta_f \rho_f c_p t_f (Y \cdot ts - (\pi D_o^2 / 4))$$

while the resistance is:

$$R_f = \frac{Y + ts - 2.D_o}{8.\pi.k_f.D_o.tf}$$

If $\tau < \tau_f = R_f.C_f$

then the time constant of the fin dominates the response characteristic of the coil and therefore the expression for the time constant is no longer valid.